Optimising the use of Recirculating Well Pairs for the Determination of Aquifer Hydraulic Conductivity

A thesis submitted in partial fulfilment of the requirement for the Degree of Master of Civil Engineering in the University of Canterbury
by M. J. Flintoft
University of Canterbury
2009

Principal Supervisor: Dr Tom Cochrane
Associate Supervisor: Prof Mark Goltz
Associate Supervisor: Murray Close
Associate Supervisor: Dr Mark Milke

Prepared and submitted by: Mark Flintoft
Student ID: 51353948
Email: mfl30@student.canterbury.ac.nz

Abstract

Hydraulic conductivity (K) is a key parameter required for the accurate prediction of contaminant transport in an aquifer. Traditionally, pump tests, slug tests, grain size analysis and, to a lesser extent, tracer tests have been employed to estimate the K of an aquifer. These methods have disadvantages in respect to assessing the K of a contaminated aquifer, for example, pumping tests generate large quantities of potentially contaminated water, slug tests interrogate only a small portion of aquifer to generate K values, and tracer tests are costly to perform. The recirculating well pair (RWP) system, assessed in this study, attempts to minimise these disadvantages while producing accurate estimates of K.

The RWP system uses two wells, each screened in two positions; one screen injects water and the other extracts water from the aquifer. One well extracts water from the lower screen and injects it into the aquifer via the upper screen, whereas the second well extracts water from the upper screen and injects it through the lower screen. When these two wells are pumped in tandem a recirculation system is created within the aquifer. No water is lost or gained from the aquifer in this system.

Hydraulic conductivity can be estimated from a RWP system by either the multi dipole or the fractional flow methods. The multi dipole method estimates K by measuring steady state hydraulic heads, whereas the fractional flow method uses a tracer test to obtain steady state concentrations at the four screens to estimate K. Both methods utilise a 3D flow model to simulate the aquifer system. Inverse modelling in conjunction with a genetic algorithm simulate the hydraulic head values obtained from the multi dipole experiments or the tracer steady state values obtained from the fractional flow method. Hydraulic

conductivity estimates are obtained by matching the simulated and observed steady state hydraulic head, or tracer steady state values.

An investigation of the accuracy of the two RWP methods, when system parameters are varied, in estimating K values was undertaken. Five multi dipole experiments were undertaken with varying dipole flow rates to assess the effect of altering dipole flow rate on estimates of K. Two experiments were also undertaken to assess the effect of altering the pumping well incidence angle as compared to the regional flow on the accuracy of K estimates. Five fractional flow experiments were conducted, four to assess the effect of changing dipole pumping rates and one to assess the influence of altering the incidence angle of the pumping wells on estimation of K. All experiments were undertaken in an artificial aquifer that allowed control of hydraulic parameters and accurate measurement of aquifer K by independent methods. Experimental results were modelled with the two RWP methods.

Results indicate that both the multi dipole and fractional flow methods provide accurate estimates of the K of the artificial aquifer (5 % to 57% greater than the actual K and -14% to 17% of the actual K, respectively). Altering the ratio between the pumping well and regional aquifer flow rates had no effect on the estimated K results in both methods. Although preliminary results were positive, further work needs to be undertaken to determine if changing the orientation of the well pairs affects the estimation of K.

Acknowledgements

I would like to thank the many people that have helped me though the process of writing this thesis. It has been a long process and without there continuing support I would not have succeeded.

Firstly, I would like to thank my employer, the Institute of Environmental Science and Research (ESR) for providing me with the funding and time that has enabled me to complete this research.

I also want to thank my colleagues at in the ESR Groundwater Group (Rod, Liping, Ross, Pieter and Alex) who have given me invaluable advice and support while I have been occupied with writing this thesis. I want to say a special thank you to Junqi Huang for showing me the ropes of the RWP model and GA and for being so patient with my innumerable questions.

I would like to thank my supervisors, Tom Cochrane, Mark Goltz, Murray Close and Mark Milke. Thank you for guiding me through this process and providing support, wisdom and constructive comments when needed.

Thanks also to my family for there unwavering love and support over the years. Finally, thanks must go to Rachel for her belief in me and her love and encouragement, without which I would never have finished.

Table of Contents

Table of Figures

Table of Tables

Glossary

Anisotropic Aquifer: An aquifer in which hydraulic properties vary in different planes.

Aquifer: A rock or sediment that is saturated and sufficiently permeable to transmit economic quantities of water to a well or spring.

Confined Aquifer: An aquifer overlain by a confining bed that is significantly lower in hydraulic conductivity.

Darcy's Law: Equation used to calculate the quantity of water flowing through an aquifer.

Dispersion: The phenomenon is which a solute in flowing groundwater is mixed with uncontaminated water thereby reducing the solutes initial concentration. Dispersion is caused by the differences in groundwater velocity due to different sized pore spaces and differences in flow velocity through larger scale geological strata.

Effective Porosity: The ratio of the volume of void spaces in a sediment or rock through which water can travel by the total volume of the sediment or rock.

Heterogeneous Aquifer: A geological formation in which properties change spatially.

Homogeneous Aquifer: A geological formation that contains the same properties in all locations.

Hydraulic Conductivity: A coefficient of proportionality relating the rate at which groundwater moves through a permeable medium to the hydraulic gradient.

Hydraulic gradient: The change in total head of a system with change in distance in a given direction.

Hydraulic head: The sum of the elevation, pressure and velocity heads at a given point in an aquifer.

Isotropic Aquifer: An aquifer in which the hydraulic properties are the same in every plane.

Packer: An inflatable device used to isolate a section of borehole from the remaining portion of the borehole.

Porosity: The ratio of the volume of void spaces in a sediment or rock to the total volume of the sediment or rock.

Storativity: The volume of water an aquifer releases or stores per unit surface area of aquifer per unit change in head.

Transmissivity: The rate at which water of a prevailing density and viscosity is transmitted through a given width of aquifer under a unit hydraulic gradient. Transmissivity is a function of the properties of the liquid, the porous media and the thickness of the aquifer.

Unconfined Aquifer: An aquifer where there is no confining beds between the aquifer and the ground surface.

Well Screen: A tubular section of well with slots, holes, gauze or continuous wire wrap used to let water into a well while keeping sediments out.

Unit Symbols

L	**Length**
T	**Time**
M	**Mass**

Unit Abbreviation

Time

s	second
hr	hour
d	day

Volume

ml	millilitre
l	litre

Length

mm	millimetre
cm	centimetre
m	metre
km	kilometre

Mass

mg	milligram
g	gram
kg	kilogram

1. Introduction

1.1 Background

Groundwater is only a small proportion of the total water on the earth (0.61%), but is critically important to humans and terrestrial ecosystems because it makes up 98% of available fresh water (Fetter, 2001). In New Zealand it has been estimated that 80 percent of fresh water is in the form of groundwater (White and Rosen, 2001). This resource is extensively used for a variety of purposes. Twenty six percent of New Zealand's population rely solely on groundwater as a source of drinking water, and a further 25% use a combination of ground and surface water sources (White and Rosen, 2001). The greatest use for fresh water in New Zealand and throughout the world is for agriculture. Since 1990 over 50% of the total water allocated for agriculture in New Zealand is groundwater. Groundwater also contributes to the base flow of streams, maintaining flow in dry conditions, sustaining ecosystems and providing recreational opportunities.

The increasing world population has lead to intensification of agriculture in order to feed and provide greater living standards for the population, placing pressure on the world's water supplies. Readily accessible surface water is approaching full utilisation, and groundwater is therefore becoming an increasingly important resource. This has been highlighted by the intense competition for surface water in areas such as the Murray – Darling basin, Australia and Colorado River, United States of America as well as the tension between Israel and surrounding nations regarding access to surface water.

As well as greater utilization, population pressure has increased the degradation of fresh water supplies, compounding supply problems. Fresh waters have been polluted with industrial chemicals, nutrient and bacterial contamination from agricultural and human effluent disposal. Groundwater has been affected to a lesser degree as compared to surface water because of the protective soil and vadose zones. These zones act as filters, straining, absorbing, transforming, and retarding contaminants before they reach groundwater. Similarly to a filter, there are limits to the flux of contamination the soil and vadose zones can mitigate. In many areas of the earth the ability for the soil and vadose zones to mitigate contamination has been over-whelmed by the quantity of contamination applied to the land surface. This has resulted in groundwater contamination. Direct contamination of groundwaters when protective soil and vadose zone layers are removed (e.g. mining) also contributes to groundwater degradation. Once contaminants reach the groundwater, they can be attenuated by natural processes to a greater or lesser extent depending on the conditions in the aquifer.

Knowledge of groundwater flow parameters is critical in predicting flow paths of contamination and for designing *in situ* remediation schemes. The success in predicting groundwater movement depends on the accurate estimation of hydraulic parameters (Bouwer, 1978). To predict groundwater flow, regional hydraulic gradient, porosity and the hydraulic conductivity (K) of the aquifer need to be ascertained. Regional hydraulic gradient is obtained by measuring the head in two wells a known distance apart. Porosity is a measure of open space in an aquifer and is usually obtained by taking a sample of the aquifer material. Hydraulic conductivity, the subject of this thesis, is more difficult to ascertain.

Hydraulic conductivity is a proportionality constant relating the rate at which water moves through a porous medium to the hydraulic gradient. The rate of water movement is quantified by the specific discharge, which is the volume of water moving through a unit area of aquifer over a specified time ($L^3/L^2/T$). Specific discharge is sometimes referred to as the Darcy velocity, with units of L/T. Henry Darcy performed the first systematic study of the movement of water through a porous media and determined the proportionality constant, K (Freeze, 1994).

Pump tests are used to estimate K by interrogating a large volume of the aquifer. These tests have the disadvantage, when dealing with contaminated aquifers, of pumping a large volume of contaminated water to the surface that will potentially have to be treated. Other methods of determining K such as slug tests and push pull tests sample small volumes of the aquifer, providing only point estimates of K. Tracer tests, which can also be used to estimate K, are costly in terms of well construction and sampling time and analysis. This thesis investigates the determination of K using a novel recirculating well pair (RWP) system, which avoids the disadvantages of conventional methods.

1.2 Assessment Methods

The RWP system consists of two pumping wells, each containing an extraction and injection screen, which circulate contaminated water in the subsurface without the need to discharge it to the surface. In an RWP system, one well pumps water from an extraction screen to an injection screen located above it, the second well pumps water in the opposite direction (Figure 1.1a). Joint operation of the wells results in a capture zone upstream of the wells and a recirculation zone between the wells (Figure 1.1b). The size of the

recirculation zone is a function of well pumping rate, the distance between the screens, distance between the wells and the aquifer K. Past studies have primarily investigated the RWP system for *in situ* remediation of groundwater (Cunningham et al., 2004; Huang and Goltz, 2005).

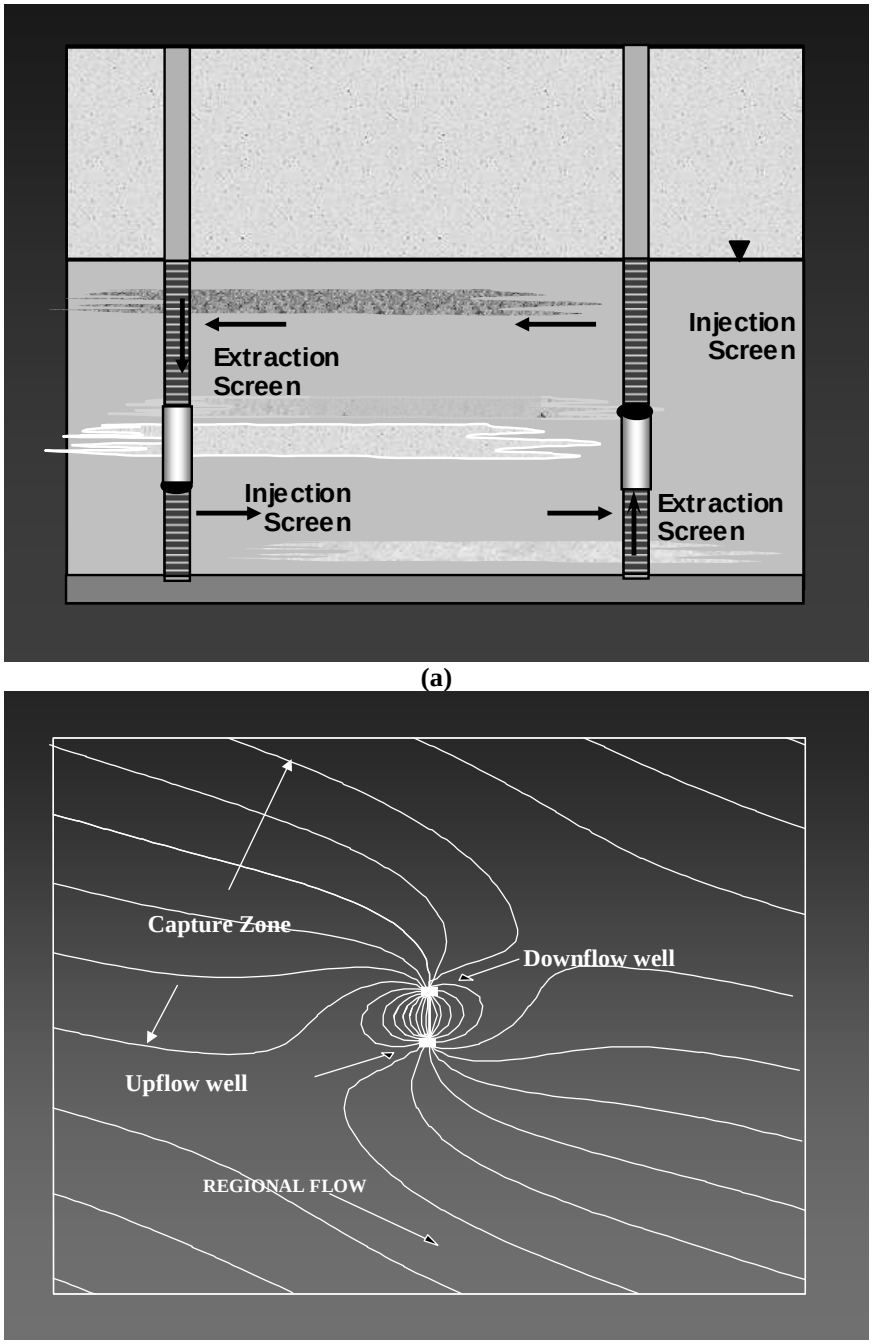

Figure 1.1: Cross-sectional a) and plan view b) depicting a Recirculating Well Pair in operation (after McCarty et al., 1998).

Goltz et al. (2008) proposed the use of RWP systems as a method to determine the K of an aquifer. This work is partially based on the earlier work in which a three dimensional analytical solution to calculate the fractional flow of groundwater circulating between a RWP system was developed (Huang and Goltz, 2005).

Two methods can be used to calculate K in a RWP system:

1. The multi dipole method
2. The fractional flow method

The multi dipole method involved estimating the vertical and horizontal K from steady-state hydraulic heads at various locations in the RWP system. The fractional flow method was based on measuring the steady state tracer concentrations at the four screens of a RWP system, with two of these screens being used to continually inject two tracers. Steady state concentrations are used to estimate the fractional flows between the four well screens. Both methods employ inverse modelling in conjunction with a genetic algorithm to estimate horizontal and vertical K values.

Recirculating well pair experiments were conducted in the ESR/ Lincoln Environmental Artificial Aquifer facility located at Lincoln University, Canterbury, New Zealand. Kim (2005) quantified the accuracy of determining the mass flux of a contaminant using the multi dipole and fractional flow methods. It was concluded that the fractional flow approach provided a reasonably accurate measure of flux and therefore conductivity (within 50% and 44% of actual K for the two experiments analysed). It was also determined that the multi dipole approach was sensitive to small hydraulic head measurement errors and therefore not useful in predicting flux.

Yoon (2006) compared the use of the RWP system with another innovative method for measuring contaminant flux, the Integral Pumping Test (IPT). The IPT method measures the head difference between piezometer and pumping wells as a function of flow in the pumping wells to determine the Darcy velocity. If concentration and Darcy velocity are known, flux can be determined. It was concluded that the fractional flow tracer test was the most accurate method (within 15% of the actual K value) followed by the IPT (within 60% of the actual K value). Yoon (2006) also determined that the multi dipole RWP method was sensitive to small hydraulic head measurement errors.

Further testing of the multi dipole method with greater accuracy in measuring hydraulic head was recommended (Kim, 2005). It was also recommended that both RWP methods be undertaken using varying well pumping rates, regional hydraulic gradients and well orientations in order to assess the robustness of the method.

This study undertakes further RWP experiments at the ESR / Lincoln Environmental artificial aquifer facility to answer some of the above questions. The artificial aquifer facility was used to perform the RWP experiments because the hydraulic parameters of the system can be controlled, unlike natural systems. Accurate independent K values of the artificial aquifer were determined for comparison with values obtained from the RWP methods.

Five RWP multi dipole experiments were performed to ascertain the effect of changing the RWP well pumping rates on the accuracy of estimated K. Three fractional flow experiments analysed by Kim (2005) and Goltz et al.(2008) were re-analysed together with two additional RWP fractional flow experiments. Four of these experiments were used to

determine the effect of changing the RWP well flow rate on the estimate of K. The fifth RWP fractional flow experiment was analysed to determine the effect of altering the incidence angle of the pumping wells to the regional hydraulic flow on the K estimate. Hydraulic heads were also measured in the fifth RWP fractional flow experiment and these values were analysed using the multi dipole approach to determine the effect of altering the incidence angle of the pumping wells to the regional hydraulic flow on the K estimate using this method.

1.3 Purpose and Objectives

The purpose of this research was to gain an improved understanding of the effects of changing RWP system parameters on estimates of K. Specifically this research sought to determine if RWP pumping rate had an effect on estimation of K values. The effect on estimated K of changing the angle between the regional groundwater flow direction and the two recirculating wells was also investigated. This work extends the research conducted to date and will enable practical applications of the RWP system to determine aquifer K.

The objective of this study was to further validate the RWP system as a method to determine aquifer K. This will be achieved for both the multi dipole and fractional flow RWP methods by:

- Determining the accuracy of the estimated K by comparing it to K determined by independent methods.

- Determining the effect of changing the flow ratio of the pumping wells and regional aquifer flow on the estimation of K.

- Determining the effect of changing the angle between the regional aquifer flow and the RWP wells on the estimation of K.

The general scope of this research was to make practical recommendations on the use and limitations of the RWP system in estimating K.

1.4 Organisation

This thesis documents the methods, analysis and conclusions drawn from a study on changing RWP system parameters on the estimation of K. Chapter 2 provides a literature review covering the current methods employed to determine aquifer K. This chapter also outlines the development of the RWP system as applied to the determination of aquifer K and a review of genetic algorithms that were used to search a parameter space for hydraulic head and fractional flow values. Chapter 3 describes the artificial aquifer in which RWP experiments were undertaken. A description of the RWP system together with the experiments carried out for this study was also included in this chapter. Chapter 4 provides results and discussion of the experiments described in Chapter 3. Determination of independent K values used to compare with K values estimated for the RWP system was also included in this chapter. An analysis of the problems encountered when the RWP system was used is also provided. A summary of the thesis, conclusions drawn from the results, and recommendations for future research is presented in Chapter 5.

2. Hydraulic Conductivity Measurement Methods

The management of groundwater quality issues requires accurate measurement of aquifer parameters to enable accurate predictive models to be constructed. The fundamental parameter controlling contaminant transport is the hydraulic conductivity (K) of the aquifer. Hydraulic conductivity values and therefore contaminant velocity vary over a wide range depending on the geology of the aquifer (Table 2.1).

Table 2.1: Ranges of hydraulic conductivity values for unconsolidated sediments (adapted from Fetter, 2001)

Material	Hydraulic conductivity (m/d)
Clay	0.000001 - 0.001
Silt, Sandy Silts, Clayey Sands, Till	0.000001 - 0.1
Silty Sands, Fine Sands	0.00001 - 1.0
Well - sorted sands, Glacial outwash	1.0 - 100
Well - sorted gravel	10 - 1000

Hydraulic conductivity can be measured by a variety of methods, each with different measurement scales, accuracy levels, sampling and equipment requirements. The superiority of one method over another is determined by the geological setting and the accuracy of results required. Contaminant transport modelling, and subsequent management, generally requires more accurate estimation of hydraulic parameters than management of groundwater quantity due to the smaller management scales. Section 2.1 summarises and describes relevant K estimation techniques, and discusses some of the advantages and disadvantages of these methods for contaminant transport studies. The recirculating well pair (RWP) system was developed as an aquifer remediation tool and then adapted to measure aquifer parameters. Section 2.2 details the application of the RWP system for determining K.

2.1 Methods for Estimating Hydraulic Conductivity

2.1.1 Grain Size Analysis

The K of an unconsolidated aquifer can be estimated by performing a grain size analysis on the sediment within the aquifer. Grain size is measured as a proxy for pore size which is problematic to measure. Several empirical formulas have been determined to relate different grain size ranges to K (Hazen, 1892; Slichter, 1899; Carman, 1937; Carman, 1938; Beyer, 1964). Selecting the correct formula for the specific grain size distribution is important to determine accurate K values (Odong, 2008). Hazen (1892) determined the most commonly used general empirical equation for K (Equation 2.1).

$$K = C_h d_{10}^2 \tag{2.1}$$

with the dimensionless constant C_h, defined in Equation 2.2.

$$C_h = (g / v)(\beta)(v(n)) \tag{2.2}$$

where g is the acceleration due to gravity, v is the kinematic viscosity of water, β is a dimensionless factor representing fabrics, grain shapes, composition, and anisotropy of the porous media, $v(n)$ is the porosity function, n is porosity and d_{10} is the grain size diameter where 10% by weight is finer and 90% coarser.

Grain size is determined by sieving for larger sediment sizes (>0.075mm), and by hydrometer and pipette analysis, or laser diffraction for small grain sizes. The hydrometer

and pipette analysis techniques rely on the difference in settling times for different grain sizes to ascertain grain size fractions.

Porosity can be calculated by oven drying a representative sample of known volume and submerging it in a known volume of water until it is fully saturated, being careful to remove entrapped air. The porosity is equal to the initial water volume minus the volume in the chamber after the saturated sample is removed (Fetter, 2001). It is difficult to accurately saturate the known volume of sample therefore it is more useful to calculate porosity using Equation 2.3.

$$n = 100 - \left[1 - \left(\rho_b / \rho_d\right)\right] \quad \textbf{(2.3)}$$

where n is the porosity, ρ_b is the bulk density and ρ_d is the particle density.

Bulk density is obtained by dividing the weight of material by its volume. Bulk density rings of set volume can be pushed into soft sediment and the material inside the ring dried and weighed to obtain bulk density. For coarser sediments, in situ volume replacement methods are used to obtain the bulk density (Dann et al., 2008). Volume replacement methods involve excavating a known mass of sediment and filling the void space with either water, sand or expanding foam to estimate the volume. The mass of material extracted from the hole is divided by the volume of the hole providing the bulk density. A literature derived particle density is generally used in this determination.

In situ porosity of aquifer material can be very difficult to measure and repacked cores rarely represent the *in situ* porosity accurately except when sediments are homogeneous. Multiple porosity measurements of intact material need to be collected to obtain a representative value for an aquifer. This can be costly and time consuming.

Empirical equations for grain size analysis provide estimates of K within one order of magnitude due to the uncertainty in calculating C_h (Palmer, 1993). Tables containing ranges of C_h values for individual grain size and uniformity are usually used because β is difficult to determine (Fetter, 2001). K estimates within an order of magnitude of the actual value are often not sufficient for contaminant transport applications.

2.1.2 Permeameter Tests

A permeameter is basically a column filled with a sample of porous aquifer material (Figure 2.1). Permeameters are used to estimate the K of discrete samples of aquifer material by measuring the flow rate and head loss across the sample. Permeameter tests can be performed with the hydraulic head held constant at both the inlet and outlet (constant head permeameter), or with a constant hydraulic head maintained at the outlet only (falling head permeameter).

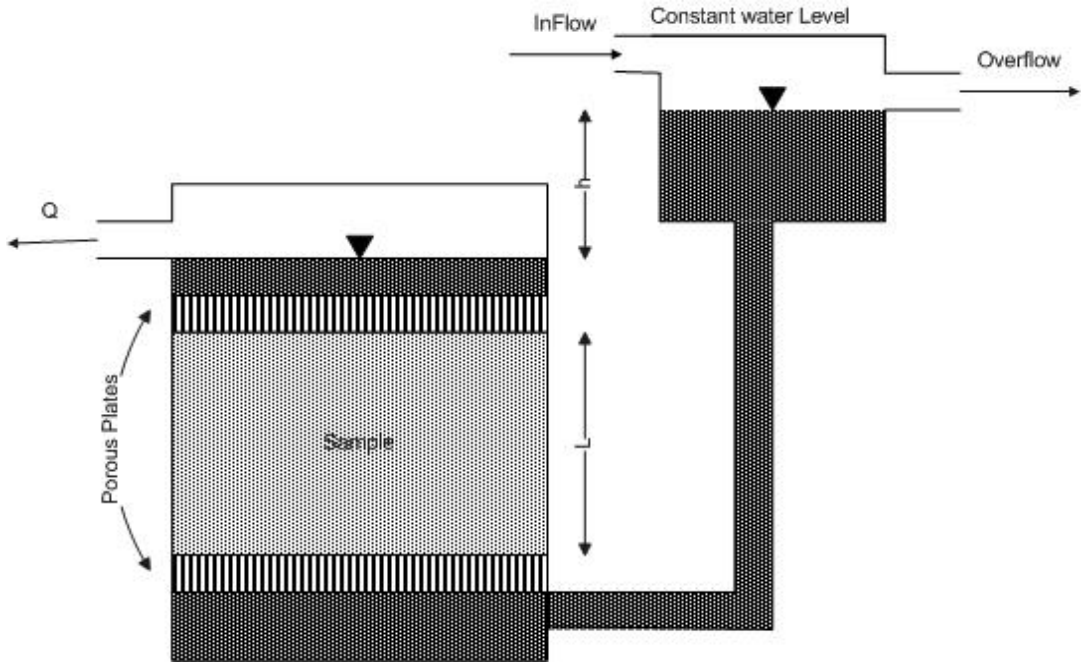

Figure 2.1: Constant head permeameter apparatus (adapted from Fetter, 2001).

Constant head permeameters are used to ascertain the K of coarse aquifer materials where water flow is large. Material of permeability higher than that of the sample is used to support the aquifer material in the permeameter to insure head losses apart from those of the sample are negligible. For a constant head permeameter, Darcy's Law can be used to calculate K (Equation 2.4).

$$K = \frac{QL}{AH} \tag{2.4}$$

where L is the length of sample, Q is the volumetric flow rate, H is the total head loss across the sample (head at the inflow minus the head at the outflow), and A is the cross-sectional area of the sample.

Constant head permeameters should be operated at a hydraulic gradient similar to that found where the core was obtained (Fetter, 2001). If the hydraulic gradient is unknown, the hydraulic gradient should not exceed one half of the sample length. A large hydraulic gradient may result in non-laminar flow, invalidating Darcy's law.

Falling head permeameters can also be used to estimate K. As the name suggests, the falling head permeameters design replaces the constant head chamber with a tube in which the change in head with time is measured. Equation 2.5, derived from Darcy's law is used to calculate K in a falling head permeameter. Falling head permeameters are more appropriate for materials with low K (Table 2.1).

$$K = \frac{d_t^2 L}{d_c^2 t} \ln\left(\frac{h_o}{h}\right) \qquad \textbf{(2.5)}$$

where L is sample length, h_o is the initial head in the falling tube, h is the final head in the falling tube, t is the time taken for the head to drop from h_o to h, d_t is the internal diameter of the falling head tube, and d_c is the internal diameter of the sample chamber.

Permeameter tests are most frequently conducted on disturbed samples that are easily obtained from commonly used drilling techniques. Disturbed samples can only produce accurate K results for uniform sands and coarse materials where the particles are spherical and therefore can pack uniformly in the permeameter column. Other sediment types are difficult to re-pack into a column to accurately reproduce the pore size distribution, connectivity of pores, packing anisotropy and bulk density in the aquifer, thereby rendering permeameter estimates inaccurate.

Conductivity values for heterogeneous materials can be obtained using intact cores of aquifer material and applying permeameter methods to these 'undisturbed' samples. Even when sample extraction is undertaken with the utmost care the act of sampling will disturb the sample to some degree, especially if cores are extracted from heterogeneous and unconsolidated formations. Disturbance will lead to inaccurate K estimates. Intact samples are predominantly obtained by coring vertically into a formation which leads to vertical conductivity being the most commonly generated parameter. Most sedimentary aquifers are anisotropic, therefore assuming isotropy may underestimate the horizontal conductivity when one measures the vertical conductivity. Generally, sediments are laid down with the long axis of particles horizontal to the ground surface resulting in reduced K values in the vertical as compared to the horizontal plane (anisotropic). To obtain more accurate horizontal conductivity values, vertical cores can be sub-cored horizontally to determine horizontal K.

To obtain accurate K estimates from permeameters, samples need to be completely saturated, excluding all air bubbles, before measurement is undertaken. Entrapped air will decrease the cross sectional flow area, reducing the measured K. Complete exclusion of air may only be achieved under vacuum in certain circumstances. Care must also be taken to minimise void space between the sample and container wall. This void space will lead to bypass flow on the edge of the permeameter, producing K values that are not representative of the sample. Edge effects are often minimised by employing a resin or paraffin wax to seal the annulus between the sample and the container wall (Cameron et al., 1990).

A major disadvantage of permeameter tests is the relatively small volume of aquifer interrogated per sample. A large number of cores need to be measured in order to obtain a representative distribution of the aquifer conductivity, especially if the aquifer is heterogeneous. Drilling multiple bore holes and conducting permeameter tests on each core may be prohibitively expensive. Even if a large number of samples are collected, Illman et al. (2008) reports that data collected from relatively small scales may not be indicative of formation properties that impact on flow and transport on a larger scale. Laboratory tests usually produce lower estimates of K values than comparable estimates from field tests (Rovey and Cherkauer, 1995). Hydraulic conductivity measured in a sandstone with permeameter tests, for example, gave a result of one thousandth the regional values (as measured by pump tests) (Rovey and Cherkauer., 1995). These scale effects are likely to be caused by fractures in consolidated material or permeable lenses in unconsolidated material that are not assessed when using small scale permeability measurements. Often these features are the primary contaminant transport mechanism in an aquifer system and therefore average K values may not be appropriate in interpreting contaminant scenarios. Permeameter test derived K values cannot be accurately scaled up and therefore should be used with caution when applied to contaminant transport applications.

Permeameter derived K values have been used to determine empirical relationships between grain size and K for use in grain size analysis. Allen-King et al. (1998) for example, used d_{10} as the representative grain size and calculated the C_h value in Equation 2.2 from permeameter tests. The resulting empirical formula was site specific and dependent on the accuracy of permeameter measurements.

2.1.3 Borehole Flow Meter Tests

The borehole flow meter test involves placing a flow meter within a well and measuring the water flow rate in the well as a function of the vertical position of the flow meter (Molz et al., 1989). This method is quick to perform and is ideal for measuring the relative vertical distribution of horizontal K values. It cannot measure the vertical conductivity of an aquifer and can by severely affected by well skin and annulus effects. Neglect of head loss across the borehole flow meter may lead to inaccuracies in horizontal K estimates (Zlotnik and Zurbuchen, 2003).

2.1.4 Slug Tests

In a slug test, the rate of rise or fall of a water column in a well is observed following a sudden, induced raising or lowering of the water column. The fall or rise of the water column in the well is usually achieved by either withdrawing or adding a known volume of water. Withdrawing or adding an equilibrated solid metal cylinder to the water column can also be used to generate a rise or fall in water level. A solution for calculating the K from a slug test using a point source piezometer was developed by Hvorslev (1951). Cooper et al. (1967) subsequently developed a procedure to interpret slug tests in confined aquifers with fully penetrating wells. These procedures plot the initial raised water level (H_o) divided by the height of the water level above the original water level as the water level falls (H) as a function of time on semi logarithmic paper. The ratio H/Ho equates to a defined function, available in tabulated form. The data are then matched to the function curves which possesses the same curvature. The value of time (t_1) on the vertical time axis which overlays the vertical axis for $Tt/r_c^2=1$ on the type curve is selected. Transmissivity (T) is calculated by Equation 2.6.

$$T = \frac{1.0 r_c^2}{t_1} \quad \textbf{(2.6)}$$

where r_c is the radius of the high conductivity zone associated with the well (if the gravel pack has a higher conductivity than the formation then a radius extending to the edge of the gravel pack should be used) and t_1 is the time determined from the H_o/H versus time plot.

Hydraulic conductivity is calculated from Equation 2.7.

$$K = T/b \quad \textbf{(2.7)}$$

where b is the aquifer thickness.

Additional slug test methods have been developed for specific aquifer configurations including the Bouwer and Rice (1976) method for fully or partially penetrating wells in unconfined aquifers and the Van der Kamp (1976) method for slug tests with under dampened responses.

The main disadvantage of slug tests is that only a small portion of the aquifer, immediately adjacent to the well, is interrogated to estimate K. The volume immediately adjacent to the well may not be representative of the aquifer K, because of bore hole construction artefacts and the influence of well skin. To prevent these disadvantages, appropriate well construction and thorough well development is crucial in obtaining an accurate K measurement from slug tests (Yang and Gates, 1997). The rise or fall of the water column should only be influenced by aquifer K and not the K of the screen or well pack. Slug tests consistently obtain lower K values than corresponding pump tests. As explained in Section

2.1.2 the larger the support volume and test period, the greater the influence high conductivity zones have on the result (Rovey and Niemann., 2001).

Slug tests that are performed in wells, rather than at a point sources isolated by well packers, produce a value of K averaged over the screen length, or uncased length of well, and therefore incorporate areas of high or low K that may be important in characterising an aquifer for contaminant transport studies.

Slow slug emplacement or withdrawal, insufficient displacement of water, disturbance of water level transducer cables and water waves caused by movement of the slug all impact on the reliability of slug tests, especially in high K aquifers. Levy et al. (1993) used pressure, instead of a mechanical slug to displace water in a well to alleviate some of the technical problems when conducting a slug test.

Slug tests are efficient and economic when compared to pump tests and the RWP system, and do not produce large amounts of potentially contaminated water. However, unless great care is taken performing slug tests, K estimates can be highly inaccurate (Sorensen et al., 2002).

2.1.5 Direct Push Methods

Direct push methods measure the *in situ* K of a formation using a screened rod that is inserted into aquifer material and through which slug test are performed. When a layer in which K measurements are desired is reached, water is injected and the flow rate though the screen and screen pressures are measured (Dietrich et al., 2008). Measurements can

also be made in hollow drill stem augers enabling estimation of K at depth (Sorensen et al., 2002). A ratio of flow rate and pressure are used as a proxy for K. These ratios can be converted to K estimates through a regression of K estimates determined from other methods. Advantages of this method include the fact that the layer sampled is not disturbed by a borehole or by the extraction of a sample, the tests are quick to perform and can estimate the vertical distribution of K. These methods do not require a permanently installed borehole. The accuracy of the method is dependent on the accuracy of the regression used. The aquifer volume that each test is measuring is small and therefore the method may produce an inaccurate estimate of the large scale K.

2.1.6 Borehole Dilution Tests

The borehole dilution test is a single well technique in which tracer is introduced into an isolated section of well and allowed to be transported out of that well by the natural hydraulic gradient. The concentration of tracer in the well is monitored over time. A mechanical mixer is required to achieve an initial uniform tracer concentration in the isolated section of well.

Freeze and Cherry (1979) estimated the groundwater velocity using a borehole dilution test (Equation 2.8).

$$V_a = \frac{W}{Ft}\ln\left(\frac{C}{C_o}\right) \quad \textbf{(2.8)}$$

where V_a is the Darcy velocity of the groundwater, W is the measuring volume of the well segment (the volume where dilution takes place), F is the cross sectional area of the measuring volume perpendicular to the direction of groundwater flow, C is the concentration of non-reactive tracer at time t, C_o is the introduced concentration of a non-reactive tracer at time 0, and t is the time since introduction of the tracer.

In practise V_a can be obtained from the slope of a plot of the natural log of C and t. Only the linear part of the dilution curve is used to calculate the groundwater velocity (Gaspar and Oncescu, 1972). If the hydraulic gradient (I) is known, Equation 2.9 can be used to calculate K.

$$K = \frac{V_a}{I} \qquad \textbf{(2.9)}$$

Borehole dilution tests require the effective porosity of the aquifer and a flow distortion factor for the well to be calculated in order to estimate K. The flow distortion factor describes the increase in flux of water through the well compared to the surrounding aquifer. This is due to the higher K of the filter pack and well annulus compared to the surrounding aquifer material (Palmer, 1993). In a similar way to the slug test results (Section 2.1.4), borehole dilution tests will be influenced by the K of material close to the well (well screen and annulus). Rigorous development of the well is needed to ensure the effects of well construction are minimised, although over development may lead to positive bias in K values. The well screen porosity should be similar to that of the aquifer to minimise the influence of the screen on the measurement.

As borehole dilution tests measure groundwater velocity at a specific site, the time required to complete these tests may be considerable. Borehole dilution tests performed in the vicinity of an extraction well require a shorter experimental time frame to complete as compared to an experiment measuring only natural groundwater velocity (Palmer, 1993). In these forced gradient borehole dilution tests the flow field is induced by an active pumping well and the velocity at the measuring point (injection well) is influenced by the K of the aquifer material between the observation well and the extraction well. An average of K over a larger area of aquifer, as compared to a standard borehole dilution test is achieved, minimising the influence of borehole construction effects. Disadvantage of this method over the standard borehole dilution test include the fact that two boreholes are required, and water is extracted from the aquifer, potentially requiring treatment if contaminated.

A velocity shadow downstream from a well may also effect bore hole dilution tests. A velocity shadow occurs when regional flow past the well is faster than flow directly down gradient of the well, over some distance (Leap and Kaplan, 1988). Borehole dilution tests measure velocity close to and downstream of the well and therefore a velocity shadow may have a significant effect. This can skew results from bore hole dilution tests that are conducted over a short period of time, if the tracer plume does not escape the influence of the well.

2.1.7 Emplacement and Pump Back Tests

The emplacement and pump back test is an extension of the borehole dilution test. A tracer is introduced into a well and allowed to 'drift' with the natural hydraulic gradient for a set time period before being pumped back to the well at a constant flow rate. The velocity of the tracer is then calculated as a function of the pumping time required to recover the tracer. Velocity is calculated from Equation 2.10.

$$v = \left(Qt_p / \pi bn\right)^{1/2} / t_* \qquad \textbf{(2.10)}$$

where v is the average linear velocity; Q is the pumping rate; t_p is the elapsed time between the start of pumping and when the centre of mass of the tracer curve is retrieved; b is the aquifer thickness; n is the effective porosity and t_* is the time the plume is allowed to drift.

If regional flow is significant over the time of pump back, Equation 2.11 can be used to calculate linear velocity (Leap and Kaplan, 1988).

$$v = \left[\left(Q/\pi nb\right)^{1/2} t^{1/2} \right] / T \qquad \textbf{(2.11)}$$

where v is the average linear velocity; Q is the constant pumping rate; t is the time the plume is allowed to drift; b is the aquifer thickness; n is the effective porosity and T is total time (time plume is allowed to drift plus pumping time).

For both methods K is determined from Equation 2.12.

$$K = \frac{vn}{I} \quad \textbf{(2.12)}$$

where v is the average linear velocity, n is the porosity and I is the hydraulic gradient.

A major advantage of this method is that the direction of groundwater flow does not need to be known before the test, as the tracer plume is returned to the injection well. The test is relatively quick to perform and requires minimal specialised equipment. The volume of aquifer that this method interrogates is dependent on the ratio of the regional groundwater velocity to the pumping flow rate. If the ratio is small the tracer plume can be allowed to drift a large distance away from the well minimising the effects of the well filter pack and skin on the calculated K.

Estimating the effective porosity and hydraulic gradient of the portion of aquifer the tracer is travelling through, especially if heterogeneous, may be problematic and lead to inaccuracies in the K values obtained by this method.

A modification of the drift and pump back method is the push pull method which involves pumping the tracer into the well instead of allowing the natural hydraulic gradient to move the tracer, before pumping it back. Injecting the tracer into the aquifer allows tests to be undertaken in a shorter time frame than natural gradient methods allow, especially in formations with low K (Pitterle et al., 2005).

2.1.8 Natural Gradient Tracer Tests

The conceptually simplest tracer method is the natural gradient tracer test. This method involves introducing a tracer into a well and monitoring one or more down gradient wells to obtain the travel time for the centre of mass of tracer. The travel time and distance between wells are used to calculate the average linear velocity of the groundwater. Equation 2.12 is then used to calculate K.

If an accurate estimate of groundwater flow direction is not known before well installation, an array of wells may be required to ensure interception of the tracer plume. In this case, the costs for well installation may be large. The accuracy of tracer tests can be compromised by indistinct breakthrough curves or poor recovery of the injected tracer if observation wells are not positioned appropriately along the tracer flow path.

The travel time of a tracer may be prohibitively large if wells are not spaced appropriately apart. If an estimate of the effective velocity in the aquifer is not known beforehand, frequent sampling may be required to insure definition of the tracer peak. Close et al. (2002) developed a technique to estimate flow direction and velocity without frequent sampling. The method involves placing permeable bags of resin that absorb tracer (rhodamine WT) in down gradient wells. Tracer is then released in an up gradient well and the resin bags observed at relatively large time periods to determine the direction and approximate velocity of groundwater. The major advantage of this method is that a number of wells and well depths can be sampled simultaneously with little cost. The groundwater velocity estimate and hence K could then be refined with a targeted sampling regime.

Tracer concentration curves obtained from natural gradient tracer tests may provide detail of other aquifer properties such as heterogeneity and dispersivity. Natural gradient tracer tests provide the most accurate estimate of K for contaminant transport studies because the tracer mimics contaminant movement within the aquifer. If the aquifer is heterogeneous the tracer will follow preferential flow paths generating larger average K values than other methods.

The hydraulic gradient is needed to calculate the K values from tracer tests. If the aquifer is heterogeneous it may be difficult to obtain hydraulic head values from the transporting portion of the aquifer in isolation. Piezometers generally provide an underestimation of the hydraulic gradient transporting the contaminant as they average the hydraulic head across the entire length screen. Piezometers measuring a point within the transporting portion of the aquifer will produce a more accurate hydraulic gradient but are difficult to install precisely.

Also, hydraulic gradient may be difficult to measure accurately from wells spaced closely together, as they may be in tracer tests, because the error in measuring water level is often comparable to the difference in water level between closely spaced wells.

Again, a measurement of the effective porosity is also required to calculate K from a tracer test. This is difficult to determine and often an estimate is used which reduces the accuracy of the K value obtained from tracer tests.

2.1.9 Forced Gradient Tracer Tests

Forced gradient tracer tests are performed by pumping or injecting water into, or out of a well in the aquifer system to create a steep hydraulic gradient. Once the system reaches steady state a tracer test is performed. The tracer test can be performed in a number of configurations. These include releasing tracer in an up gradient well and observing in the pumping well, releasing the tracer in an up gradient well and observing the tracer in one or more down gradient observation wells or releasing the tracer in an injection well and observing the plume in down gradient observation wells or well. As with natural gradient tracer tests, travel time and distance between wells are used to calculate the average linear velocity of the groundwater and then Equation 2.12 is used to calculate K.

The steep hydraulic gradient created in a forced gradient tracer test increases tracer velocity resulting in completion of experiments in a shorter time period when compared to natural gradient tracer tests, especially in aquifers with low K. Pumping of a down gradient well during a tracer test also lowers the uncertainty in flow direction. This means that less wells could be potentially installed as compared to a natural gradient tracer test to intercept the plume.

A variation on a single well forced gradient tracer test is the double forced gradient tracer test. These tests are performed by pumping a down gradient well and injecting water into an up gradient well (usually water sourced from the down gradient well) (Grove and Beetem, 1971). An alternative method involves pumping the down gradient well, disposing of the resulting water, and injecting fresh water into the up gradient well. In both methods the system is pumped until steady state is achieved and then a tracer is introduced into the injection well and monitored at the extraction well. Ideally all tracer injected in the

upstream well is captured by the downstream well forming a closed cell. Recirculation of water eliminates the need to source injection water and to dispose of potentially contaminated extraction water. This system is similar to a RWP system with one half of the circulation system running along the surface (in a pipe) rather through the aquifer as in the RWP system. This system has been used to determine natural attenuation rates in an aquifer for such contaminants as nitrate. Double forced gradient tracer tests can be interpreted with numerical models.

Vandenbohede and Lebbe (2006), conducted a double forced gradient tracer test while measuring drawdown data simultaneously. The aim was to combine the benefits of pump and tracer tests and to eliminate the drawbacks in determining aquifer hydraulic properties. Drawdown observations are sensitive to specific elastic storage, concentration observations are sensitive to dispersivity and effective porosity and both are sensitive to vertical and horizontal conductivity (Vandenbohede and Lebbe, 2006). It was shown that combining these observations derived more reliable estimates of aquifer parameters than if one data set was used. Similarly the RWP method produces both drawdown and concentration data but these data are not combined in this study. If separate data sets are combined to generate more accurate hydraulic parameters, weighting of the data may be required if the goal of the analysis is to study contaminant transport or aquifer quantity.

2.1.10 Specific Capacity Tests

Specific capacity data can be used to estimate the K of an aquifer. Specific capacity data are generated from pumping a well and observing the drawdown at several measured flow rates. These observations are routinely undertaken in water production wells to gauge the

optimal production pumping rate and positioning of the pump. The majority of commercial wells drilled will possess specific capacity data from which an estimate of K can be made. Specific capacity (SC) is calculated from Equation 2.13.

$$SC = Q/(h_0 - h) \tag{2.13}$$

where Q is the pump flow rate and h_o-h is the drop in water level at that flow rate.

Theis et al. (1963) first proposed a method to estimate T and therefore K (if aquifer thickness is known) from specific capacity data. The Theis method has several disadvantages, firstly, storativity has to be estimated, and secondly it assumed that the well is 100% efficient. The Theis method uses Equation 2.14 to calculate transmissivity.

$$T = \frac{Q}{(h_o - h)} \frac{2.3}{4\pi} \log \frac{2.25Tt}{r^2 S} \tag{2.14}$$

where T is transmissivity, Q is flow rate, $(h_o$-$h)$ is the change in head of the well, t is the length of time the well is pumped, r is the radius of the pumping well and S is the storativity.

This equation is solved by measuring the change in head over time and then estimating the T (or T and S simultaneously) by fitting the drawdown versus time curve. T is then adjusted to obtain a calculated value of specific capacity close to that of the measured value.

Razack and Huntley (1991) found that this method generally under estimated the value of T, due to turbulent well losses. Razack and Huntley (1991) devised an empirical relationship from known T values (from pumping tests) and the associated specific capacity measurement. For an alluvial ground water basin in Morocco the relationship in Equation 2.15 was determined.

$$T = 15.3\left(\frac{Q}{h_o - h}\right)^{0.67} \quad \textbf{(2.15)}$$

where T is the transmissivity, Q is the pumping rate and h_o-h is drawdown (m).

This relationship has a correlation co-efficient of 0.63. Additional authors have developed empirical relationships for other groundwater systems (Bal, 1996; Mace, 1997). These empirical relationships are system and site specific as demonstrated by an increasing correlation co-efficient as the area that the relationship is calculated from decreases. Hydraulic conductivity can be determined from Equation 2.7. K derived from empirical relationships and specific capacity data are inaccurate and therefore not suitable for contaminant transport studies.

2.1.11 Pump Tests

A pump test is conducted by extracting water from a pumping well at a constant rate and observing drawdown in observation wells at a distance from the pumping well. Two types of pumping tests are utilized to calculate T; steady state, where the pumping continues until a steady state is approached in the observation wells, and transient, where water level drop in observation wells is measured with time. Transient pump tests are more common

because steady state conditions are rarely obtained in practical time periods. Many analytical solutions to interpret pump tests are available and these operate under a variety of assumptions according to the geological setting (Fetter, 2001; Bouwer, 1978).

Steady state methods to evaluate K are based on the Theim equation (Equation 2.16).

$$T = \frac{Q \ln(r_2 / r_1)}{2\pi(s_1 - s_2)} \quad \textbf{(2.16)}$$

where T is the transmissivity, Q is the pumping rate, and s_1 and s_2 are the measured draw downs at the radial distance from the pumping well of r_1 and r_2 respectively.

Hydraulic conductivity can be calculated by dividing T by the aquifer thickness (Equation 2.7). Theoretically, the water level in observation wells will never reach equilibrium but they may approach equilibrium sufficiently to obtain a reasonable estimate of K.

A mathematical analysis of the transient effects of drawdown in an idealised confined aquifer was produced by Theis (1935). Equation 2.17 is adapted from this analysis.

$$T = \frac{Q}{4\pi(h_0 - h)} W(u) \quad \textbf{(2.17)}$$

where Q is the pumping rate, h is the hydraulic head after pumping, h_o is the initial hydraulic head, T is the transmissivity, and $W(u)$ is the well function which can be found in well function tables (Wenzel, 1942).

A graphical method has been developed to calculate the transmissivity which involves plotting the well function versus *1/u* on log-log paper (type curve). Then the drawdown versus time is plotted on log-log paper and superimposed onto the type curve. Arbitrary match points of *W(u), 1/u*, drawdown and time are determined. These values together with the pumping rate and radial distance are then substituted into Equation 2.17 to calculate T. Transmissivity values are converted to K by using Equation 2.7. Variations on curve matching technique can be used for a variety of other aquifer geometries (e.g. leaky aquifers, unconfined aquifers) (Fetter, 2001). Numerous commercial computer programs are available to analyse pump tests to obtain aquifer parameters as well as non-commercial analysis packages such as Function.xls (Hunt, 2005).

The accuracy of pump tests is dependent on a number of assumptions being meet including bounding of the aquifer on the top and bottom with a confining layer, infinite lateral extent, homogeneous aquifer, and Darcy's law being valid (Fetter, 2001). All assumptions are rarely met in real situations. Vandenbohede and Lebbe (2003) state that pump tests tend to overestimate K of a measured permeable layer. This overestimation is cause by the underestimation of water contributed from layers bounding the permeable layer. Measurements can also be inaccurate if clogging or corrosion of screens occurs or if there was incomplete development of the well.

Pump tests average K values over a large and representative aquifer volume. This averaging will not identify higher K zones that are important in contaminant transport if the aquifer is heterogeneous in nature. Pump tests do not yield the vertical conductivity of the aquifer.

Pump tests can produce non-unique estimates of K if the aquifer geometry is not well defined. Pump test drawdown curves may match several type curves of differing aquifer geometries resulting in uncertainty of the true aquifer K value if aquifer geometry is not known.

Pump tests also produce large quantities of water, and disposal of this water, if contaminated, may be expensive. Installing pumping wells and observation wells and running pump tests is also costly.

Studies have been undertaken using both pumping tests and tracer tests to obtain a more accurate understanding of the distribution of K within an aquifer (Dann et al., 2008). Studies that compare pumping tests to tracer tests have concluded that the different tests average K zones in the aquifer differently resulting in differing estimates of K (Neimann et al., 2000; 2005; Thorbjarnarson et al., 1998). Pump tests are three dimensional and therefore average heterogeneous K distributions arithmetically whereas tracer tests are two dimensional and therefore average heterogeneous K distributions geometrically. This results in lower K values for tracer tests as compared to pump tests. This has implications when we compare the RWP system derived K values with K values derived from tracer tests. Further discussion on this topic is undertaken in Chapter 4.

2.1.12 Dipole Flow Tests

The dipole flow test (DFT) creates a vertical recirculation system in a single well and is used to estimate horizontal and vertical conductivity of the adjacent aquifer material. The recirculation cell is formed by isolating an injection and extraction screen section with impermeable packers and then pumping between sections (Figure 2.2).

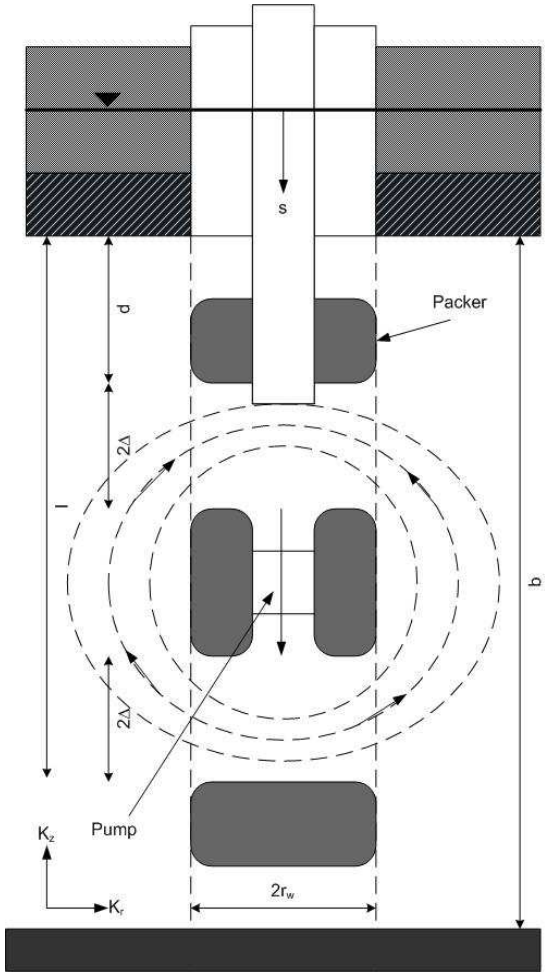

Figure 2.2: Schematic of the dipole flow test (adapted from Kabala, 1993).

No water is withdrawn or added to the aquifer in this method. Hydraulic conductivity is estimated by measuring the head changes in the two dipole screens. Kabala (1993) developed solutions for transient analysis of DFT's and Zlotnik and Ledder. (1996) developed analytical solutions from steady state head draw downs. Sutton et al. (2000) analysed the addition of a tracer to the DFT that enabled the anisotropy ratio to be more accurately defined and an estimate of longitudinal dispersivity to be obtained. Sutton et al. (2000) also used a stream tube approach to semi analytically model the peak arrival and centre of mass for the tracer in the system.

Zlotnik and Zurbuchen (1998) found that in a homogeneous aquifer the head differences between the upper (S_U) and lower ($|S_L|$) DFT screen $h = S_U + |S_L|$ can be used to estimate K of an aquifer (Equation 2.18).

$$K_{\Delta h} = \frac{2Q}{\Delta h} f_i \qquad \textbf{(2.18)}$$

where Q is the pumping rate, h is the head difference between chambers, Δ is half the length of the screen and f_i is a shape factor.

This yields the K estimate that is characteristic of the DFT support volume which extends radially and vertically on the order of several times the distance between the screens from the well. If the aquifer is heterogeneous the magnitude of the head in each chamber can be different and in such cases the DFT can yield a higher resolution of K by interpreting each chamber separately using Equation 2.19.

$$K_U = \frac{2Q}{\Delta S_U} f_{U,} K_L = \frac{2Q}{\Delta |S_L|} f_L \qquad \textbf{(2.19)}$$

where the shape factors depend on the hydrogeological setting and the dipole probe geometry. Generally $f_U = f_L = f_i$ when aquifer boundaries do not affect the DFT.

The DFT emphasises vertical flow which provides good resolution of K anisotropy ratio. Johnson and Simon (2007) conducted tracer tests to evaluate the DFT method for aquifer

remediation and determined that much of the flow was occurring close to the dipole. The small scale of the test especially in the horizontal direction may result in horizontal K values that are not applicable to contaminant transport modelling. The small support volume may also result in a large influence of well skin and short circuiting of flow through the well annulus. Kabala (1993) states that meticulous well development and/or specialist well installation may be needed to remediate this problem.

Like the borehole dilution test and flow meter test, vertical profiles of horizontal conductivity can be gained by running sequential DFTs on different portions of the aquifer by altering the position of the dipole flow apparatus.

2.2 Recirculating Well Pair System.

The first application of RWP systems were for *in situ* aquifer remediation. The RWP system establishes a recirculation zone between the two pumping wells. When a chemical or biological remediation agent is added to the RWP system an *in situ* treatment zone is created. Recirculation allows multiple passes through the reaction zone enabling efficient remediation. The technology has been successfully used to stimulate bioremediation of contaminated groundwater (McCarty et al., 1998; Gandhi and Kitanidis, 2002). Christ et al. (1999) developed a two dimensional analytical model that defined the relationship between capture zone, interflow, and treatment efficiency for the RWP system for given environmental and design parameters (e.g. distance between pumping wells, flow rate, natural groundwater velocity). Cunningham et al. (2004) extended the work of Christ et al. (1999) by estimating the fraction of captured water that was recycled between the wells, and the travel time distribution in the recirculation zone also using a two dimensional

model. Cirpka et al. (2001) and Gandhi and Kitanidis (2002) used numerical models to investigate the RWP system. A three dimensional analytical solution for steady state flow in a homogeneous, anisotropic contaminated aquifer was then developed to calculate the interflow between wells and to map the capture zone of the RWP system (Huang and Goltz, 2005).

Goltz et al. (2008) proposed two methods for determining K from RWP systems:

- the multi-dipole method
- and the fractional flow method

The multi-dipole method is an extension of the method used by Kabala (1993), Zlotnik and Ledder (1996) and Xiang and Kabala (1997) for the DFT (Section 2.1.12). The fractional flow method uses a tracer test to determine the interflow between the two dipoles. The interflow is directly related to the K of the aquifer.

This section describes the modelling processes employed to determine the K of an artificial aquifer from the RWP system. A brief outline of how these methods were developed is followed by a description of the two methods used to obtain K in this study. In addition, the method of inverse modelling to determine the results is described

2.2.1 Multi Dipole Method

The analytical model for the multi-dipole method was developed by Christ et al. (1999) and Huang and Goltz (2005) to simulate the complex flow patterns generated by a RWP system for use as a contaminant remediation technology. This method was extended to measure K using a RWP system (Goltz et al., 2008) and to measure contaminant mass flux in groundwater (Goltz et al., 2009).

Goltz et al. (2008) utilises the theory of superposition to extend the analytical solutions obtained by Kabala (1993), Zlotnik and Ledder (1996) and Xiang and Kabala (1997). The principle of superposition states that if there are several pumping sources or sinks in an aquifer system, the effects of these sources or sinks on the total hydraulic head at any point in the system are additive (Bouwer, 1978). In simpler terms, if water is pumped (or injected) from several wells in a single aquifer, the drawdown (or mounding) at any point in the aquifer is calculated as the sum of the draw downs (or mounding) at that point caused by each individual pumping (or injection) well. Thus the draw downs at any point in the aquifer can be calculated by summing the draw downs caused by each injection and extraction screen in the RWP system.

Goltz et al. (2008) formulated a solution for the multi dipole test that may be applied to determine horizontal and vertical hydraulic conductivities using a RWP system with both wells pumping. At steady state in a confined aquifer of infinite lateral extent, recognising that there is no net extraction or injection of water into the system, the governing equation (Equation 2.20) and boundary conditions (Equation 2.21a-c) can be expressed as:

$$k_r \frac{1}{r_i} \frac{\partial}{\partial r} \left(r_i \frac{\partial s_i}{\partial r_i} \right) + k_z \frac{\partial^2 s_i}{\partial z^2} = 0, \; i = 1, 2, \ldots N_w \qquad \textbf{(2.20)}$$

$$\frac{\partial s_i}{\partial r_i} = \begin{cases} Q_i / [2\pi r_w k_r (z_t^i - z_b^i)], & z_b^i \le z \le z_t^i \\ 0, \; otherwise \end{cases}, \; r_i = r_w \qquad \textbf{(2.21a)}$$

$$\sum_{i=1}^{Nw} s_i = 0, r_i \to \infty \qquad \textbf{(2.21b)}$$

$$\frac{\partial s_i}{\partial z} = 0, z = 0, b \qquad \textbf{(2.21c)}$$

where $s_i(r, z)$ is the drawdown from the operation of the i^{th} well screen (s_i >0 for drawdown; s_i <0 for mounding, i= 1,2, …N_w); N_w is the number of well screens (extraction plus injection); r_i is the radial co-ordinate with respect to the i^{th} well screen; z is the vertical co-ordinate with respect to the lower confining layer of the aquifer; Q_i is the pumping rate of well I (Q_i >0 for injection; Q_i<0 for extraction); z_t^i and z_b^i are the vertical co-ordinates of the top and bottom, respectively, of the i^{th} well screen; r_w is the radius of the i^{th} well; and b is the thickness of the aquifer.

Figure 2.3 illustrates the parameters used in Equations 2.20 and 2.21a-c.

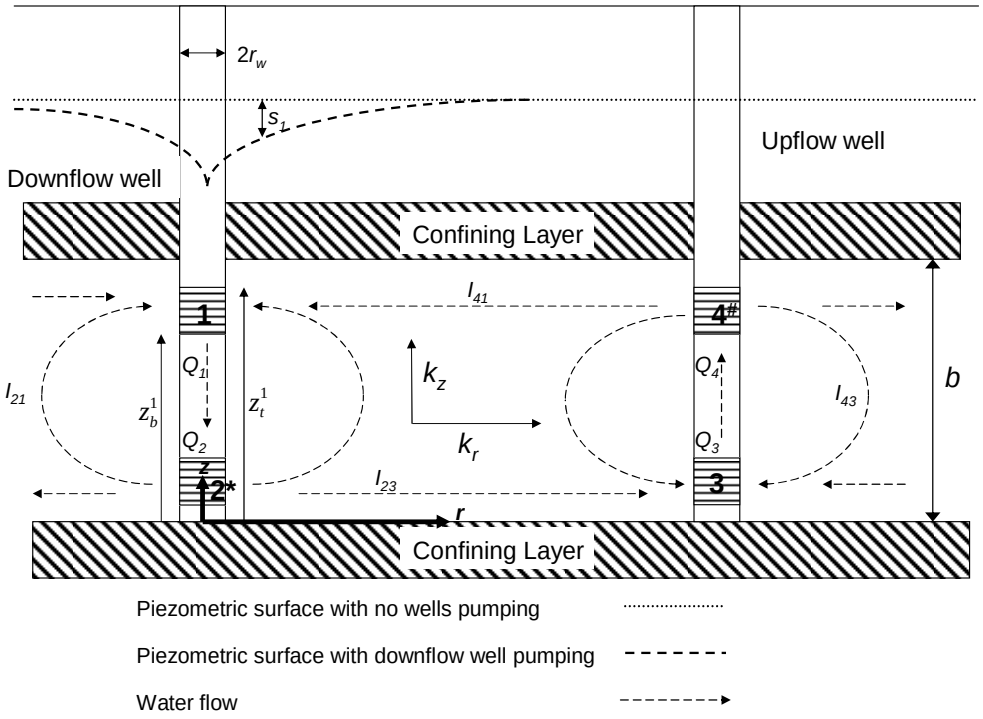

Figure 2.3: Schematic of the flows during the operation of a Recirculating Well Pair (Goltz et al. 2008). Where r_w=well radius, s_1=drawdown, b=aquifer thickness, Q_{1-4} = pumping rates of the well screens, $I_{(i,i)}$ = fractional flow between well screens, k_z=vertical K, k_r=horizontal K, Z_b^n and Z_t^n = coordinates of the top and bottom of well screen n.

Goltz et al. (2008) then solved Equations 2.20 and 2.21a-c for the drawdown at any point (x, y, z) for N_w partially penetrating wells (the four screens of the recirculating well pair system).

The RWP system was trialled in an artificial aquifer and therefore Goltz et al. (2008) also modified the equation to reflect the conditions encountered in this aquifer. A description of the artificial aquifer can be found in Section 3.1. The modifications incorporated constant head boundaries at the up and down gradient constant head chambers and no flow boundaries at the sides of the aquifer. The no flow boundaries and constant head boundaries were incorporated into the model by placing imaginary wells symmetrically on the opposite side of the boundary as the real wells, and having these wells pump or inject

water at an identical flow rate as the actual wells. In the artificial aquifer the pumping wells are surrounded on four sides by boundaries, therefore an infinite number of image wells are needed to simulate this situation. With the positions of the image wells determined, the drawdown at any point in the system can be calculated by superposition. Superposition can also be used to account for a sloping piezometric surface with the calculated piezometric surface prior to pumping being subtracted off the surface calculated during pumping. Goltz et al. (2008) incorporated an infinite number of image wells and generated the formula for the drawdown (*s*) at the spatial co-ordinates *x,y,z (s(x,y,*z)).

To increase the accuracy of the method, heads were measured at various points in the RWP system. Heads were also measured at various pumping rates to determine the effect on K estimation. Hydraulic conductivity values were then substituted into the formula (Goltz et al. 2008) and hydraulic head estimates for each observation point *(s(x, y, z))* were determined. The resulting set of calculated hydraulic head values are compared to the set of measured head values. This process is then repeated with another K value until the measured and calculated hydraulic head values attain the best match. An objective function was used to obtain the best match (Equation 2.22).

$$F_{obj} = \frac{1}{1 + \sum_{i=1}^{N} \left(H^{i}_{meas} - H^{i}_{calc} \right)^2} \qquad \textbf{(2.22)}$$

where H^{i}_{meas} and H^{i}_{calc} indicate the measured and calculated hydraulic heads at the i^{th} flow rate, and *N* is the total number of head measurements.

This process would take a prohibitively large amount of computing time to maximise the objective function if the routine was choosing values of K randomly and without direction. Therefore a genetic algorithm is used to evaluate the objective function. The genetic algorithm is described in Section 2.3.

2.2.2 Fractional Flow Method

The fractional flow method is based on measuring the interflow between the four screens in a RWP system with a tracer test (Goltz et al., 2008). The interflow is determined by measuring the proportion of tracer from each injection screen (two tracers were used) that reach the two extraction screens when the system reaches steady state. With known fractional flow between screens, well injection and extraction rates, and system dimensions, an inverse three dimensional flow model can be used to estimate values of horizontal and vertical K.

Fractional flow is defined as the fraction of flow entering an extraction screen that originated in an injection screen. For example, I_{ij}, is the fraction of water being drawn into the j^{th} extraction screen that originated in the i^{th} injection screen. The fractional flow depends on four parameters:

- geometry of the recirculating wells: the closer the extraction and corresponding injection screens are together the greater the fractional flow
- pumping rates of the wells: the greater the pumping rate the higher the fractional flow

- regional gradient: the greater the gradient the less fractional flow occurs because a greater proportion of tracer travels downstream of the recirculating well pair system.
- magnitude of site heterogeneity
- hydraulic conductivity of the aquifer material

In the experimental RWP system, the first three of the above parameters can be measured accurately; therefore the K of the aquifer formation is the only unknown in the system because the artificial aquifer was assumed to be relatively homogeneous. In a field situation, the heterogeneity of an aquifer may not be well characterised and therefore an 'average' K for the aquifer will be determined.

If we introduce tracer A into the up flow well and tracer B into the down flow well, assume steady-state, and apply a mass balance at each of the well screens, we obtain four simultaneous equations (Equation 2.23a-d).

$$A_1 I_{12} + A_4 I_{42} = A_2 \quad \textbf{(2.23a)}$$

$$B_1 I_{12} + B_4 I_{42} = B_2 \quad \textbf{(2.23b)}$$

$$A_1 I_{13} + A_4 I_{43} = A_3 \quad \textbf{(2.23c)}$$

$$B_1 I_{13} + B_4 I_{43} = B_3 \quad \textbf{(2.23d)}$$

where A_i is the concentration of tracer A measured at the i^{th} well screen, B_i is the concentration of tracer B measured at the i^{th} well screen and Iij represents the fraction of water being drawn into the j^{th} extraction screen that originated at the i^{th} injection screen.

Figure 2.4 illustrates the fractional flow between screens used in Equations 2.23a-d.

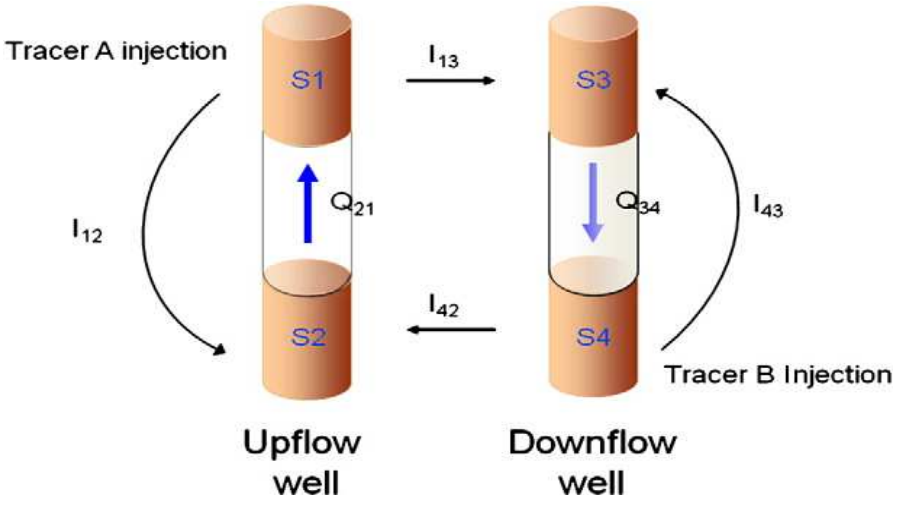

Figure 2.4: Recirculating well pair fractional flow (Adapted from Goltz et. al., 2009).

If we measure the concentrations of tracers A and B at the injection and extraction screens of both wells in the system we can solve the four simultaneous equations with the unknowns being the fractional flows (I_{21}, I_{23}, I_{41} and I_{43}). Knowing the four fractional flow values, we then use an inverse numerical model to estimate the K value. Flow rates, screen and well spacing were determined in such a manner as to guarantee a proportion of tracer travels laterally and not 100% vertically.

To calculate K values an assumed K value is generated and MODFLOW (Harbaugh, 2005) is used to calculate the hydraulic head and flow velocity field resulting from operating the RWP system at steady state. The particle tracking program MODPATH (Pollock, 1989) is

then used to obtain the proportion of particles that originate at an injection screen that terminate at each extraction screen (interflow). The proportions of simulated particles calculated in MODFLOW are then compared to the measured interflows for each screen and tracer. An objective function was then defined (Equation 2.24).

$$F_{obj} = \frac{1}{1 + \frac{1}{N}\sum_{i}^{Ninj}\sum_{j}^{Next}\left|I_{ij}^{meas} - I_{ij}^{calc}\right|} \quad \textbf{(2.24)}$$

where I_{ij}^{meas} and I_{ij}^{calc} are the measured and calculated fractional flows, respectively, N_{inj} and N_{ext} are the number of injection and extraction screens respectively, and N is the total number of well screens.

The goal is to find the value of K that maximises the objective function. As with the multi dipole approach, a GA is used to efficiently find the value of K that maximises the objective function.

2.3 Genetic Algorithm

A genetic algorithm (GA) developed by Carroll (1996) was used to determine values of horizontal and vertical K that maximised the objective functions (F_{obj}) for both the multi dipole and fractional flow methods.

There are three main methods used to search a parameter space for a set of parameters that match observed data: calculus based, enumerative and random (Carroll, 1996). Calculus based methods search the local area adjacent to the initial starting point for the optimal

value and have no facility to expand the search once an optima is reached. If the search area has local optima as well as a global optimum, calculus based methods may get 'stuck' on local optima. This means that they are not robust enough to search a complex and multimodal environment such as the one that characterises the problem encountered in this thesis. Enumerative methods evaluate every point in the search space one at a time, guaranteeing that the global optima will be found. In a large search space, as we have in this problem, the time and computer power needed to search the entire parameter space would be prohibitive and therefore this method is not suited to this problem. Random search algorithms search the parameter space in a random but not directionless process. Genetic algorithms are a random search tool.

Genetic algorithms are a random search technique developed by Holland (1975) and belong to the family of non-formal optimisation techniques. Genetic algorithms have the advantage over more formal optimisation methods of favouring good solutions while allowing the search to continue in a random manner beyond the bounds of the local optima. Genetic algorithms are based on Darwinian evolution. As discussed further, below, a population of individuals is manipulated by cross–over, random mutations and the survival of the fittest (elitism) for several generations until the population converges on a superior solution.

Genetic algorithms initially produce a random population of individuals created from parameters in the parameter space and each individual is assigned a fitness value. These individuals of different parameters can be thought of as strings of different alleles, similar to chromosomes. In the present study, the parameters are individual K estimates. Fitter individuals obtain higher objective function (F_{obj}) values, meaning that the calculated head

or interflow values are a closer match to the observed values. The fittest individuals from the initial population are retained and placed in a mating pool while the less fit individuals are ‘killed off’. The surviving individuals are randomly mated within the mating population and a random cross–over location on the string is assigned. Mating between two strings takes place with a probability that is defined in the GA set-up parameters (Pcross). The ‘children’ of fit individuals will have characteristics contained in both ‘parents’. The mating population is then ‘killed’ except for a small number of the very fit individuals (elitism). Elitism is an operator that ensures that the chromosome set of the fittest individuals are retained in subsequent populations. After a population is generated, a check is undertaken to insure that the fittest individual from the previous generation is retained. If it is not, then the chromosomes of the best individual in the previous generation is mapped into a random individual of the present generation.

Parents are replaced by children plus elitists in the next population. Before this replacement occurs a small proportion of the population will be mutated with a defined probability (Pmutate), adding new characteristics into the population. These mutations correlate to searching a new random area of solution space thereby avoiding local optima in the search area. Much like natural selection the overwhelming majority of mutations are less fit than the original ‘parent’ and therefore will be ‘killed off’ in the next generation, but occasionally an increase in fitness of an individual will occur. A flow diagram of the process used for the GA for this study is shown in Figure 2.5.

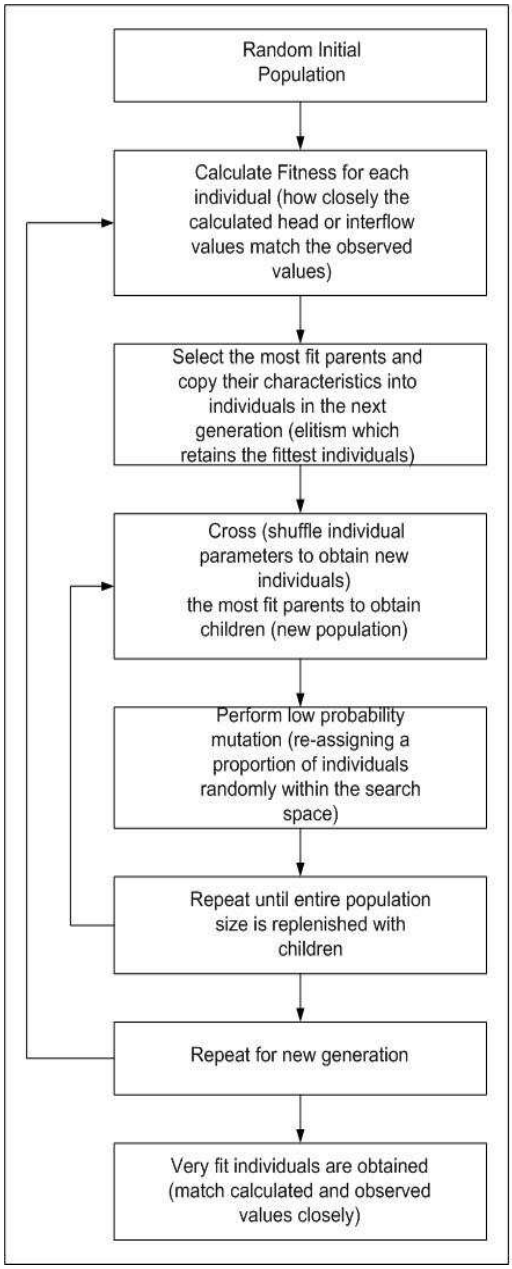

Figure 2.5: Flow diagram of the Genetic Algorithm procedure.

Genetic algorithms are an aggressive search technique, and could quickly converge to a local optima if it were not for mutations that maintain diversity (Cieniawski et al., 1995). This is because GAs rapidly eliminate strings with poor fitness until all individuals are identical resulting in a population that lacks diversity. Figure 2.6 illustrates the output of a typical GA from the present study. It can be seen that by the 14^{th} generation, the best fitness of the population is not increasing and that the average fitness is approximately

equal to the best fitness. This indicates that diversity in the population is low and therefore a local optimum has been reached. A mutation event occurs at generation 38 introducing new alleles into the population. Most of the new combinations were less fit than the best fitness value obtained so far, but crosses of the new individuals with the old have produced individuals of better fitness by generation 46. Therefore the mutation introduced some alleles that had a greater fitness than the previous generation. This cycle of introducing mutations continues but in this example further mutations are producing little or no advantage over previous generations. This study has limited the GA runs to 200 generations as little change in the fitness was achieved by continuing the algorithm.

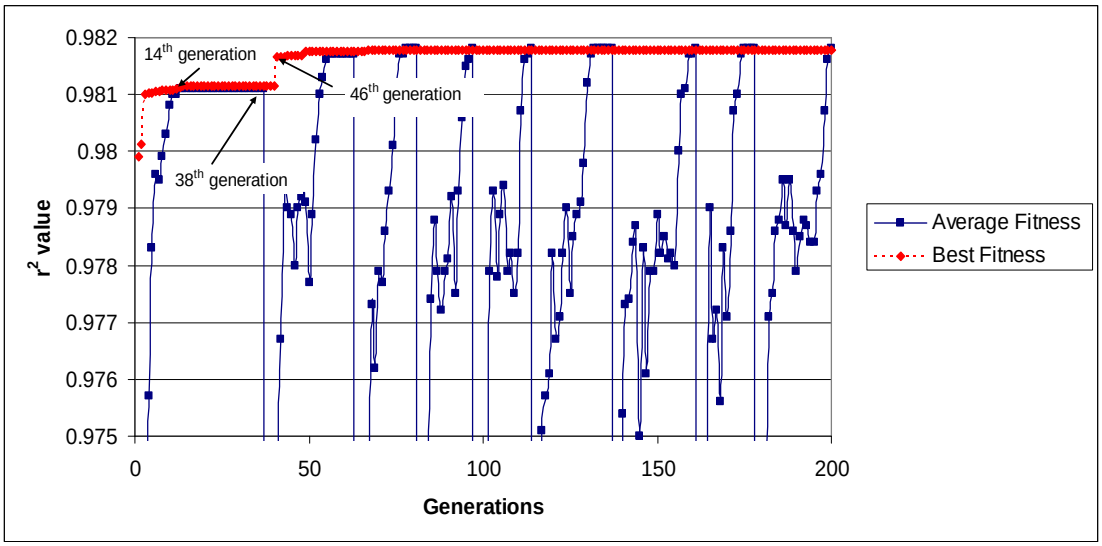

Figure 2.6: Genetic Algorithm output average r^2 and best r^2 vs number of generations.

The R squared value in the case above has not matched the observed values precisely (r^2 not equal to 1). This may mean that the GA, with more searching (greater number of generations) may locate a more optimal solution, that our model is imprecise in some aspect, or that there is measurement error in our observations.

Using cross-over and mutation to maintain and increase individual fitness renders GAs intrinsically more computationally efficient than total enumeration (Cieniawski et al., 1995). The retaining of fit alleles means that not every search space has to be evaluated. But if the mutation rate is too high and becomes the primary search technique then the benefits of the efficiency gains of the GA are diminished because every search space will need to be evaluated.

The handling of constraints is one shortcoming of the GA method. Cieniawski et al. (1995) state that constraints can be included by clever formulation which uses the length of the string as a constraint or which limits the values which can be placed within the strings alleles. Penalty functions are more commonly used. These assign poor fitness to strings that violate constraints. In the GA used in this project (Carroll, 1996) the search space is confined by inputting minimum and maximum values for vertical and horizontal K. If the string does not correspond to a value within the range of the parameter space, the individual is randomly reassigned within the range, rather than being assigned a poor fitness. To limit the search area, horizontal K was limited to 10 to 300 m/d based on previous experimental work undertaken in the artificial aquifer (Close et al., 2008) and results determined in Section 4.1.

Cieniawski et al. (1995) also cites the large number of function evaluations that need to be performed as a disadvantage of GAs. For each generation the performance of each string (individual) must be evaluated which can be very time-consuming and is often the limiting operation of the GA. This evaluation, although slow, is faster than evaluating the entire search space, as carried out with enumerative methods.

3. Description and Modelling of the Artificial Aquifer and Recirculating Well Pair System

This chapter describes the equipment and methodology used to estimate hydraulic conductivity (K) using the recirculating well pair (RWP) method. Experiments were carried out in an artificial aquifer enabling the complete control of aquifer parameters and the independent determination of K. A description of the artificial aquifer is presented in Section 3.1. An outline of previous studies that determined the K of the artificial aquifer is given in Section 3.2. The RWP system is described in Section 3.3. Section 3.4 describes the methodology used for each of the experiments undertaken in this study. Finally, Section 3.5 outlines the modelling procedures used to simulate the RWP system within the artificial aquifer and the genetic algorithm (GA) used to optimise the K values.

3.1 Artificial Aquifer Description

All RWP experiments were conducted in a large scale three-dimensional artificial aquifer at Lincoln University, New Zealand. The artificial aquifer was 9.5m long, 4.7m wide and 2.6m deep and was uniformly packed with sand of medium grain size (0.6-1.18mm). The bulk density of the aquifer material was estimated by dividing the mass of sand placed in the aquifer by the aquifer's volume resulting in an average bulk density of 1490 kg/m^3. Total porosity was estimated from the bulk density and a particle density of 2650 kg/m^3 (Equation 3.1).

$$n = 100[1 - \rho_b / \rho_d] \quad \textbf{(3.1)}$$

where n is the total porosity as a percent, ρ_b is the bulk density and ρ_d is the particle density.

Total porosity of the artificial aquifer was calculated to be 44%. Although efforts were made to achieve homogeneous packing of the aquifer during construction, some variation in sand density within the aquifer exist. This was demonstrated by Bright et al. (2002) with a tracer test that determined that there were differing K values throughout the artificial aquifer.

Water used for the aquifer was sourced from a well screened at approximately 85m depth. The water, when withdrawn from the well, was close to saturated with air. This was a concern as previous studies determined that dissolved air coming out of solution (forming air bubbles) blocked pore space within the aquifer affecting K values (Close et al., 2008). However, the problem was solved by the construction of a de-aeration tower which stripped dissolved air from the water before entering the artificial aquifer. Air entrapment in the aquifer before the tower was built may have changed the K in some areas of the aquifer permanently. All experiments in this study were carried out after the de-aeration tower was constructed.

Constant head tanks, located at the up gradient and down gradient boundaries of the aquifer, were used to maintain a constant gradient across the aquifer. A weir system was used to adjust this gradient as desired (Figure 3.1). The base and sides of the aquifer were constructed of impermeable material (butyl rubber on concrete). Upstream and downstream walls, facing the header tanks were constructed of permeable material allowing uniform flow of water, to and from the aquifer. The aquifer material was covered

with an impermeable liner to form a confined aquifer and a thick gravel layer was deposited on the liner to prevent the liner lifting with large water pressures (Figure 3.2a). The water levels in both constant head tanks were maintained at a higher level than the top impermeable layer, rendering the aquifer confined. Water input into the aquifer was monitored over the course of the experiments with a logged flow meter. The aquifer operated as a closed system except for the flow input and output at either end, therefore the aquifer is a steady-state system.

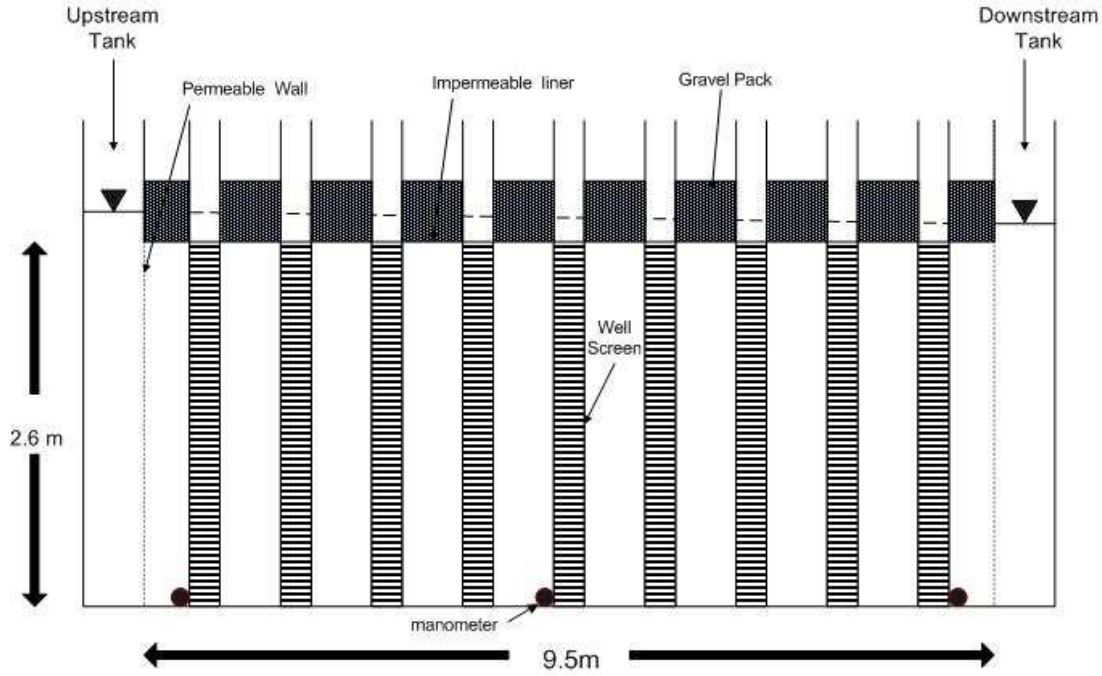

Figure 3.1: Lateral view of the artificial aquifer (Modified from Close et. al. 2008).

The hydraulic gradient of the aquifer was measured using three uniformly spaced manometers located on the base of the aquifer and running across the full width of the aquifer (Figure 3.1). The 3 manometer tubes were fixed to the side of the aquifer and the head in each is measured by a fixed scale. As the manometer tubes ran the width of the aquifer they provided an average head value across that transect of the aquifer.

The aquifer has 45 monitoring wells installed, spaced on a 1m by 1m grid (Figure 3.2b). The wells were designed to accommodate internal samplers that obtained discrete samples from 0.4, 1.0, 1.6 and 2.2m depths. These samplers were used for tracer experiments to obtain K and dispersivity estimates for the aquifer. The samplers were removed from the wells containing the RWP system.

(a)

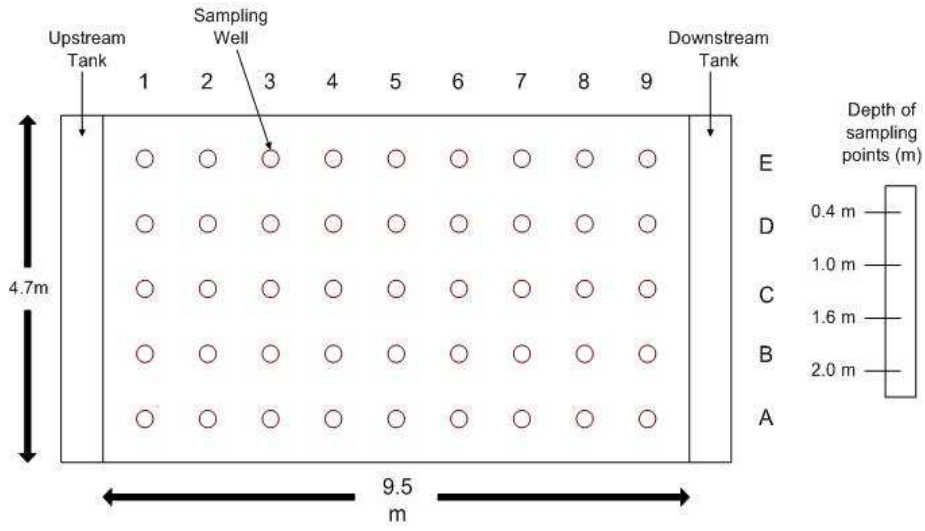

(b)

Figure 3.2: Artificial aquifer used in the recirculating well pair experiments (a) and plan view of sampling well distribution in the aquifer (b).

The monitoring wells were constructed of rigid poly vinyl chloride pipe with an outer diameter of 33mm and internal diameter of 25mm. The wells are covered externally with a

small mesh size nylon well 'sock' to exclude aquifer material from the well. The wells penetrate the aquifer fully and are slotted in 70mm sections separated by 80mm of un-slotted pipe (Figure 3.3). There are six slots in each section, each with a width of 1.5mm. The total porosity for the screen was calculated to be 4.1%. Pairs of wells were used for the RWP experiments. Further details of the artificial aquifer system are described in Close et al. (2008).

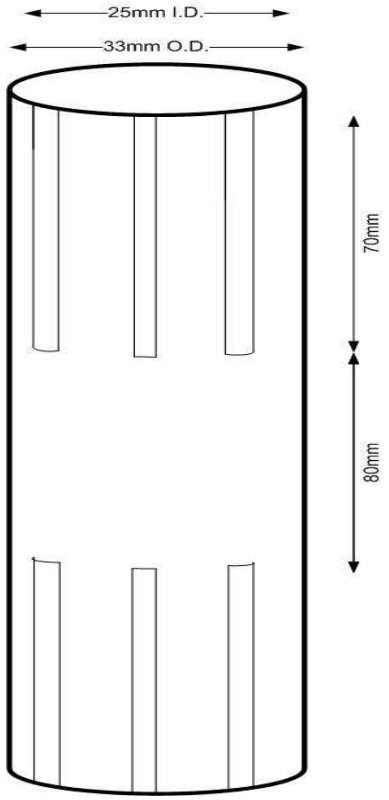

Figure 3.3: Schematic of a section of well screen.

3.2 Determining the Hydraulic Conductivity of the Artificial Aquifer

An accurate estimate of the K of the artificial aquifer was required to validate the RWP method. Values determined from an independent method of calculating K were compared to the values obtained from the RWP method to gauge accuracy. Several methods have been used to determine the K of the artificial aquifer:

1: Hazen Grain Size Analysis.

2: Darcy's Law

3: Tracer Tests

4: Mass Flux Back Calculation

5: Unconfined Heads

This section gives a brief outline and the results of each K method. Section 3.2.6 gives a brief discussion on the vertical K of the artificial aquifer.

3.2.1: Hazen Grain Size Method

The K of the sediment was estimated using the Hazen method (Equation 3.2). This empirical method uses a grain-size distribution curve and formula to predict K.

$$K = C(d_{10})^2 \qquad \textbf{(3.2)}$$

where K is the hydraulic conductivity, C is the Hazen co-efficient, and d_{10} is the effective grain size.

Using an effective grain size of 0.6mm (0.0006m) and a Hazen co-efficient of 80 (Fetter, 2001), K of the artificial aquifer was calculated to be 249 m/d.

3.2.2: Hydraulic Conductivity from Darcy's Law

Darcy's Law was used to calculate the K of the artificial aquifer by measuring the specific discharge per unit hydraulic gradient (Equation 3.3).

$$K = \frac{Q}{AI} \tag{3.3}$$

where Q is flow rate, A is the cross-sectional area and I is the hydraulic gradient.

Flow rate was measured by a logged flow meter on the inflow pipe. There is no net loss or gain of water through the aquifer, and therefore the inflow is equal to the discharge. The hydraulic gradient was calculated by dividing the difference between the up gradient and down gradient piezometer readings by their separation distance.

Using Equation 3.3, Close et al. (2008) determined that K values for the artificial aquifer range from 160 to 208 m/d, with an estimated uncertainty of between 6 and 22% (higher uncertainties at lower flows and gradients).

3.2.3: Tracer Tests

Hydraulic conductivity was also calculated by conducting tracer tests to obtain the pore water velocity (Equation 3.4).

$$K = \frac{V\eta_e}{I} \quad \textbf{(3.4)}$$

where V is the pore water velocity, η_e is the effective porosity and I is the hydraulic gradient.

Bright et al., (2002) estimated the K values of individual cells (blocks of aquifer material encapsulating a sampling point) using a modification of Equation 3.4. The modification was required because the tracer test was conducted with a reactive tracer (rhodamine WT). The distribution co-efficient of the tracer was determined experimentally and this co-efficient was used in Equation 3.5 to calculate the retardation factor.

$$R = \frac{(\rho_b k_d)}{n} + 1 \quad \textbf{(3.5)}$$

where n is porosity, ρ_b is bulk density of the material and k_d is the distribution co-efficient in the linear adsorption isotherm.

The retardation factor can be used to calculate the velocity of the tracer from Equation 3.6.

$$u = V_w/R \quad \textbf{(3.6)}$$

where u is the tracer velocity, V_w is the water velocity and R is the retardation factor.

Equations 3.4, 3.5 and 3.6 were combined to obtain the K (Equation 3.7).

$$K = \frac{\left(n + \rho_b k_d\right)}{I} u \qquad \textbf{(3.7)}$$

where u is the travel velocity of the tracer, I is the hydraulic gradient, n is porosity, ρ_b is bulk density of the material and k_d is the distribution co-efficient in the linear adsorption isotherm.

Table 3.1 shows the distribution of K values in the artificial aquifer calculated by Bright et al. (2002). Kim (2005) estimated missing values by the quadratic Shepard method (shaded squares). The transect number or column is the distance down gradient of the header tank, the row is the position across the width of the aquifer; results are given at four sampling depths (Figure 3.2b).

Velocity values used to construct Table 3.1 were measured from the up gradient header tank to the sample point without taking into account any variation in the permeability in the screen separating the header tank and the aquifer material. Although the screen was designed to have a sufficiently high permeability relative to the aquifer material, experiments have revealed that the screen has a low permeability relative to the aquifer material (Burbery, 2008, pers.com.). This is possibly due to clogging or degradation of the screen material. This screen would reduce measured velocities used in Table 3.1 and therefore give an under estimate of the actual K values in the artificial aquifer. The K

values in Table 3.1 were generated prior to construction of the de-aeration tower (Section 3.1). Air entrapment in the aquifer had the potential to reduce the conductivity of the aquifer in the period when these results were obtained. Thus the K values reported by Bright et al. (2002) and used by Kim (2005) and Yoon (2006) were not used in this study.

Table 3.1: Hydraulic conductivity of each cell (m/d) determined by Bright et al. (2002). Kim (2005) estimated values in the shaded boxes using the quadratic Shepard method.

Transect (number of measured conductivities)	Row	Depth			
		0.4m	1.0m	1.6m	2.2m
1st (19)	A	151	110	102	204
	B	151	132	83	93
	C	110	110	79	110
	D	132	100	93	91
	E	132	102	132	102
3rd (18)	A	214	200	174	224
	B	158	151	158	110
	C	166	166	166	178
	D	166	166	170	191
	E	245	204	151	151
5th (15)	A	288	148	138	138
	B	229	174	171	199
	C	151	158	174	216
	D	229	184	218	240
	E	263	151	174	155
7th (11)	A	214	237	232	123
	B	195	194	173	131
	C	145	158	174	229
	D	174	156	180	240
	E	214	152	135	155
9th (8)	A	347	316	267	166
	B	186	207	182	114
	C	479	276	257	263
	D	251	216	224	240
	E	288	191	171	191

Further tracer experiments to determine the K and dispersivity using rhodamine WT and bromide as tracers were conducted by Close et al. (2008). It was determined that rhodamine WT was retarded with respect to bromide and therefore only the bromide tracer test results are shown in this study.

Hydraulic conductivity values were estimated by fitting breakthrough curves from each sample point with the curve fitting program, CXTFIT (Toride et al., 1995), to estimate pore water velocity which was then used in Equation 3.4 to calculate K values. Close et al. (2008) reported K values obtained from velocities calculated from the header tank to each sample point (Table 3.2). Grey squares denote cells in which no data were available (wells 5C and 9E were not available for sampling at all depths).

Table 3.2: Hydraulic conductivity of each cell (m/d) determined by Close et al. (2008).

Transect (number of measured conductivities)	Row	Depth			
		0.4m	1.0m	1.6m	2.2m
2.75 (20)	A	450.07	118.58	93.36	104.32
	B	95.42	79.51	89.05	101.44
	C	96.19	87.84	95.04	125.46
	D	94.43	84.21	95.11	134.41
	E	125.89	92.11	100.89	94.45
4.75 (15)	A	620.73	293.17	102.90	85.04
	B	198.61	123.93		96.55
	C				
	D	109.30	92.56	101.64	107.94
	E	130.70	103.18	107.52	101.23
6.75 (19)	A	576.29	367.20	215.10	145.00
	B	272.21	134.08	96.97	103.98
	C		86.90	108.90	110.83
	D	115.74	93.39	109.14	112.46
	E	137.80	105.64	112.35	113.77
8.75 (14)	A	423.32	240.98	181.03	128.41
	B	274.50		119.45	103.70
	C	123.38	103.63	108.37	111.26
	D	134.30		113.88	137.90
	E				

As is shown in Table 3.2, there are large variations in the estimated K values. High K values are located in the upper sample points (0.4m) in the A row. Close et al. (2008) hypothesised that differential packing of the aquifer may have caused these heterogeneities.

This method of calculation leads to correlation of K values down a flow path. For example the K value calculated at a point 8.75m from the up gradient header tank will depend on the K values from the header tank to 2.75, 4.75 and 6.75, as well as the K at 8.75. If there are heterogeneities in any section of aquifer from the up gradient header tank to the sample

point at 8.75m then these will affect the K value assigned to the 8.75m point. Although there will be correlation of K values down the aquifer, values further down gradient will be closer to the average value of the aquifer than those up gradient. The low permeability header tank wall will, as in the analysis of Bright et al. (2002), lead to an under estimation of the K value of the aquifer. These values were obtained after the construction of the de-aeration tower and therefore aquifer clogging with air did not have an effect on these results.

Rather than using the correlated K values measured between the header tank and the sampling wells, uncorrelated well to well velocities were used to determine the K values for comparison with K values obtained from the RWP system. These values are presented in Section 4.1.

3.2.4: Mass Flux back-calculation

Kim (2005) calculated the mass flux (M_f) of a contaminant in the artificial aquifer using RWP methods to calculate K, and samples taken from the RWP system to measure the contaminant concentration. In these experiments mass flux of the contaminant was known. As the mass flux was known, K could be determined for the aquifer with Equation 3.8.

$$K = \frac{M_f}{iC} \tag{3.8}$$

where M_f is the mass flux, K is the hydraulic conductivity, i is the hydraulic gradient and C is the concentration of the contaminant.

Kim (2005) used both multi dipole and fractional flow methods to calculate the K. In the artificial aquifer the concentration of the contaminant was known because it was introduced at the aquifer feed water. Kim (2005) compared calculated mass flux values to the actual mass flux in the artificial aquifer as calculated from Equation 3.9.

$$M_f = \frac{QC}{A} \tag{3.9}$$

where Q is the flow rate of the total aquifer and A is the cross sectional area of the aquifer and C is the concentration of the contaminant.

This equation can only be employed in controlled situations, like those in the artificial aquifer, as the area of the contaminant plume the input concentration and the flow rate are difficult to measure in a real situation. By comparing the known mass flux (calculated from Equation 3.9) with the mass flux calculated from the K obtained from the RWP system it is possible to calculate the actual K of the aquifer. This is achieved by calculating the percent difference between the calculated and actual flux and using this percentage to derive the K value. Table 3.3 shows the calculated fluxes and K values assuming the aquifer was isotropic using the multi dipole method. Three multi dipole experiments were analysed (1, 2 and 3) and the K and mass flux estimated from the multi dipole method are shown. The actual flux travelling through the aquifer is also shown. Dividing the actual flux by the estimated flux and multiplying by the estimated K produces an estimate of the actual K of the aquifer (Calculated K). The same calculations can be applied to the fraction flow method (Table 3.4). Two experiments are analysed for this method, with experiment one using the four steady state estimation methods used by Kim (2005).

Table 3.3: Hydraulic conductivity calculated from multi dipole method (data from Kim 2005).

Experiment	Isotropic K (m/d) estimated by Kim (2005)	Mass Flux (g/m^2*d)		Calculated K (m/d)
		Estimated by Kim (2005)	Actual	
1	1.13	0.016	2.48	**175**
2	20.16	0.298	2.4	**162**
3	16.35	0.234	2.48	**173**

Table 3.4: Hydraulic conductivity calculated from the fractional flow method (data from Kim 2005).

Experiment	Estimation method	Isotropic K (m/d) estimated by Kim (2005)	Mass Flux (g/m^2*d)		Calculated K (m/d)
			Estimated by Kim (2005)	Actual	
One	1	230	3.29	2.48	**173**
	2	243	3.47	2.48	**174**
	3	230	3.29	2.48	**173**
	4	234	3.35	2.48	**173**
Two		143	2.12	2.4	**162**

3.2.5: Unconfined Head Method

Hydraulic conductivity, when the aquifer was unconfined, was calculated with a method that assumes 1D flow. The water level in the artificial aquifer was set to below the confining layer to achieve unconfined conditions. A modification of the Darcy equation was used to calculate K (Equation 3.10).

$$K = \frac{2QL}{w(dh^2)} \qquad \textbf{(3.10)}$$

where Q is the pumping rate, L is the length between the observation wells, w is the aquifer width, and dh is the difference between the water level at the 1st and 2nd observation points.

Equation 3.8 was used to calculate an average K for the artificial aquifer sands of 217.2 m/d with a geometric mean of 214m/d (Burbery, 2008, pers. comm.). Row by row K

values were also calculated with the results ranging from 255 m/d for row B to 166 m/d for row D.

3.2.6 Vertical Conductivity

No independent measurement of vertical K of the artificial aquifer has been performed. The aquifer is packed with coarse sand of approximately uniform grain size (0.6-1.18mm) and therefore should pack isotropically (hydraulic properties equal in all directions). The possibility exists that the packing procedure created layers of different sand densities or that the continuous flow of water through the aquifer has created layering of the sediments resulting in vertical conductivity being less than the horizontal conductivity. There is no direct evidence for this assumption. Kim, (2005) determined that using isotropic values for K to calculate mass flux gave a more accurate estimation of the mass flux than using anisotropic K values, which lends some weight to the assumption that the artificial aquifer is isotropic. The present study calculates K values assuming both isotropic and anisotropic conditions.

3.3 Description of the Physical Recirculating Well Pair System

A small scale RWP system was constructed based on large scale systems constructed by McCarty et al. (1998) and Cunningham et al. (2004) to evaluate remediation technologies. The large scale systems were installed in dedicated wells with dual screens specifically constructed for the system. The large scale systems employed pumps located in the wells. The wells in the artificial aquifer were designed for multilevel sampling and therefore were fully screened. The narrow well diameter could not accommodate down-hole pumps,

limiting flow rate to the maximum that could be pumped from tubing with a diameter smaller than the well diameter.

Although the RWP design is limited by well construction there are many advantages of trialling the RWP system in the artificial aquifer. These include the relatively uniform K field, independently determined K, and the ability to control the hydraulic gradient. The well design in the artificial aquifer did not include a well pack, eliminating this complication in estimation of K.

Two RWP systems were utilised for the experiments in this study. Fractional flow experiments 1, 2 and 3 used a system constructed of polyvinyl chloride; the second system used in fractional flow experiments 4, 5 and the series of multi dipole experiments was constructed of stainless steel (Figure 3.4). Both systems utilised rubber inflatable packers.

Figure 3.4: Single dipole of the stainless steel recirculating well pair system.

The PVC system could not achieve the high flow rates desired for later experiments due to restricted flow caused by the limited diameter of the pump tubing installed. A redesigned system with larger diameter pump tubing and constructed of stainless steel was used in later experiments. Both systems possessed identical geometry. A schematic of the system is illustrated in Figure 3.5. As the systems are similar, only the stainless steel system will be described.

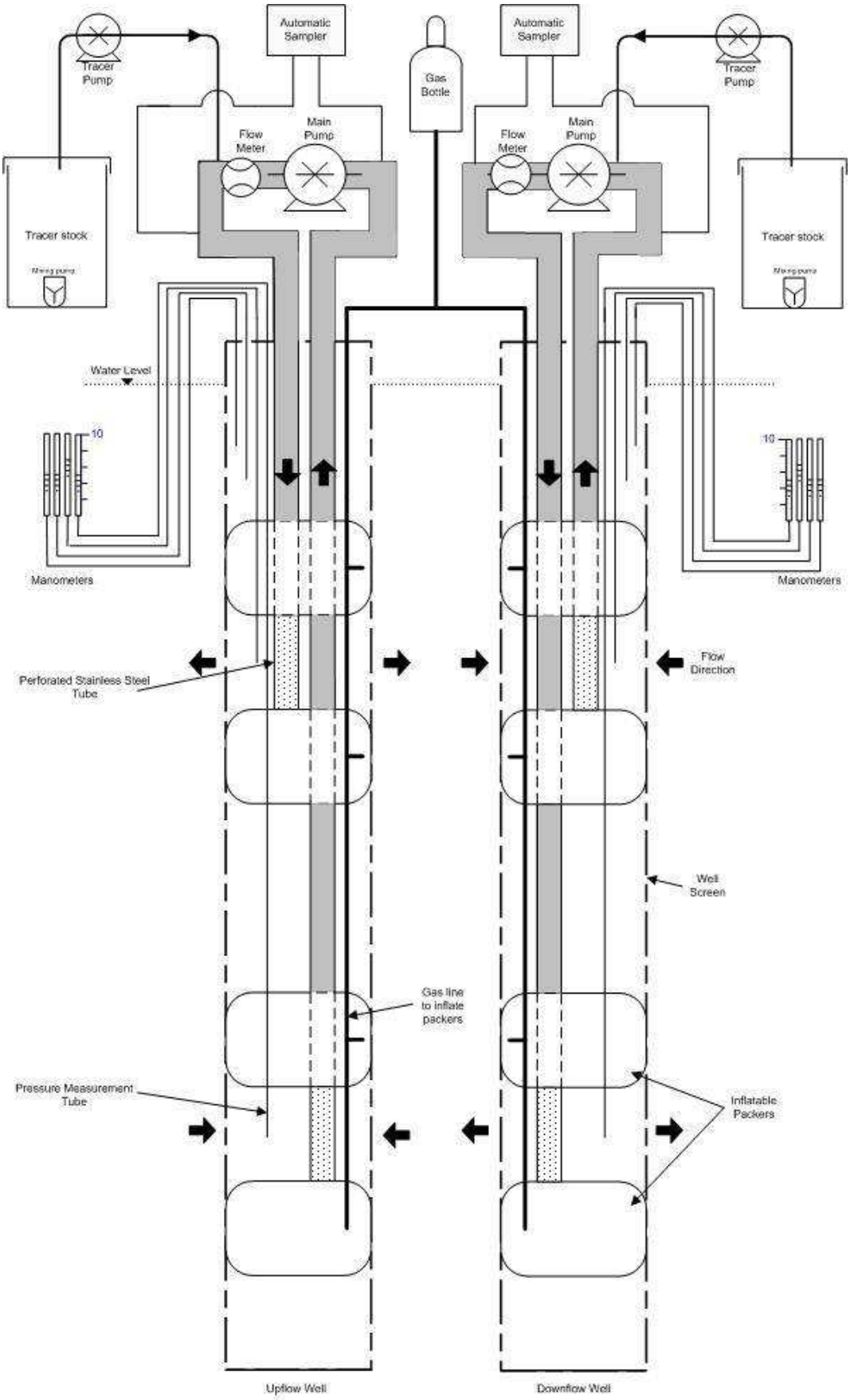

Figure 3.5: Schematic of the recirculating well pair system used in this study.

Each well contained four inflatable rubber packers which enclose an injection and extraction screen creating a dipole in each well (Figure 3.6). Figure 3.6 also depicts the pump tubing carrying the water (injection or extraction) and the manometer tube used to measure head in this screen. One of the well pairs (Up flow) consisted of the extraction screen in the lower portion of the aquifer and the injection screen in the upper part of the aquifer with the other well in the pair (Down flow) having the opposite configuration. The narrow diameter of the wells in the aquifer precluded the use of down well pumps and therefore water was pumped from the extraction screen to the surface of each well with large capacity peristaltic pumps (Masterflex, Model no: 77410-05) and then re-injected into the aquifer via the injection screens (Figure 3.5).

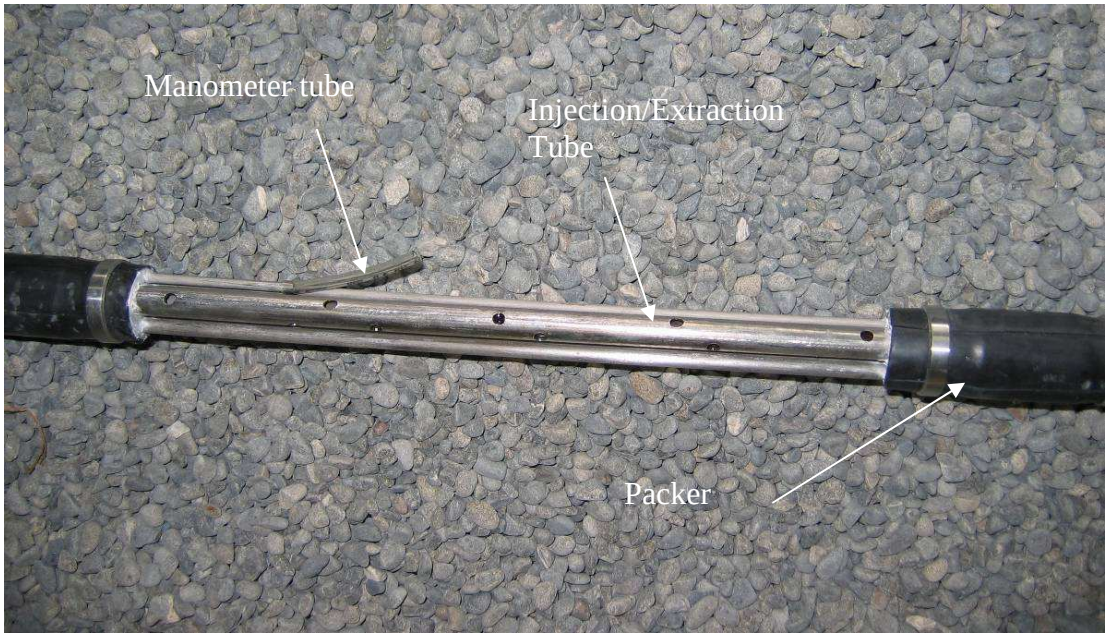

Figure 3.6: Detail of an injection or extraction screen.

The flow rate of each dipole was monitored using inline flow meters installed in each dipole. The flow rates of both dipoles were balanced to within 0.20 m^3/d for all experiments. Injection and extraction screens are 225mm long, enclosing two 70mm slotted sections of well casing separated by 80mm of blank casing. The distance between

the upper and lower screen is 1.28m. The packers were 80mm long, constructed of rubber and inflated from the surface with inert gas. The packers, when inflated, sealed against areas of blank well casing above and below the two sections of slotted well casing. Pumped water exited or entered the screens via a tube with uniformly distributed holes ensuring even distribution of flow.

Four manometers were placed in each well (dipole) to measure the hydraulic head at four depths. Two of these manometers were located in the extraction and injection screens (Obs 3, 4, 7 and 8). The manometers measured the pressure (either positive or negative) of the water leaving or entering the aquifer formation. The 2 remaining manometers were located 400 and 500mm above the centre of the top screen (Obs 1, 2, 5 and 6). These two points measured the mounding or drawdown above the screens (Figure 3.7).

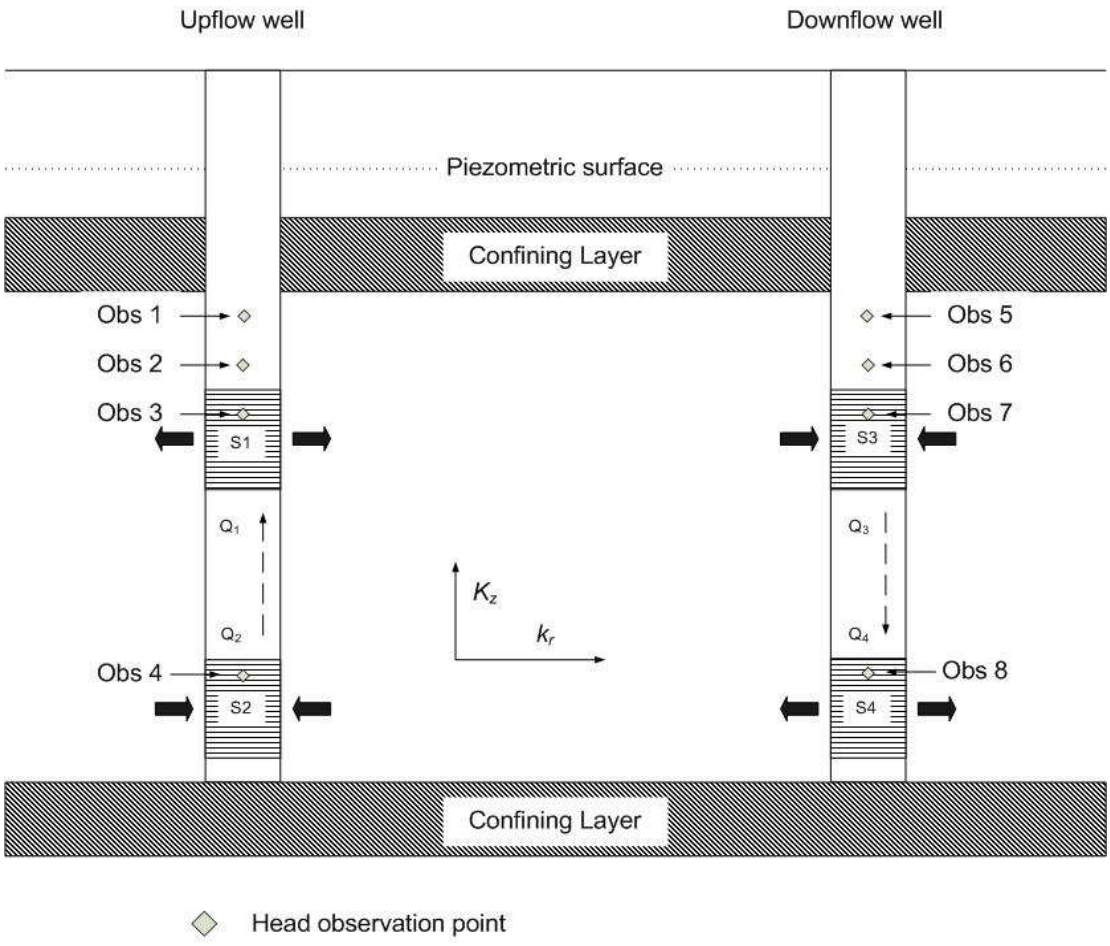

Figure 3.7: Position of manometers to measure hydraulic head and screens from which tracer concentration was sampled.

The manometers consisted of narrow gauge open ended tubes that ran from the observation point to a bank of manometers fastened to the side of the aquifer. Measurements were recorded from the manometers for each flow rate after a period of stabilisation. This stabilisation period was ascertained to have finished when there was no movement in the manometer readings. Twenty four hours were deemed to be sufficient in the artificial aquifer for the current study.

The fractional flow RWP experiments utilised two sample points for each dipole, effectively sampling the concentration at the four screens (S1, S2, S3 and S4 in Figure 3.7). The water from the extraction screens was pumped to the surface and then re- injected

through the injection screens enabling the sampling of the screens to occur on the surface (Figure 3.5).

Tracer was injected into the water flow on the surface after the extraction sample was obtained, and before the pump (Figure 3.5). The pump assisted in mixing the tracer with the extraction water, but to guarantee fully mixed tracer an inline static mixer was placed in the flow after the pump. The injection sample was taken after the inline mixer ensuring a representative sample. Two peristaltic pumps (Masterflex, Model no. 07553-70) were used to inject concentrated tracer into the two dipole flows at a constant rate. Nitrate, chloride and bromide were used as tracers. Two tanks containing the stock (nitrate, chloride or bromide) were constantly mixed using a pump throughout the course of the experiments.

Thirty millilitre samples were taken via a data logger controlled peristaltic pump system at 12 hourly intervals throughout the experiments. Samples were frozen to ensure no degradation of the tracers before analysis was completed. Samples were analysed by a Flow Injection Analyser (Foss Analytical FIAstar 5000). Source water concentrations of the tracers were also measured and this background concentration of tracer was subtracted from the samples reported in the experiments used in this study. Samples from various wells downstream of the dipole flow cell, together with samples from a well located between the dipole wells were analysed but the results were not used in this study as they would not be available in a practical application of the method in the field.

3.4 Experiments performed in the Artificial Aquifer

To study the effect of changing the pumping flow rate and the incidence angle of the wells relative to regional flow on the accuracy of the RWP system to estimate K, additional experiments were carried out. Five multi dipole experiments at 5 progressively larger flow rates were undertaken. These experiments were called multi dipole experiments 1 to 5 (MD1-MD5). The effect of incidence angle was determined by comparing the results of two combined (multi dipole and fractional flow) experiments. These two experiments were identical except for the incidence angle of the wells to regional flow and consequentially the distance between the wells. These experiments will be called multi dipole 6 (MD6) and multi dipole angle (MDA).

Similarly, for the fractional flow approach, 4 experiments were analysed with differing flow rates to determine if changing flow rates affected the accuracy of the method. Experiment 1 and 2 were analysed by Goltz et al. (2008), Kim (2005) and Yoon (2006). These data were re-analysed and 2 additional experiments were carried out to determine the accuracy of the method with differing flow rates. These experiments will be labelled fractional flow experiments 1- 4 (FF1 – FF4). As discussed above a combined experiment was also conducted to determine if incidence angle affected the accuracy of the fractional flow method. This experiment will be labelled fractional flow experiment 5 (FF5).

Each experiment utilised a pair of wells within the aquifer (Figure 3.8). The wells utilised for the multi-dipole experiments were:

- MD1 7B and 7D
- MD2 7B and 7D
- MD3 7B and 7D
- MD4 7B and 7D
- MD5 7B and 7D
- MD6 7B and 7D
- MDA 5B and 7D

For the fractional flow experiments the following wells were utilised:

- FF1 6B and 6D
- FF2 6B and 6D
- FF3 6B and 6D
- FF4 7B and 7D
- FF5 5B and 7D

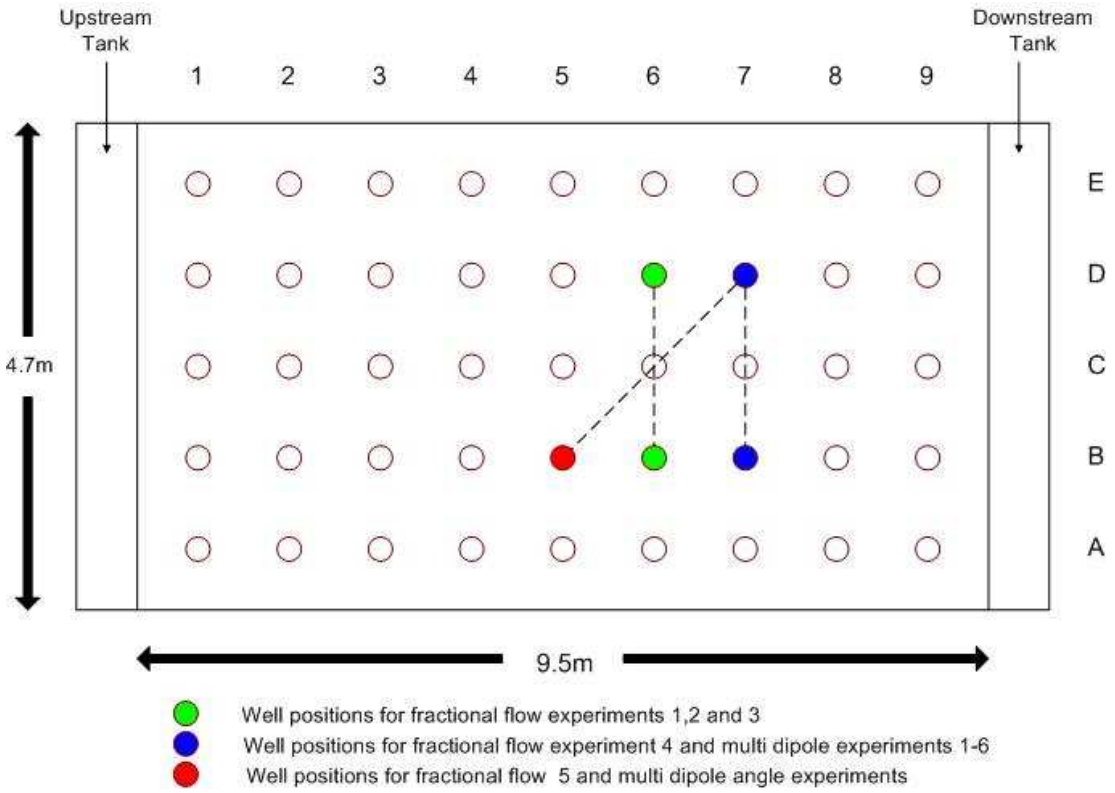

Figure 3.8: Detail of the positions of the recirculation well pairs.

The remaining parameters used for these experiments are given in the following sections.

3.4.1 Multi Dipole Method

A series of five experiments were undertaken to test whether change in flow rate of the pumping wells affects the accuracy of the multi dipole method. The five experiments were conducted sequentially without altering aquifer parameters. Therefore, the average regional aquifer flow over the course of the 5 experiments was held constant. The average flow was 2.78 m^3/d (Figure 3.9). This regional flow rate produced a hydraulic gradient of 0.0011 in the artificial aquifer.

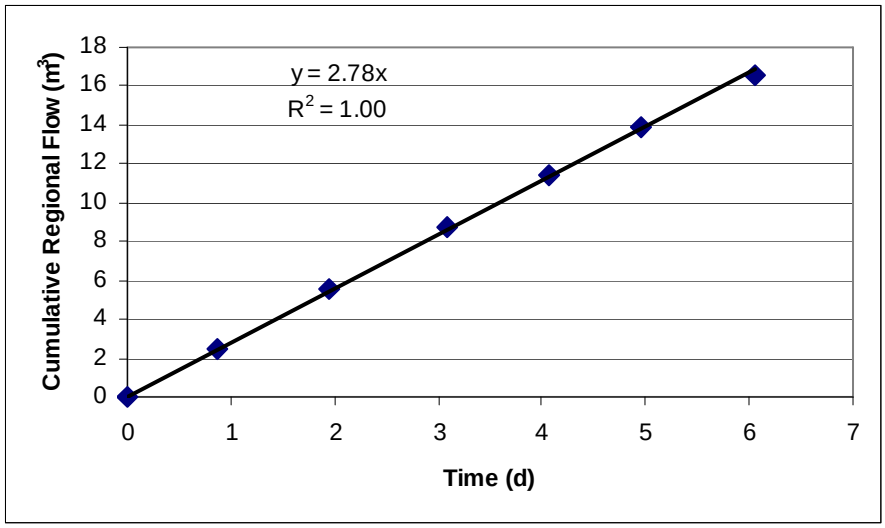

Figure 3.9: Cumulative regional flow rate during multi dipole experiments.

The five experiments were undertaken in wells 7B and 7D (Figure 3.8). Table 3.5 details the well screen intervals and flow rates tested (a negative flow rate denotes extraction and a positive flow rate denotes injection). Flow rates of each dipole were balanced to approximately equal (maximum difference = 0.20 m^3/d) and then the manometers were allowed to stabilize. Manometer readings were recorded after approximately 24 hours for each flow rate step.

Table 3.5: Screen Parameters and flow rates for the multi dipole method.
***xw is the distance from the up gradient boundary, yw is the distance from the right hand boundary when orientated in the direction of flow, zwb is the height of the base of the screen from the bottom of the aquifer and zwt is the position of the top of the screen from the base of the aquifer.**

					Q (flow rate)				
	xw	yw	zwb	zwt*	MD1	MD2	MD3	MD4	MD5
Screen	(m)	(m)	(m)	(m)	(m^3/d)	(m^3/d)	(m^3/d)	(m^3/d)	(m^3/d)
S1	5.75	1.35	1.84	2.06	-1.54	-3.02	-4.25	-5.85	-7.12
S2	5.75	1.35	0.34	0.56	1.54	3.02	4.25	5.85	7.12
S3	5.75	3.35	1.84	2.06	1.37	3.01	4.27	5.65	7.20
S4	5.75	3.35	0.34	0.56	-1.37	-3.01	-4.27	-5.65	-7.20

MD6 and MDA were also analysed with the multi dipole method to determine whether the incidence angle of the RWP system in relation to the regional flow affected the accuracy of

results obtained. Both of these experiments had six manometers (Obs 2, 3, 4, 6, 7 and 8). The regional flow of the aquifer over the course of MD6 was 3.06 m^3/d (Figure 3.10).

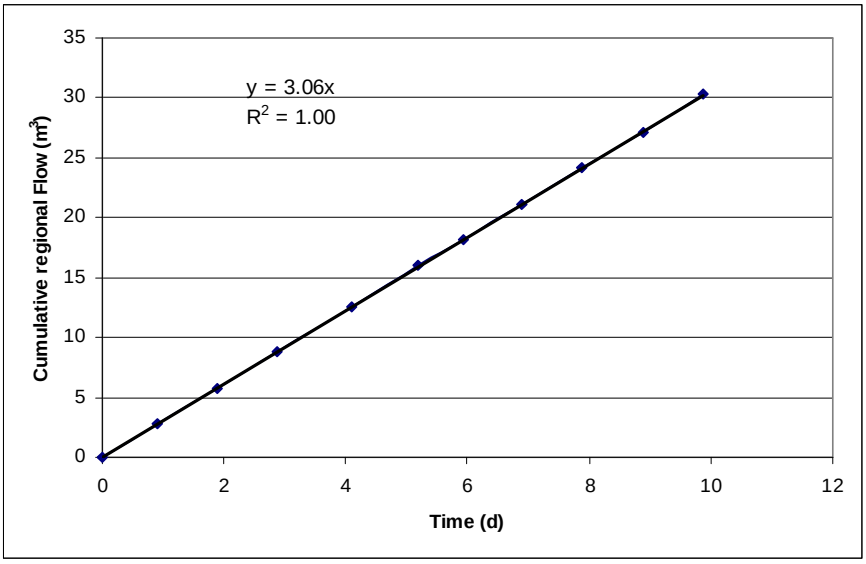

Figure 3.10: Cumulative regional flow rate during MD6.

The regional flow produced a hydraulic gradient of 0.0013 in the artificial aquifer. MD6 was undertaken in wells 7B and 7D (Figure 3.8) with flow rates and screen positions shown in Table 3.6. Flow rates for each dipole were balanced to approximately equal and then the manometers were allowed to stabilize. Manometer readings were recorded after approximately 24 hours.

Table 3.6: Screen Parameters and flow rates for MD6.

Screen	xw (m)	yw (m)	zwb (m)	zwt (m)	Q (m^3/d)
S1	6.75	1.35	1.84	2.06	-6.51
S2	6.75	1.35	0.34	0.56	6.51
S3	6.75	3.35	1.84	2.06	6.58
S4	6.75	3.35	0.34	0.56	-6.58

The regional flow in the aquifer over the course of MDA was 2.68 m^3/d (Figure 3.11).

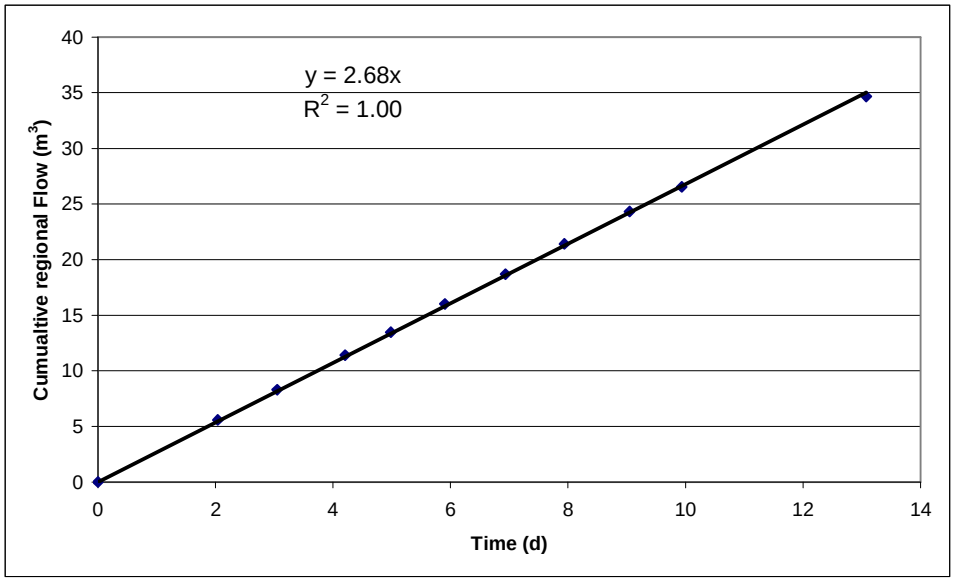

Figure 3.11: Cumulative regional flow rate during MDA.

The regional flow produced a hydraulic gradient of 0.0013 in the artificial aquifer. MDA was undertaken in wells 5B and 7D (Figure 3.8) with the flow rates and screen positions shown in Table 3.7. Flow rates of each dipole were balanced to approximately equal and then the manometers were allowed to stabilize. Manometer readings were recorded after approximately 24 hours.

Table 3.7: Screen Parameters and flow rates for MDA.

Screen	xw (m)	yw (m)	zwb (m)	zwt (m)	Q (m^3/d)
S1	4.75	1.35	1.84	2.06	-6.63
S2	4.75	1.35	0.34	0.56	6.63
S3	6.75	3.35	1.84	2.06	6.44
S4	6.75	3.35	0.34	0.56	-6.44

3.4.2 Fractional Flow Method

Five experiments were carried out using the fractional flow approach. FF1, 2, 3 and 4 were undertaken to determine if altering the pumping flow rates affects the accuracy of the

method. FF5 tested the effect the incidence angle of the RWP system in relation to the regional flow had on the accuracy of results by placing the wells at 45 degrees to the regional flow and replicating the flow rate of FF4.

For each experiment the flow rates of each dipole were approximately balanced and run for 12 hours prior to the start of the experiment to allow the recirculating cell between the dipoles to develop and reach steady state. Screen position and the corresponding screen flow rates are shown in Table 3.8.

Table 3.8: Screen parameters and flow rates for the 5 fractional flow experiments.

Experiment	Screen	xw (m)	yw (m)	zwb (m)	zwt (m)	Q (m^3/d)
FF1	S1	5.75	1.35	1.84	2.06	-1.14
	S2	5.75	1.35	0.34	0.56	1.14
	S3	5.75	3.35	1.84	2.06	1.45
	S4	5.75	3.35	0.34	0.56	-1.45
FF2	S1	5.75	1.35	1.84	2.06	-2.22
	S2	5.75	1.35	0.34	0.56	2.22
	S3	5.75	3.35	1.84	2.06	2.39
	S4	5.75	3.35	0.34	0.56	-2.39
FF3	S1	5.75	1.35	1.84	2.06	-2.32
	S2	5.75	1.35	0.34	0.56	2.32
	S3	5.75	3.35	1.84	2.06	2.59
	S4	5.75	3.35	0.34	0.56	-2.59
FF4	S1	6.75	1.35	1.84	2.06	-6.51
	S2	6.75	1.35	0.34	0.56	6.51
	S3	6.75	3.35	1.84	2.06	6.58
	S4	6.75	3.35	0.34	0.56	-6.58
FF4	S1	4.75	1.35	1.84	2.06	-6.63
	S2	4.75	1.35	0.34	0.56	6.63
	S3	6.75	3.35	1.84	2.06	6.44
	S4	6.75	3.35	0.34	0.56	-6.44

Regional flow rate in the aquifer and the hydraulic gradient of the aquifer were monitored throughout each experiment. Cumulative regional flow in the artificial aquifer for each experiment is shown in Figure 3.12.

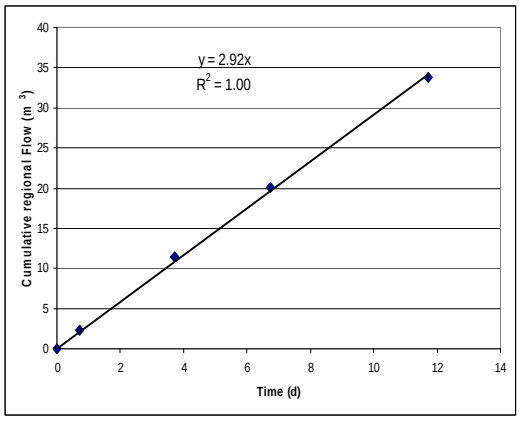

FF1

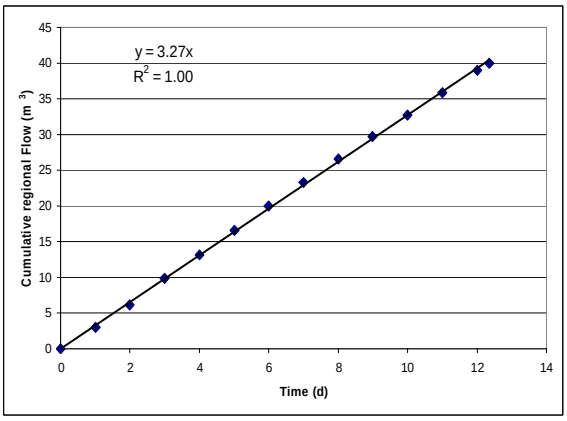

FF2

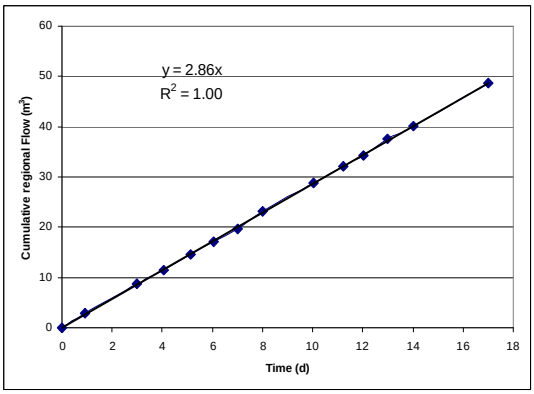

FF3

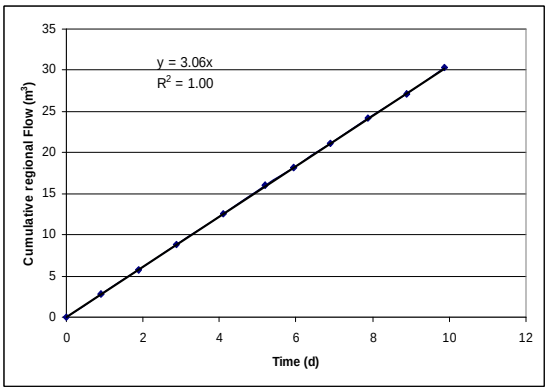

FF4

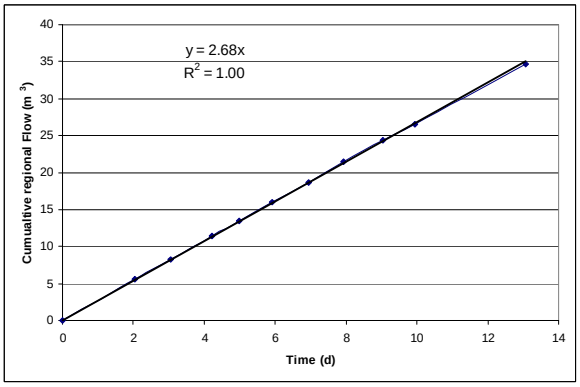

FF5

Figure 3.12: Cumulative regional flow for the 5 fractional flow experiments.

Solutions of bromide and nitrate or chloride were made from water sourced from the artificial aquifer. Tracer solutions were constantly stirred throughout the length of the experiments to maintain a uniform concentration in the tracer tanks. Peristaltic pumps were

calibrated and used to inject tracer into each dipole. Samples were taken frequently for each experiment to define the concentration curves from each screen for each dipole.

A summary of the initial conditions for the 5 fractional flow RWP experiments is presented in Table 3.9.

Table 3.9: Summary of the parameters for the 5 fractional flow experiments.

	Aquifer Flowrate (m^3/d)	Hydraulic Gradient	Pumping Rate ($m^{3/}$d)		Angle (degrees)	Tracers	Injection Concentration (mg/L)
			UpFlow Well	DownFlow Well			
FF1	2.92	0.0014	1.14	1.45	90	Br	5.5
						Cl	6.1
FF2	3.27	0.0015	2.22	2.39	90	Br	8.2
						NO_3	8.1
FF3	2.86	0.0014	2.32	2.59	90	Br	14.2
						NO_3	7.2
FF4	3.06	0.0013	6.52	6.54	90	Br	6.3
						NO_3	6.8
FF5	2.68	0.0013	6.62	6.44	45	Br	6.3
						NO_3	11.2

3.5 Description of the Modelling Technique

MODFLOW (Harbaugh, 2005) was used to construct a simulation of the artificial aquifer for both the multi dipole and fractional flow methods. MODFLOW is a three dimensional block centred finite difference simulator developed by the United States Geological Survey (USGS). Both multi dipole and fractional flow methods utilise output from MODFLOW to define the dimensions, boundaries, and hydraulic gradient of the artificial aquifer system. The fractional flow method then runs MODPATH for each iteration of the genetic algorithm. MODPATH determines the interflow values that are compared to the measured interflow values. Therefore, an accurate model of the system is required for MODFLOW to simulate the correct K values accurately for the two methods.

A GA was then used to determine the K values that provide the closest match between the calculated hydraulic head or interflow values and the observed hydraulic head or interflow values.

3.5.1. MODFLOW

The artificial aquifer was represented by a 3D grid in MODFLOW. Experiments FF1-4 and MD1-5 were represented by grids consisting of 121 columns (aquifer length), 100 rows (aquifer width) and 26 layers (aquifer depth) (Figure 3.13 – 3.14). Experiments FF5 and MDA were represented by grids with 147 columns, 100 rows and 26 layers (Figure 3.15). Experiments FF5 and MDA used 147 columns because the two wells in these experiments are offset with regard to the long axis to form the angle in this experiment. Grid square size maximised resolution and accuracy of MODFLOW simulations in the vicinity of the pumping wells. In areas of the aquifer at a greater distance from the pumping wells grid square size increased in order to minimise the computational time needed to run MODFLOW. The diameter of the dipole wells in the artificial aquifer was 0.025m. This diameter was used as the minimum mesh size in the MODFLOW model. Grid size was increased from 0.025m to 0.0375m and then to 0.05 and finally 0.1m as the distance from the injection or extraction screens increased.

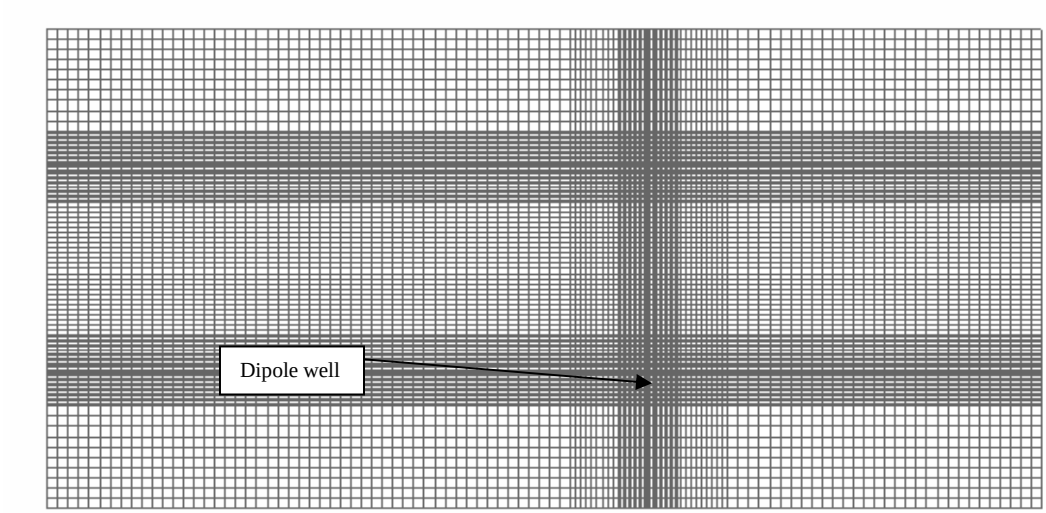

(a)

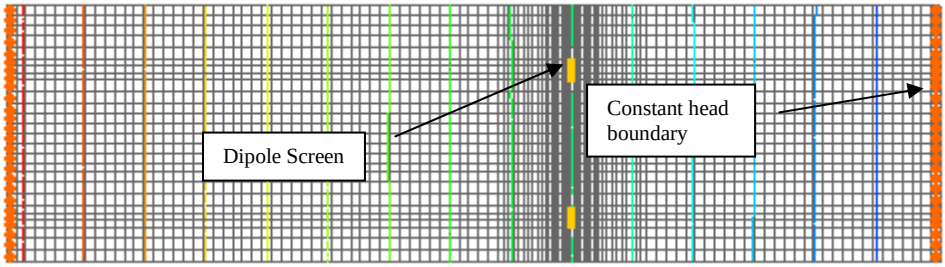

(b)

Figure 3.13: Plan (a) and cross section (b) view of the mesh used to model experiments FF1-FF3 where wells were positioned in row 6 of the artificial aquifer.

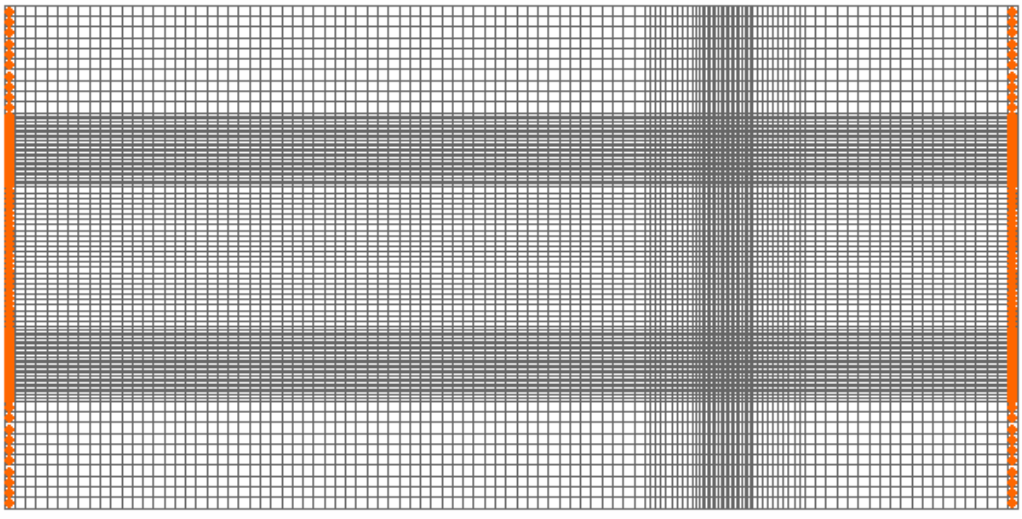

(a)

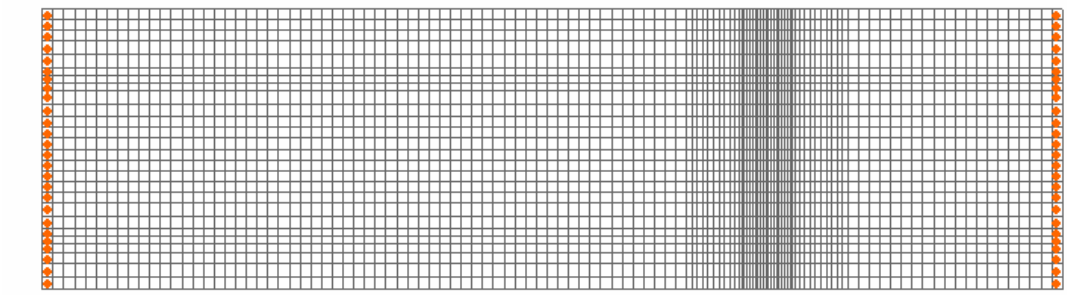

(b)

Figure 3.14: Plan(a) and cross section (b) view of the mesh used to model experiment FF4 and MD1 – MD5 where wells were positioned in row 7 of the artificial aquifer.

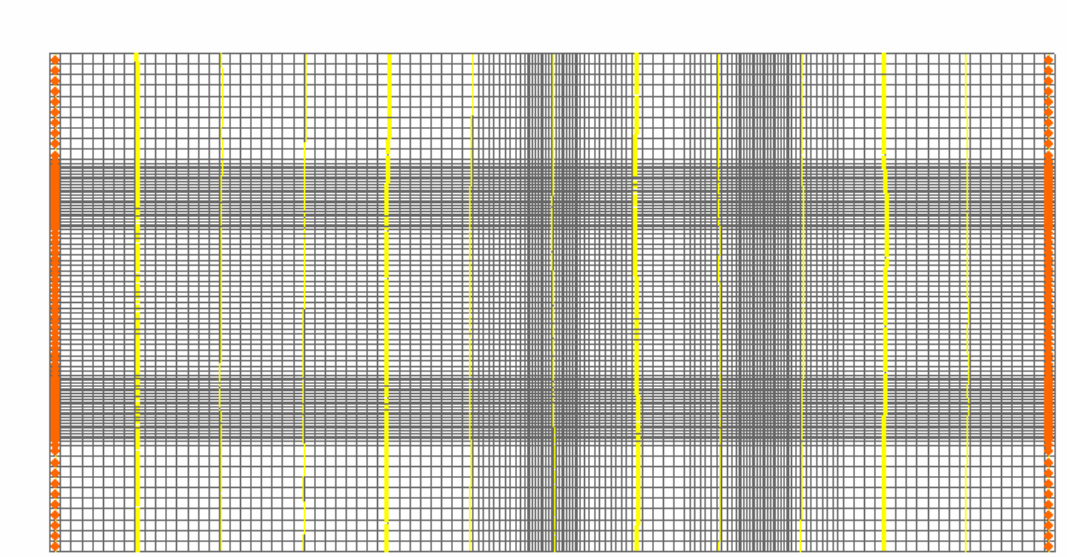

(a)

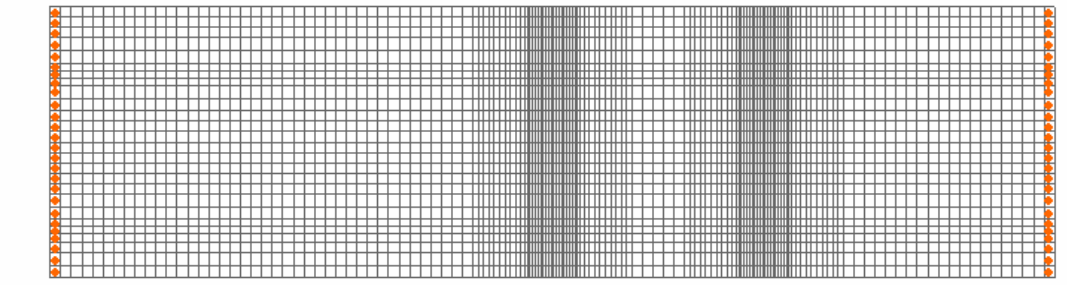

(b)

Figure 3.15: Plan(a) and cross section (b) view of the mesh used to model FF5 and MDA where the wells were positioned in rows 5 and 7.

Injection and extraction screens were represented in MODFLOW as 1 column, 1 row and 3 layers (Figure 3.13).

Constant head boundaries were defined at the first and last column of the model according to the gradient of the aquifer for each experiment (Table 3.10).

Table 3.10: Constant head values used in the RWP models.

Experiment	Up Gradient (m)	Down Gradient (m)
FF1	2.798	2.783
FF2	2.798	2.783
FF3	2.797	2.783
FF4 and MD6	2.796	2.783
FF5 and MDA	2.795	2.783
MD1 -MD5	2.795	2.785

The following options were selected in MODFLOW:

- the grid system was set as confined
- a forward run was specified
- steady state flow was selected
- layer by layer flow package was used
- PCG2 (preconditioned conjugate-gradient-2) solver package was specified

The packers positioned above and below the well screens to prevent short circuiting of the flow were included in MODFLOW by assigning the cells above and below the well screens as no flow cells (ibund=0). For each experiment, MODFLOW was initially run with only the constant head boundaries active, which produced the starting heads (before pumping) for each cell in the grid.

Cells that correspond to the screens were reassigned as pumping cells (3 cells for each screen). The pumping rate for each screen was the total pumping rate divided by 3, and this value assigned to each cell in the screen. Positive pumping rates denote injection into the

well and negative pumping rates denote extraction from the well. MODFLOW was used to create input files for the multi dipole and fractional flow RWP models.

3.5.2. Recirculating Well Pair Models and Genetic Algorithm

The multi dipole RWP model requires two additional files to run together with the MODFLOW output files. One file contains the observation point names and the co-ordinates according to the MODFLOW grid system (Figure 3.16). The other file contains the head values at the two constant head boundaries, the number and the MODFLOW cell co-ordinates of the pumping or injection cells, as well as the number, names, MODFLOW cell co-ordinates, and head values of each observation point (Figure 3.17).

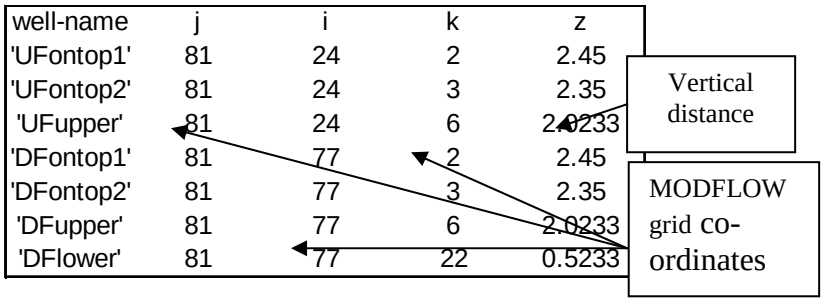

Figure 3.16: Example of observation point input file for MODFLOW MD4.

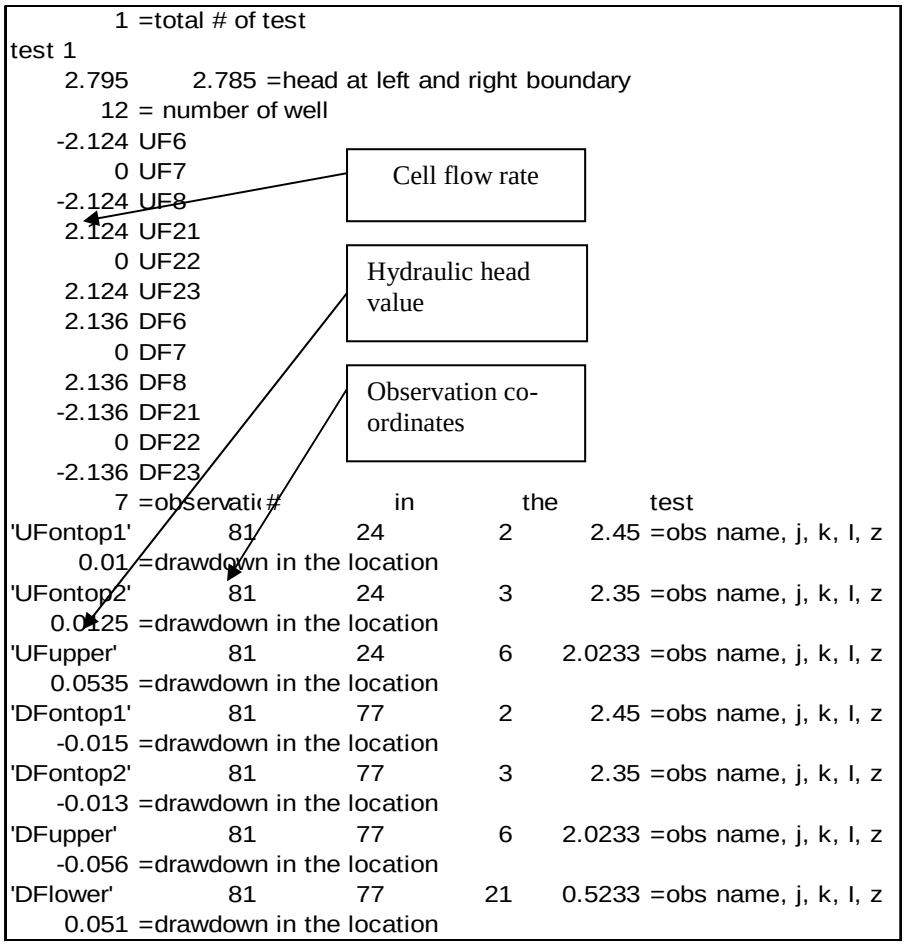

Figure 3.17: Example of input file for MODFLOW MD4.

The fractional flow approach requires a file containing the physical co-ordinates of the well position, flow rate of each of the pumping and injection wells, and the concentration values at each screen. For each tracer only 3 of the 4 screen concentration values are required as the extraction and injection concentrations in the screens that are not injecting the tracer are theoretically identical. The two concentration values (measured at the injection ad extraction screen of the well that is not injecting the tracer) were averaged to obtain the values used in this study. A controlling parameter that determines if the model uses one or the other or both of the tracers is also included in this file (Figure 3.18).

```
following data can be edited by user, the values are concentrations at steady state
6.75,3.35,1.84,2.06,-6.58 =xw,yw,zwb,zwt,well rate for well 3
6.75,3.35,0.34,0.56,6.58  =xw,yw,zwb,zwt,well rate for well 4
6.75,1.35,1.84,2.06,6.51  =xw,yw,zwb,zwt,well rate for well 1
6.75,1.35,0.34,0.56,-6.51 =xw,yw,zwb,zwt,well rate for well 2
21.8d0
15.0d0
9.4d0
7.1d0
11.1d0
17.4d0
3                         =myop,    1=just use downflow(NO3)        2=just use upflow(Br) 3=use both
```

Figure 3.18: Example of Fractional flow input file.

Input parameters for the fractional flow approach are listed and discussed in the results section. An example input file for the GA used to optimise the hydraulic heads or fractional flows is shown in Figure 3.19 and a brief explanation of the main parameters is given below.

.

```
$ga
irestrt=0,
microga=1,
npopsiz=   30,
nparam=    2,
pmutate=0.05d0,
maxgen=200,
idum=-1000,
pcross=0.5d0,
itourny=1,
ielite=1,
icreep=1,
pcreep=0.04d0,
iunifrm=1,
iniche=0,
nchild=1,
iskip=0,     iend=0,
nowrite=1,
kountmx=5,
parmin=    10d0,1d0,
parmax=    300d0,1d0,
nposibl=2*32768,
nichflg=2*1,
$end
```

Figure 3.19: Example of genetic algorithm input file.

Irestrt is whether the GA is a new run or whether to continue from the last run. 0 = new run.

Npopsiz is the population size of the generation, we set this to 30

Nparam is the number of parameters to be evaluated; we have two parameters horizontal conductivity and the ratio of horizontal to vertical conductivity therefore this value was set to 2.

Pmutate is the jump mutation probability which is the probability that an individual's chromosomes will be mutated as compared to the previous generations. This was set to 0.05.

Maxgen is the maximum number of generations which is set to 200.

Pcross is the cross over probability. This means that half the individuals will be crossed and the other half will not participate in mating, instead they will survive to the next generation. Set to 0.5.

Ielite a number one here guarantees that the best individual is transferred into the next generation. Set to 1.

Parmin Min minimum parameter values. Set to 1 and 10

Parmax Max maximum parameter values. Set to 10 and 300

The genetic algorithm produces a file containing the optimum values of horizontal and vertical K, a file containing the fitness (r^2) of each individual in each generation, and the fitness of each generation. The multi dipole approach also produces a file comparing the measured and calculated head values. A flow diagram of the entire modelling process is shown in Figure 3.20.

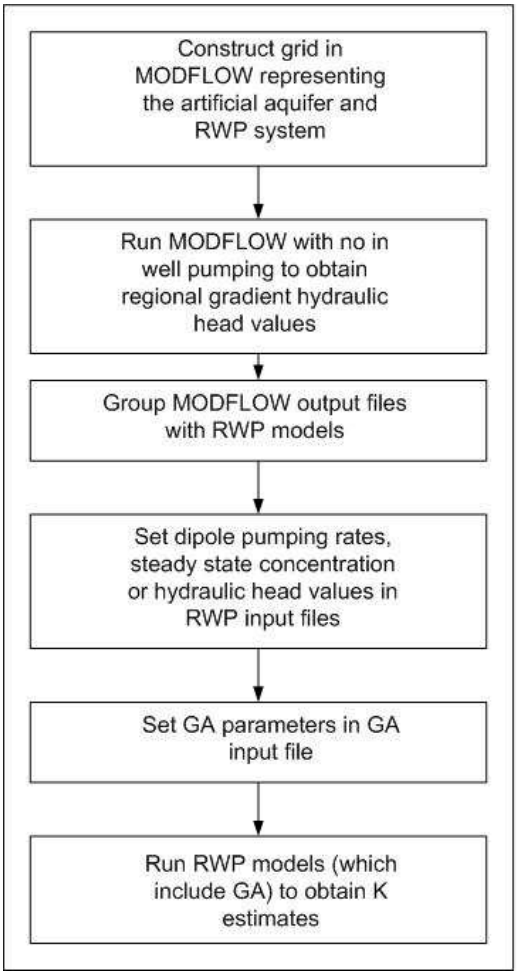

Figure 3.20: RWP system modelling process.

4. Results and Discussion

This chapter presents the results of the artificial aquifer recirculating well pair (RWP) experiments and the subsequent modelling of these results to produce estimates of hydraulic conductivity (K). Section 4.1 describes the rationale behind, and the results of, an analysis of the K values of the artificial aquifer determined from previous data. The results of this analysis are used to determine the accuracy of the estimates obtained by the RWP methods.

Hydraulic head results from the multi dipole experiments are described in Section 4.2 together with a discussion of potential sources of error in applying these hydraulic heads in the model. The K values obtained from the multi dipole modelling are then presented in Section 4.3 together with an analysis of the influence of pump rate and incidence angle on the accuracy of the results. A sensitivity analysis of the values is also presented. A discussion on the discrepancy between actual K values and those estimated by the multi dipole RWP model are presented in Section 4.4.

Breakthrough curve graphs from the fractional flow approach are shown in Section 4.5 together with a discussion on how the steady state concentration values were obtained. Section 4.6 presents the estimated K values obtained from applying the steady state concentration values to the fractional flow model. These results are then compared to the K values of the aquifer determined in Section 4.1. Effects of changing the flow rate and incidence angle of the well pairs are also discussed.

4.1 Independent Determination of the Hydraulic Conductivity of the Artificial Aquifer

This section establishes the K value of the artificial aquifer that will be used to compare with the estimated K values obtained by the RWP method. Table 4.1 summarises the K values obtained in previous studies. The methods used to obtain these values are described in Section 3.3. These methods measure K at different scales and incorporate differing measurement errors which can account for the variability between the measurements.

Table 4.1: Summary of hydraulic conductivity values obtained from previous studies.

Method		Hydraulic Conductivity (m/d)	Range (m/d)
Hazen Grain size		249	
Darcy's Law (Close 2008)			160 -206
Tracer test (Bright 2002)		181	79- 479
Tracer test (Close 2008)		155	80- 621
Mass Flux method	**Dipole**	170	162- 175
	Fractional Flow	171	162- 174
Unconfined Heads		217	166- 255

Hydraulic conductivity values determined from Darcy's law (Equation 3.3) for the experiments undertaken in this study are presented in Table 4.2. Aquifer flow rate (Q) and hydraulic gradient (I) are given in the table and a value of 12.22 m^2 was determined as the cross-sectional area of the artificial aquifer. The calculated error shown in Table 4.2 represents the sum of the errors in measuring of the hydraulic gradient and the aquifer flow rate.

Table 4.2: Hydraulic conductivity values determined from Darcy's law for the present experiments.

	Data obtained	Hydraulic Gradient (I)	Aquifer Flowrate (Q) (m^3 d^{-1})	K=Q/AI (m/d)	Calculated Error
FF1	**April 2003**	0.00149	2.92	160	+/- 13
FF2	**March 2004**	0.00154	3.27	174	+/- 15
FF3	**September 2004**	0.00143	2.86	164	+/- 18
FF4 and MD6	**January 2006**	0.00132	3.06	190	+/- 13
FF5 and MDA	**March 2006**	0.00126	2.68	174	+/- 12
MD1-5	**November 2007**	0.00109	2.78	209	+/- 18
Average				178	+/- 15

The K values in Table 4.2 are similar to the values calculated for the various methods in Table 4.1, with the exception of the grain size analysis. The results in Table 4.2 were obtained over a period of several years. The aquifer permeability, and therefore K, may have altered over this time period due to clogging from fines or bacterial growth, or from flushing of fines. These processes together with error in the measurement of parameters may account for the variations in K seen in Table 4.2.

The K values in Table 4.2 are calculated from parameters derived for the entire aquifer and therefore provide an average K value for the aquifer. These K values could be used to compare to the values of the RWP system if the artificial aquifer was totally homogeneous and isotropic. This, however is not the case, as has been demonstrated in previous studies (Close et al., 2008). This heterogeneity may have arisen from non-uniform packing or differential compaction of sand during the aquifer construction or from redistribution of fines throughout the life of the artificial aquifer.

The RWP system calculates an average K value of the aquifer from within the area of aquifer affected by the pumping. To obtain a K value for the same area of aquifer with which to compare to the K obtained by the RWP system this study reinterpreted the individual tracer test data obtained by Close et al. (2008), and shown in Table 3.3, to obtain

sample point to sample point velocities. Close et al. (2008) used the curve fitting program, CXTFIT (Toride et al., 1995) to fit breakthrough curves at each sample point and to calculate the velocity of the tracer mass for each breakthrough curve. These velocities were calculated from the header tank to the individual sample points. These results incorporate the velocity profile of the entire flow path from the header tank to the sample point. The RWP system, when pumping creates a dipole flow cell in a portion of the artificial aquifer; therefore K is only estimated for that portion of aquifer. Therefore, to obtain accurate estimates of K for the portion of aquifer in which the RWP system was operated, a method of converting the whole aquifer tracer tests to tracer tests that matched the area of the RWP recirculating cell was performed.

To achieve this, the velocities between adjacent sample points were calculated for sets of breakthrough curves. The travel times determined from the centre of mass of the breakthrough curves at two sample points, one immediately down gradient of the other were subtracted to obtain the time travel time between the two points (Figure 4.1).

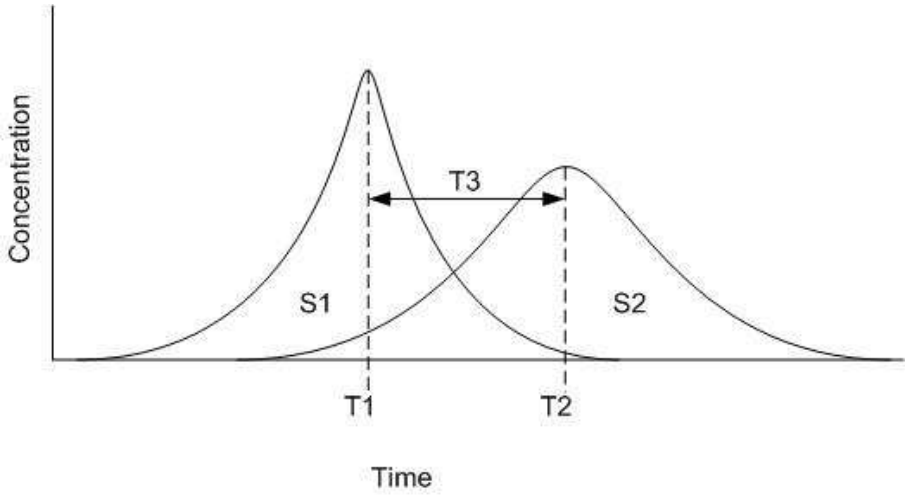

Figure 4.1: Sample point to sample point velocity method.
S1 is an up gradient sample point and S2 is the sample point immediately down stream of S1 T1 and T2 are the travel times for the centre of mass to reach S1 and S2. T3 is the difference between T2 and T1 which is the travel time between the two sample points.

Sample points that did not have complete breakthrough curves associated with them were excluded from this analysis. Also, for this study, breakthrough curves that CXTFIT was unable to match accurately were matched manually. The distance between each pair of adjacent sample points was divided by the time the peak takes to travel between the two points to give the velocity of the tracer between them (Equation 4.1).

$$V = \frac{S_2 - S_1}{T_2 - T_1} \quad \textbf{(4.1)}$$

where S_1 is the distance from the header tank to the first sample point, S_2 is the distance from the header tank to the second sample point immediately down gradient of the first sample point, T_1 is the time taken for the centre of mass of the tracer peak to reach the first sample point and T_2 is the time taken for the centre of mass of the tracer peak to reach the second sample point.

Velocity values calculated from Equation 4.1 in conjunction with the artificial aquifer porosity value (0.44) and hydraulic gradient (0.0089) were substituted into Equation 3.4 and a K distribution table for the artificial aquifer was produced (Table 4.3). This K estimation method assumes that the tracer travels directly from sample point to sample point with the regional hydraulic gradient.

Table 4.3: Distribution of hydraulic conductivities calculated by well to well tracer travel time.

Well ID	Sample Point Depth (m)	Hydraulic Conductivity (m/d)			
		Header Tank-2.75m	2.75m - 4.75m	4.75m - 6.75m	6.75m - 8.75m
A	0.4	NA*	NA*	NA*	NA*
	1	NA*	322	404	123
	1.6	103	132	237	130
	2.2	115	NA*	160	102
B	0.4	105	218	299	311
	1	104	238	183	NA*
	1.6	98	NA*	114	219
	2.2	112	100	140	113
C	0.4	106	NA*	NA*	156
	1	97	NA*	95	325
	1.6	105	NA*	133	117
	2.2	138	NA*	113	124
D	0.4	104	153	148	322
	1	93	118	105	NA*
	1.6	105	123	146	147
	2.2	148	93	137	205
E	0.4	138	152	174	NA*
	1	101	136	123	NA*
	1.6	111	130	138	NA*
	2.2	104	124	177	NA*

***Sample points with missing data or undefined breakthrough curves**

Hydraulic conductivities in the zone from the header tank to 2.75m are significantly lower than those in the aquifer as a whole (Table 4.3). The average K value for the header tank to 2.75m zone of the aquifer is 110 m/d as compared with an average of 178 m/d for the entire aquifer. The low K zone may be the result of bacterial growth or physical clogging of the screen separating the header tank and the artificial aquifer medium (Burbery, 2008, pers. comm.). Hydraulic conductivity values measured from the header tank to the sampling points will be reduced due to this low K zone, as compared to the well-to-well

values calculated in Table 4.3. The low K zone at the header tank screen will not affect K values calculated by Darcy's Law (Table 4.2) because the manometers used to measure the hydraulic gradient of the aquifer are located within the aquifer (Figure 3.1). However, the K values measured by Bright et al. (2002) and used by Kim (2005) and Yoon (2006) to compare with the estimated K values derived in their theses will be affected by this zone.

To obtain a localised K value for each of the three well configurations used in the present study (Figure 3.8), the sample point to sample point values obtained for the area in the vicinity of the well pair were averaged. For fractional flow experiments 1, 2 and 3 (FF1-3), which were carried out in row 6 (5.75m), the K data obtained from 4.75m to 6.75m were averaged. Fractional flow experiment 4 (FF4) and multi dipole experiments 1-6 (MD1-6) were carried in row 7 (6.75m) and therefore data from 4.75m to 8.75m were averaged. Fractional flow experiment 5 (FF5) and the angle multi dipole experiment (MDA) were conducted with one dipole in row 5 (4.75m) and the other dipole in row 7 (6.75m) and therefore data from 2.75m to 8.75m were used to obtain a comparative K value. The results of this averaging are compiled in Table 4.4. The edges of the artificial aquifer show preferential flow (Close et al., 2008) and therefore average K values without the edge rows (Row A and E) were also calculated.

Table 4.4: Hydraulic conductivity values calculated from the average of well to well results for the sections of aquifer in which the RWP experiments were untaken.

		FF 1, 2, 3		FF 4, MD1-6		FF 5, MDA	
Data Used	Average of entire aquifer	4.75m -6.75m	4.75m -6.75m Rows B,C,D	4.75m -6.75m and 6.75m - 8.75m	4.75m -6.75m and 6.75m - 8.75m Rows B,C,D	2.75m -4.75m, 4.75m -6.75m and 6.75m - 8.75m	2.75m -4.75m, 4.75m -6.75m and 6.75m - 8.75m Rows B,C,D
Average (m/d)	155	168	147	175	174	170	168
Median (m/d)	118	143	137	146	146	139	143
Max (m/d)	583	404	299	404	325	404	325
Min (m/d)	80	95	95	95	95	93	93
Count	62	18	11	31	21	44	28

The greatest proportion of flow during the operation of a RWP system is in the vicinity to the well system (Cunningham et al., 2004). Figure 4.2 shows a MODFLOW simulation of the head gradient generated by the RWP system. The path lines of particles generated by MODPATH at the injection screen are also shown. Each arrow in the figure represents an elapsed time period of 0.2 days. Flow occurs perpendicular to all the piezometric contours therefore large amounts of water enters the system from upstream and down stream of the pumping wells. The greatest contribution to the K values obtained for the aquifer will be from the areas with the steepest piezometric surface, which is the area closest to RWP system (rows B, C and D).

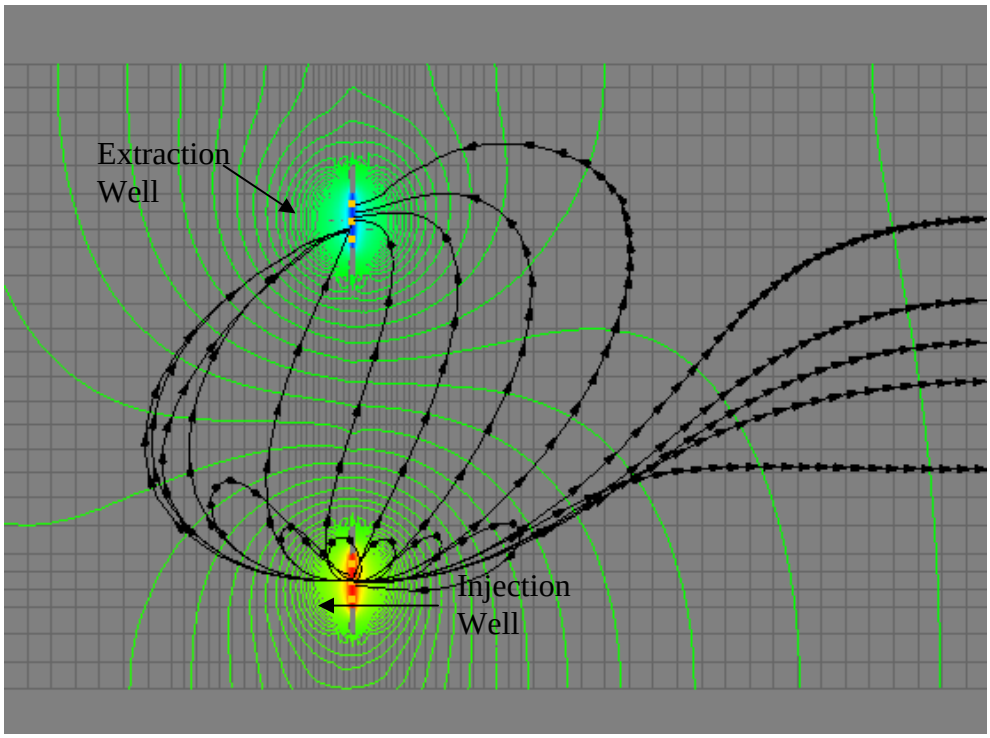

(a)

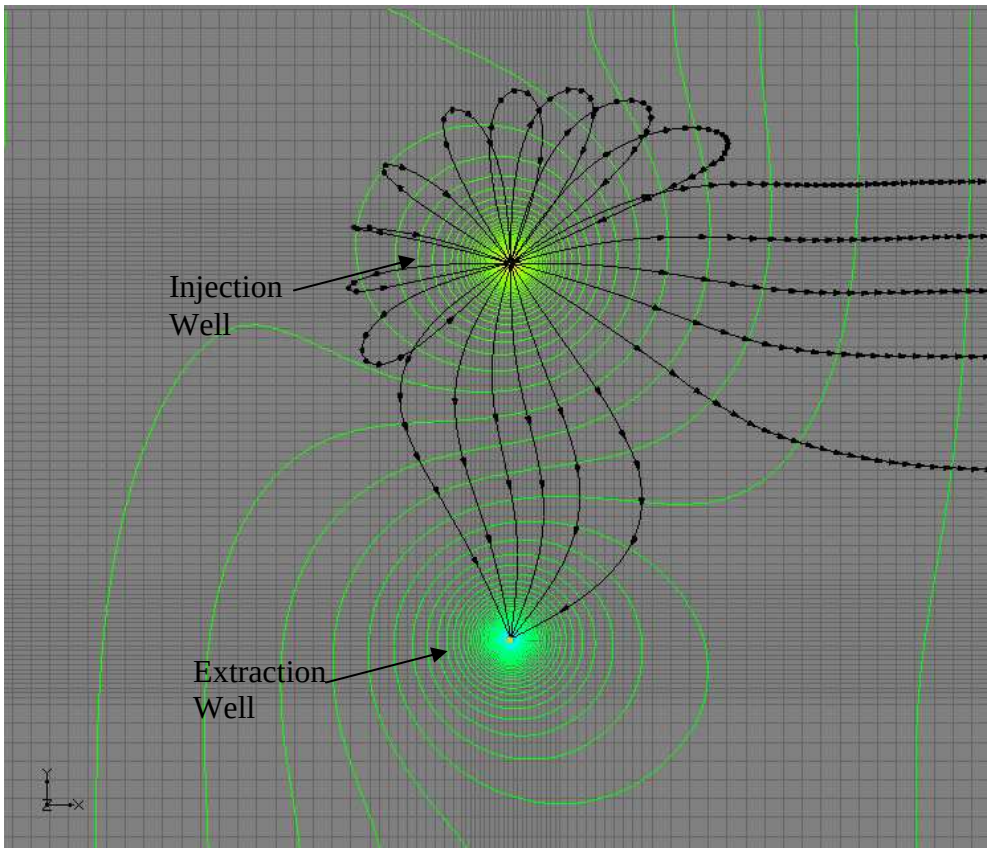

(b)

Figure 4.2: Lateral (a) and plan (b) view of a MODFLOW simulation of the operation of the RWP system. Black lines represent the paths of particles from the injection well. Each arrow represents the position of the particle after 0.5 days. Green lines link areas with the same hydraulic head.

The K values used to ascertain the accuracy of the RWP methods are therefore the average K values calculated in the vicinity of the RWP system:

- FF 1, 2, 3: **147** m/d
- FF 4 and MD 1-6: **174** m/d
- FF 5 and MDA: **168** m/d

4.2 Multi Dipole RWP Experimental Results

4.2.1 Hydraulic Head Results

The hydraulic heads (draw down (-) or mounding (+)) recorded for the five flow rates used for the multi dipole experiments (MD1-5) are shown in Table 4.5. The 8 observation point positions are shown in Figure 3.7. Five hydraulic head values were excluded from the K analysis because they significantly deviated from the expected linear relationship with increasing flow rate as compared to the remainder of the hydraulic head values (Figure 4.3-4.5). The outliers are attributed to measurement error. The 5 values excluded are marked with an asterisk in Table 4.5.

Table 4.5: Hydraulic head values obtained from the RWP multi dipole experiments (MD 1-5) from 8 observation points.

	Pumprate		Obs 1	Obs 2	Obs 3	Obs 4	Obs 5	Obs 6	Obs 7	Obs 8
Experiment	UpFlow	Downflow								
	(m^3/d)	(m^3/d)	(m)	(m)	(m)	(m)	(m)	(m)	(m)	(m)
MD1	1.54	1.37	0*	0.0045	0.036*	-0.015	-0.0045	-0.004	-0.005*	0.0165
MD2	3.02	3.01	0.006	0.007	0.0415	-0.0285	-0.0085	-0.0085	-0.0355	0.032
MD3	4.25	4.27	0.01	0.0125*	0.0535	-0.059*	-0.015	-0.013	-0.056	0.051
MD4	5.85	5.65	0.0115	0.0125	0.0715	-0.061	-0.0185	-0.017	-0.0765	0.065
MD5	7.12	7.20	0.0145	0.0145	0.097	-0.071	-0.0215	-0.02	-0.096	0.098

***values excluded from the study**

Table 4.6 shows the hydraulic head values measured for experiments MD6 and MDA. These experiments used 6 observation points the positions of which are again shown in Figure 3.7. These observations were used to determine the effect of changing the incidence angle of the wells on the K estimates obtained.

Table 4.6: Hydraulic head values for MD6 and MDA.

Experiment	Pumprate UpFlow (m^3/d)	Pumprate Downflow (m^3/d)	obs1 (m)	obs3 (m)	obs4 (m)	obs5 (m)	obs7 (m)	obs8 (m)
MD6	6.51	6.58	0.0137	0.0795	-0.099	-0.0129	-0.1076	0.0615
MDA	6.63	6.44	0.0186	0.0925	-0.1300	-0.0158	-0.1159	0.0618

4.2.2 Factors Influencing Hydraulic Head

The RWP multi dipole method uses hydraulic head values to estimate K. The model assumes that hydraulic head results are solely influenced by the well and aquifer geometry, pumping rate and regional flow, which are known, and by the aquifer K, the parameter to be estimated. Additional factors can influence the measured hydraulic head values apart from those mentioned above. To generate accurate K estimates these additional factors need to be incorporated into the multi dipole RWP model. The additional factors that can influence the measured hydraulic head include:

- turbulent flow to the well, leading to well loss
- overdevelopment or clogging of the aquifer adjacent to well
- heterogeneity of the aquifer (as the multi dipole RWP model was developed assuming homogeneity, which has been shown to not be the case in the artificial aquifer)

Turbulent flow leading to well loss

An investigation to determine if turbulent flow was occurring is described in this section. Water flow can be either laminar or turbulent. In contrast to turbulent flow, laminar flow occurs when water molecules travel in smooth paths parallel to solid boundaries. Laminar

flow is dominated by viscous flow and therefore hydraulic heads vary linearly with increase in velocity (Bouwer, 1978). The majority of natural groundwater flow is laminar. Turbulent flow develops when inertial forces become dominant. This may occur if aquifer pore spaces and groundwater velocities are large. In groundwater systems turbulent flow can occur in the vicinity of pumping wells which create steep hydraulic gradients and therefore fast velocities. The RWP system creates steep hydraulic gradients between the screens in a single well vertically (Figure 4.2a), and between the wells horizontally (Figure 4.2b). Head losses vary exponentially with increasing velocity when flow is turbulent. Turbulent flow is characterised by a parameter called the Reynolds number, which is dimensionless, and expresses the ratio between inertial and viscous forces in a fluid. If non-laminar flow occurs, models relying on Darcy flow such as MODFLOW (used in this study) will yield inaccurate results.

Departures from laminar flow have been reported at Reynolds numbers ranging from 60 to 600 and have been experimentally shown to occur at Reynolds numbers of 1 to 10 (Fetter, 2001). An analysis to determine the Reynolds number for the experiments conducted in this study was undertaken. MD5 possessed the highest flow rate of the experiments carried out for this thesis (7.2 m^3/d) and therefore was the most likely experiment to exhibit non-laminar flow. The fastest velocities in the RWP system occurred at the pumping or injection screens where flow is restricted. Reynolds number was calculated from Equation 4.2.

$$R = \frac{\rho v D}{\mu} \qquad \textbf{(4.2)}$$

where R is the Reynolds number, ρ is the density of water, v is the velocity, D is the average grain size of the aquifer material and μ is the viscosity.

The velocity at the screen was calculated with equation 4.3.

$$v=Q/A_s \quad \textbf{(4.3)}$$

where v is velocity, A_s is screen area and Q is flow rate.

Using Equation 4.2 and the values listed below, the Reynolds number for MD5 was calculated to be 58.

v=0.066138m/s (calculated from Equation 4.3)

ρ =999kg/m^3

D =0 .001m (average grain size of aquifer material (range 0.6-2mm)

μ = 0.00114kg/m.s

The Reynolds number indicates that the system has the potential to generate turbulent flow, invalidating the assumptions used in MODFLOW. The region of restricted flow, and therefore high Reynolds number, was at the well screen and aquifer immediately adjacent to it. This area was a small proportion of the aquifer but may be important as hydraulic head values were measured within the well screen. Calculating well loss will indicate if the head values measured within the well are the actual values of the aquifer or are a combination of head values of the aquifer and well. The head of the aquifer is needed if the K of the aquifer is to be determined.

The multi dipole RWP model assumes that hydraulic head values observed in the pumping well are the result of head losses incurred from within the aquifer adjacent to the pumping well (formation loss), which is a function of the K. This assumption allows the K of the formation to be calculated from the head loss. Hydraulic head can also occur due to restricted (non-laminar) or enhanced flow through the filter pack (if present) and the well screen. This hydraulic head is termed well loss. Well loss can be calculated for a well installed in a homogeneous, isotropic, confined aquifer of infinite extent and pumping at a constant discharge rate (Equation 4.4) (Avci, 1992).

$$s(t) = B(t)Q + CQ^P \quad \textbf{(4.4)}$$

where *s(t)* is time dependent drawdown, *B(t)* is the Cooper-Jacob approximation of the Theis well function, *Q* is constant discharge rate, *C* is the well loss co-efficient and *P* is the exponent of well discharge.

B(t)Q represents formation drawdown and CQ^P represents drawdown from well loss. Formation loss varies linearly with *Q* because aquifer flow is laminar, whereas the well loss component will vary according to a power function (Q^P) due to turbulent flow through the screen and gravel pack (if present). In general, for relatively low pumping rates, the well loss co-efficient (*C*) will be zero and therefore neglected, but for high pumping rates, or for a low quality of well completion, it may represent a significant proportion of the total loss. The well radius and screen length may have a large effect on the entrance velocity into the well screen. The experiments conducted for this thesis used wells with small well diameter, inefficient screen design and limited screen area (Figure 3.3) due to the original design of the artificial aquifer. These factors increase screen velocity and may

lead to well loss. Appropriate well construction utilising sufficient screen or slot area and sufficient radius will keep well loss to a minimum (Bear, 1979).

A step drawdown test in the artificial aquifer for the Integral Pumping Test (IPT) method was conducted (Goltz, 2006, pers. comm.). Analysis of the step drawdown test resulted in Equation 4.5.

$$S_W = 28.2Q^{1.46} \quad \textbf{(4.5)}$$

where *Sw* is drawdown due to well loss and *Q* is the pumping rate.

The hydraulic head values used in the IPT method were corrected and then re-calculated to obtain K values which were used to measure contaminant flux. The corrected values improved the match between the calculated and observed flux values as calculated by the IPT method. The IPT method is similar to a forced gradient tracer test (Section 2.1.9) where water is withdrawn from a standard extraction well and re-injected into an injection well up gradient to create a recirculation cell within the aquifer. The RWP well configuration, used in this thesis, was non-standard and therefore results obtained from the IPT step drawdown test may not be transferable to the RWP system. To obtain a step drawdown test for the RWP well configuration, the 5 multi dipole tests were re–interpreted.

The 5 multi dipole experiments were conducted at 5 flow rates and therefore can be analysed together as a step drawdown test. A step drawdown test is usually conducted by pumping a well at a known *Q*, and measuring the resulting drawdown at steady state, then progressively increasing the flow rate and making further observation. This is repeated for

4 or 5 Q values. $B(t)$, C and P are then evaluated graphically (Rorabaugh, 1953) or with computer based methods (Avci, 1992).

Plots of Q versus hydraulic head for all observation points are shown in Figures 4.3-4.6. Observation points exhibited a linear flow rate versus hydraulic head response, as expected. Both screens show similar magnitude of drawdown as compared to mounding with some exceptions (identified as outliers). These outliers are thought to be caused by measurement error. This indicates that only the first (linear) part of the step drawdown equation (Equation 4.4) is needed to describe the hydraulic head response and therefore well loss was not included in the analysis of these experiments.

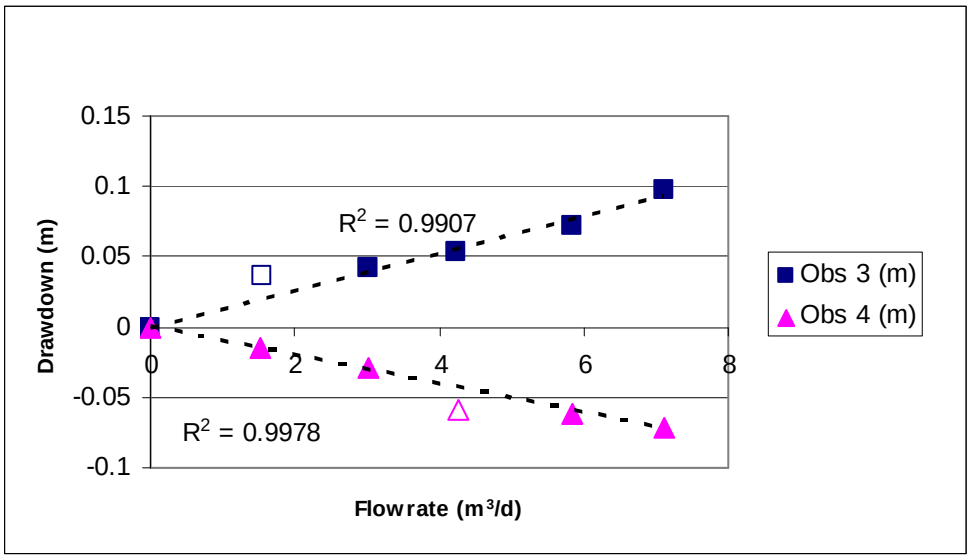

Figure 4.3: Flow rate vs. hydraulic head for observation points 3 and 4. R^2 values calculated excluding outliers (outliers shown as unshaded symbols).

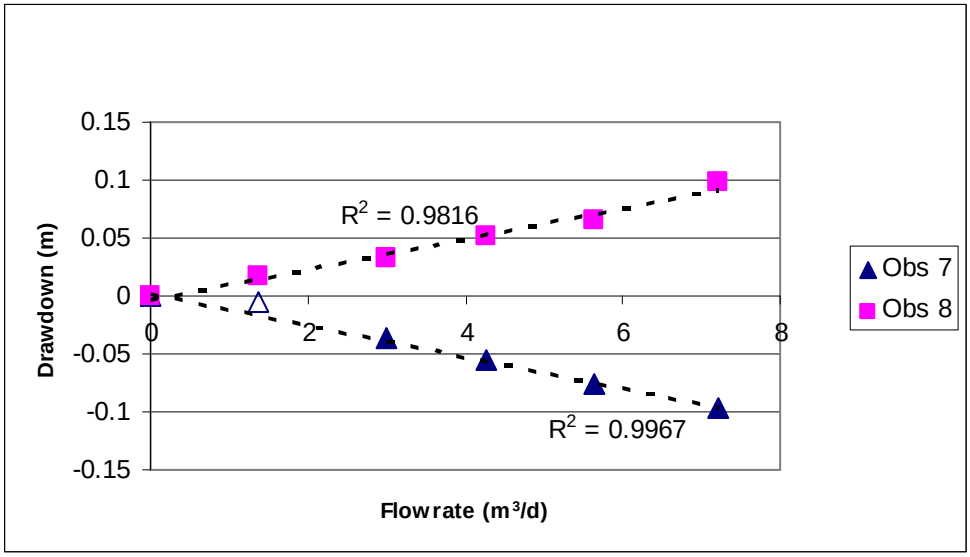

Figure 4.4: Flow rate vs. hydraulic head for observation points 7 and 8. R^2 values calculated excluding outliers (outlier shown as unshaded symbols).

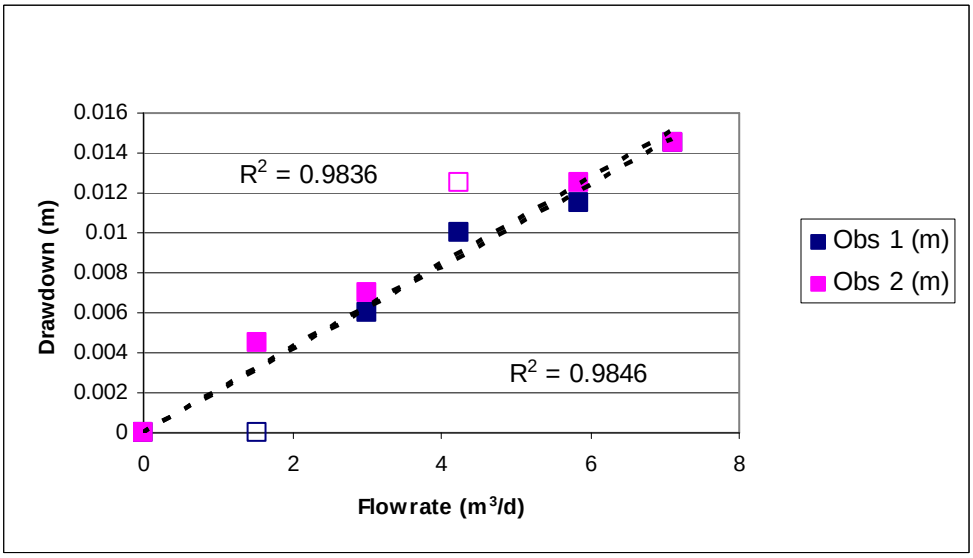

Figure 4.5: Flow rate vs. hydraulic head for observation points 1 and 2. R^2 values calculated excluding outliers (outliers shown as unshaded symbols).

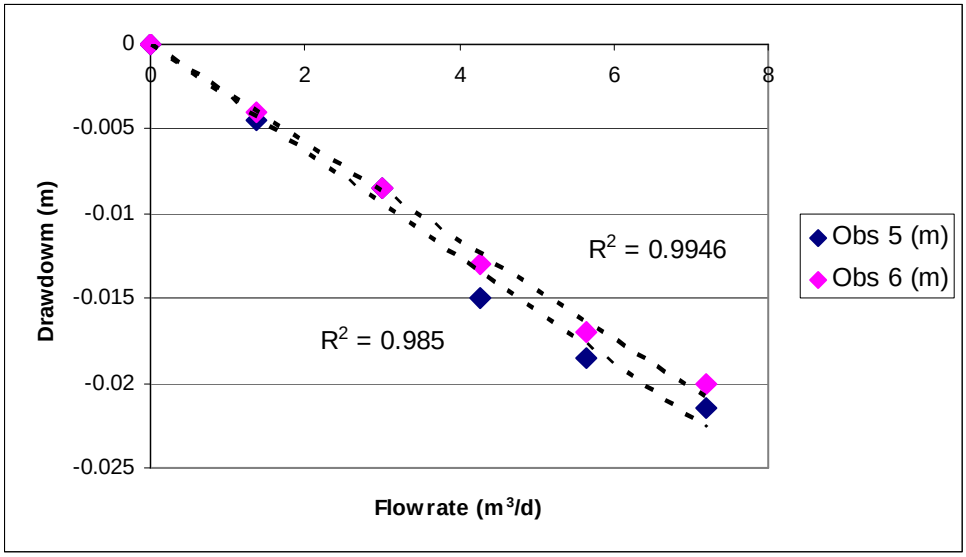

Figure 4.6: Flow rate vs. hydraulic head for observation points 5 and 6.

In field applications of the multi dipole method a step drawdown test should be conducted to determine if well loss is occurring. The well loss value calculated at the flow rate that the multi dipole test is carried out can then be added or subtracted from the hydraulic head or mounding values used in the model.

Overdevelopment and clogging of the aquifer adjacent to well

Fine material transported by pumping during a RWP experiment may alter the formation K in the vicinity of the extraction screens, or clog the injection screens. The recirculating nature of the RWP experiments may capture fines from the area around the extraction screen and re-inject these fines into the formation at the injection screen. Peursem et al., (1999) found that continuous pumping in a vertical recirculation well, which is essentially equivalent to a single well in a RWP system, plugs the formation with fines.

Extraction or deposition of fines may have a significant effect on the hydraulic head values obtained from the RWP system. The longer the duration of pumping the more pronounced

the effects of re-working of the fines. The five multi dipole experiments were conducted over a 5 day period limiting potential reworking of the fines within the system. Each of the five fractional flow experiments, on the other hand, were conducted over a 10-14 day period which may be sufficient to produce significant re-working of fines. The experiments were carried out in sequence, with an increase in pumping rate with each additional experiment which may result in later experiments being affected to a greater extent. As discussed above, there was a linear increase in hydraulic head with increasing pumping rate which indicates that there was no progressive effect with increasing flow rate.

High K zones in the vicinity of the pumping wells used in this study were detected using the unconfined head method (Burbery, 2008. pers. comm.) (Section 3.3.5). This may indicate over development of the aquifer from the continuous pumping or aquifer heterogeneity. Re-working of fines can be examined more easily by plotting the absolute drawdown values of the injection and extraction screens (Figures 4.7). The four observation points have approximately equal relative flow rates and therefore should produce equal drawdown values. Observation point 4 deviates from the other sample points, with an average difference of -0.0165m from observation point 3. This deviation could indicate over development of the aquifer in the vicinity of this screen from pumping, or could result from an area of high K around the screen due to aquifer heterogeneity. A consistent error in the measurement of the drawdown at this screen may also result in this deviation. The measurement technique for all screens was identical and the systems checked thoroughly so this hypothesis is unlikely.

Kim (2005) observed non-uniform drawdown values for observation points above the well screens which he interpreted as measurement error. The observation points in this study

above the wells screens (Figure 4.5 and 4.6) did not exhibit the deviations found by Kim, (2005). This may be the result of greater accuracy of measurement. The deviations observed in observation point 4 could also result from aquifer heterogeneity, discussed in the following paragraphs.

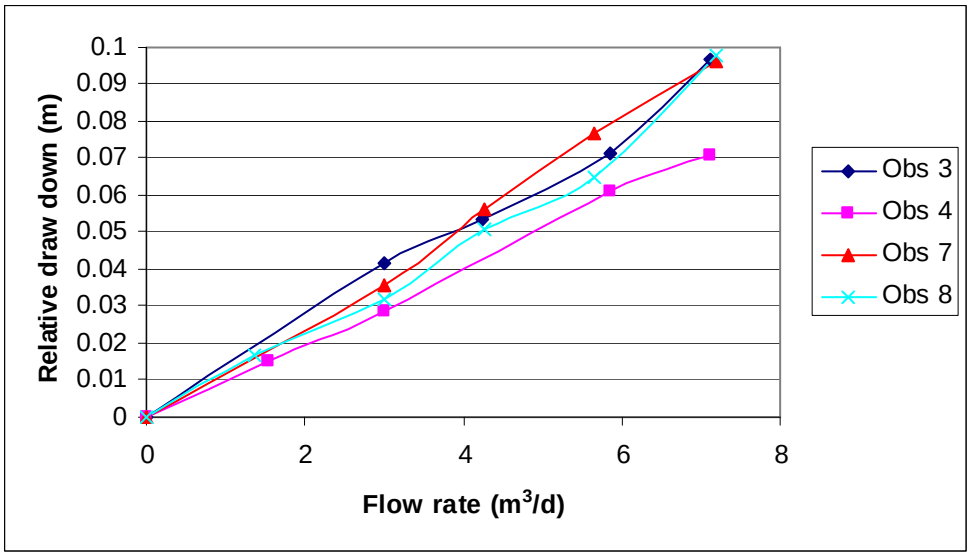

Figure 4.7: Absolute drawdown of observation points 3, 4, 7 and 8.

Aquifer Heterogeneity

The K values determined in Table 4.3 can be compared to the drawdown in the well screen to assess if aquifer heterogeneity is causing the deviation in observation point 4. The K values in the column labelled 4.75m - 6.75m and 6.75m-8.75m in row B and D of Table 4.3 correspond to the portion of the aquifer where the observation points are located (Figure 3.7). The average K value calculated in the vicinity of observation point 3 was 264 m/d, and 146 m/d for observation point 4. The average K values calculated in the vicinity of the second dipole were 192m/d for observation point 7 and 159 m/d for observation point 8. The high conductivity values produced for observation points 3 and 7 are the result of a high conductivity zone in the upper layer of the aquifer (Close et al., 2008). This layer

was not reflected in the observed drawdown values. Observation point 4, which showed lower hydraulic head compared to other observation points, gave the lower K value, which is the opposite of what would be expected if the K values were influencing the hydraulic head. The K values calculated in Table 4.3 may not be sensitive enough to pick up the fluctuations in K that are influencing the observed hydraulic heads. Also, the K distribution of the artificial aquifer could have altered slightly over the time period from when the tracer test results were gathered and when the RWP experiments were carried out.

The centres of the upper well screens were 0.65m from the top impermeable layer and the centres of the lower well screens were 0.45m from the bottom of the aquifer. If the closer impermeable layer were influencing observed hydraulic heads the lower screens should show larger relative hydraulic head values as compared to the upper screens. This is not the case. Therefore the pumping or injection screens are located at a sufficient distance for the impermeable layers to have a minimal effect on hydraulic head.

Table 4.6 showed the hydraulic head values measured in MD6 and MDA. Observation point 3 and 8 are measured in injection screens and observation points 4 and 7 are measured in extraction screens. The hydraulic head in the injection screen is consistently less than the hydraulic head observed in the extraction screens. These two experiments were conducted over a greater time period than MD1-5 which may influence this response. MD1-6 was conducted in the same wells therefore the heterogeneity of the aquifer should have an equal effect on these experiments. These results are not consistent with the results obtained for the multi dipole experiments. This inconsistency may influence the estimated K values obtained from the RWP methods.

Clogging of the aquifer as a result of the introduction of air bubbles may also influence the observed hydraulic head values. Air entrapped in aquifers may result in spatial and temporal changes in K as the amount of entrapped air alters (Zlotnik et al., 2007). When applied in a field situation, the pumps and all pipe work in a RWP system is located within the aquifer and therefore the chance of air ingress would be minimal after installation. Air entrapped with RWP installation would dissolve into the aquifer water with a rate that would depend on aquifer chemistry, pressure and temperature. In the system used in this thesis, water was pumped from the extraction screen to the surface through the pump and down to the extraction screen. This system greatly enhances the possibility of air entering the aquifer and altering the K. The packers used in the system were inflated with N_2 and therefore could be a source of entrapped gas. The pressure of the packers was measured to ensure a leak free system. There was no evidence of introduction of air or N_2 into the system.

In summary, we have determined that there is no well loss in the RWP system. Although clogging and over development of the formation in the vicinity of the screens may be occurring this can not currently be quantified. Therefore in the following multi dipole analysis the measured hydraulic head results will be utilised by the multi dipole RWP model unaltered.

4.3 Multi Dipole RWP Modelling Results

Estimates of both horizontal and vertical K values (anisotropic) for MD1-5 obtained from the application of the multi dipole RWP model are presented in Table 4.7. Hydraulic conductivity values were estimated using different combinations of hydraulic head

observation points. Modelled K estimates were compared with a K value of 174m/d derived from tracer tests (Section 4.1), and the percent of the actual K tabulated. An indication of the fit between the hydraulic head values calculated by the model to estimate K and the observed hydraulic head values is given as a root mean square deviation (RSMD). The square of the sample correlation co-efficient (r^2) is also calculated. The number of generations taken by the GA to obtain no further change in estimated K is also shown.

Table 4.7: Multi dipole RWP model results for experiments MD 1-5 assuming anisotropy.

Experiment	Observation points used	Estimated Horizontal K m/d	% of actual K	Estimated Vertical K m/d	RMSD (m)	Estimated to actual draw down (r^2)	GA Generations
MD 1 1.46 m^3/d	1,2,4,5,6,8	228	131	455	2.74E-03	0.99	92
	1,2,5,6	40	23	4	2.12E-03	1.00	20
	4	375	216	60	4.00E-03	1.00	27
	4,8	269	155	190	2.00E-03	0.98	108
	8	247	142	71	5.00E-03	1.00	31
MD 2 3.02 m^3/d	1,2,3,4,5,6,7,8	216	124	432	4.90E-03	0.98	87
	1,2,5,6	75	43	136	2.29E-03	1.00	54
	3,4	282	162	60	5.00E-03	0.95	16
	3,4,7,8	300	172	39	4.39E-03	0.97	6
	7,8	300	172	48	9.49E-03	1.00	14
MD 3 4.26 m^3/d	1,2,3,5,6,7,8	217	124	190	7.63E-03	0.97	63
	1,2,5,6	64	37	127	3.12E-03	0.99	29
	3	246	141	71	2.00E-03	1.00	19
	3,7,8	278	160	28	3.32E-03	0.99	38
	7,8	219	126	52	9.85E-03	0.99	7
MD 4 5.75 m^3/d	1,2,3,4,5,6,7,8	215	124	215	9.62E-03	0.96	71
	1,2,5,6	73	42	145	4.27E-03	0.99	69
	3,4	300	172	43	5.15E-03	0.96	13
	3,4,7,8	308	177	18	5.94E-03	0.97	20
	7,8	261	150	54	7.62E-03	0.97	28
MD 5 7.16 m^3/d	1,2,3,4,5,6,7,8	204	117	203	1.23E-02	0.97	139
	1,2,5,6	77	44	150	4.95E-03	0.99	68
	3,4	298	171	29	1.20E-02	0.91	6
	3,4,7,8	293	169	15	1.10E-02	0.94	39
	7,8	216	124	136	1.58E-03	0.99	123

Table 4.8 presents the estimated K for MD1-5 produced by the multi dipole RWP model when vertical and horizontal K are equal (isotropic). Table 4.9 and 4.10 present the results of MD6 and MDA. MDA was performed on a 45 degree angle to the direction of regional

flow and MD6 is the matching experiment performed on a 90 degree angle and used to compare with MDA. The value used to gauge the accuracy of MD6 was 174m/d and for MDA, 168m/d (Section 4.1).

Table 4.8: Multi dipole RWP model results for experiments MD 1-5 assuming isotropy.

Experiment	Observation points used	Estimated Horizontal K m/d	% of actual K	RMSD (m)	Estimated Vertical K m/d	Estimated to actual draw down (r2)	GA Generations
MD 1 1.46 m^3/d	1,2,4,5,6,8	249	128	2.74E-03	249	0.98688	6
	1,2,5,6	61	32	2.12E-03	61	0.99424	6
	4	306	157	4.00E-03	306	1	33
	4,8	257	133	2.00E-03	257	0.98052	5
	8	213	110	5.00E-03	213	0.99999	33
MD 2 3.02 m^3/d	1,2,3,4,5,6,7,8	238	123	4.90E-03	238	0.98132	14
	1,2,5,6	73	38	2.29E-03	73	0.9976	4
	3,4	236	122	5.00E-03	236	0.94787	30
	3,4,7,8	240	124	4.39E-03	240	0.97298	3
	7,8	244	126	9.49E-03	244	0.99467	13
MD 3 4.26 m^3/d	1,2,3,5,6,7,8	213	110	7.63E-03	213	0.97443	4
	1,2,5,6	62	32	3.12E-03	62	0.99259	3
	3	212	109	2.00E-03	212	1	49
	3,7,8	216	112	3.32E-03	216	0.99136	95
	7,8	219	113	9.85E-03	219	0.98886	5
MD 4 5.75 m^3/d	1,2,3,4,5,6,7,8	228	117	9.62E-03	228	0.96968	19
	1,2,5,6	71	37	4.27E-03	71	0.98746	6
	3,4	242	125	5.15E-03	242	0.95501	6
	3,4,7,8	230	119	5.94E-03	230	0.96713	7
	7,8	219	113	7.62E-03	219	0.96642	178
MD 5 7.16 m^3/d	1,2,3,4,5,6,7,8	215	111	1.23E-02	215	0.95972	1
	1,2,5,6	74	38	4.95E-03	74	0.98674	11
	3,4	232	120	1.20E-02	232	0.90708	5
	3,4,7,8	217	112	1.10E-02	217	0.94364	39
	7,8	203	105	1.58E-03	203	0.98799	14

Table 4.9: Multi dipole RWP model results for MD6.

	Observation points used	Estimated Horizontal K m/d	% of Actual K	Estimated Vertical K m/d	RMSD (m)	Estimated to actual draw down (r^2)	GA Generations
Isotropic	1,5	97	56	97	1.00E-03	1.00	7
	1,3,4,5,7,8	206	118	206	1.60E-02	0.96	2
	3,4,7,8	206	118	206	1.89E-02	0.96	1
Anisotropic	1,5	82	47	20	1.00E-03	1.00	16
	1,3,4,5,7,8	228	131	103	1.63E-02	0.96	124
	3,4,7,8	264	152	27	1.92E-02	0.96	6

Table 4.10: Multi dipole RWP model results for MDA.

	Observation points used	Estimated Horizontal K m/d	% of Actual K	Estimated Vertical K m/d	RMSD (m)	Estimated to actual draw down (r^2)	GA Generations
Isotropic	1,5	78	46	78	1.58E-03	1.00	8
	1,3,4,5,7,8	180	107	180	2.24E-02	0.95	5
	3,4,7,8	181	108	181	2.65E-02	0.95	8
Anisotropic	1,5	82	49	20	2.83E-03	1.00	16
	1,3,4,5,7,8	191	114	123	2.25E-02	0.95	53
	3,4,7,8	193	115	117	2.65E-02	0.95	37

The multi dipole models using sample points 1, 2, 5 and 6 for the analysis gave an estimate of K that was significantly less than the K value determined for the aquifer (Section 4.1). These values ranged from 40 to 97 m/d, or 23 % to 56% of the aquifer K value. These observation points produced greater hydraulic head values than estimated by MODFLOW if K values calculated in Section 4.1 are used. These observation points had low hydraulic head change compared to observation points 3, 4, 7 and 8 because of their greater distance from the injection or extraction screens (Table 4.7 and 4.8).

Initially it was hypothesised that the difference in estimated K using the observation points 1, 2, 5 and 6 was caused by errors in measuring the small hydraulic head changes in these observation points. Small measurement errors in these observation points equate to large errors in estimates of K. A sensitivity analysis was therefore undertaken on observation points 1, 2, 5, and 6 for MD 4 to determine if measurement error could result in the large differences in observed and modelled hydraulic head values. Increasing or decreasing the observed hydraulic heads by as much as 20% did not account for the discrepancy between K estimated by the multi-dipole method and the actual K value of the artificial aquifer (Figure 4.8). A 20% change in the hydraulic head values equates to an average difference of 0.003m over the 4 sample points whereas the difference between the observed and modelled values on average is 0.01m for MD4. The accuracy of the measurement

technique was plus or minus 0.0005m. Therefore, low K estimates obtained are not accounted for by measurement error or by errors in measuring the position of the sample point (vertical position).

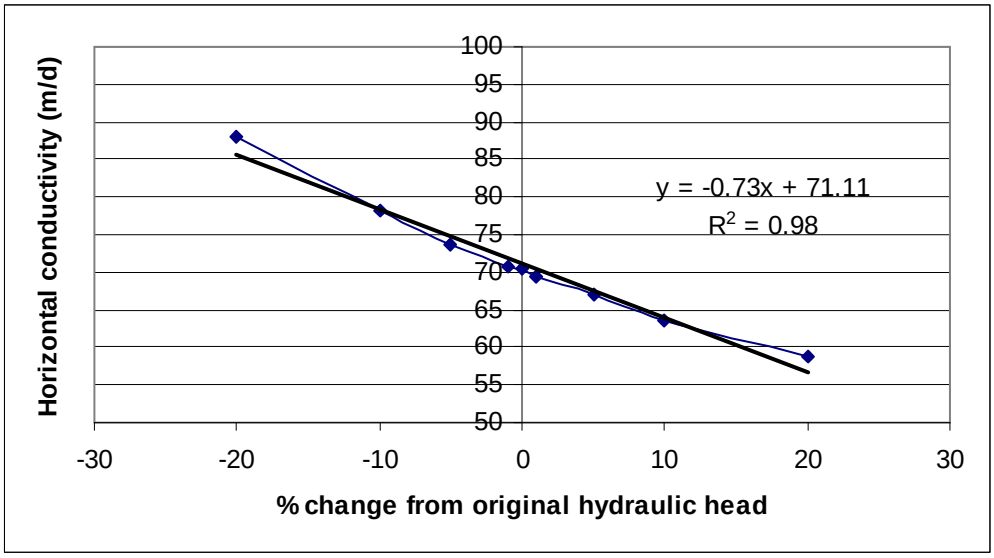

Figure 4.8: Sensitivity of observation points 1, 2, 5, and 6.

Figure 4.9 illustrates the differences between the hydraulic head estimated by MODFLOW, the multi dipole RWP model, and the observed values. The change in hydraulic head over vertical distance is small above the packers therefore error in vertical position would not account for the hydraulic head discrepancies.

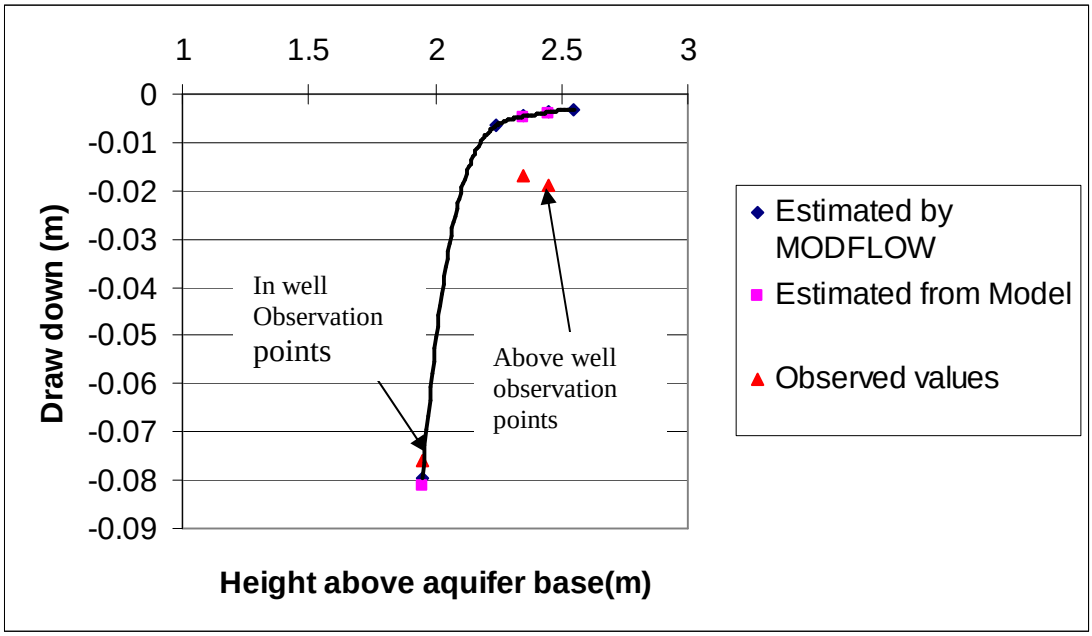

Figure 4.9: Comparison of observed head, head estimated by MODFLOW and head estimated by the multi dipole RWP model.

Another possible reason why the RWP multi dipole model did not match observed hydraulic head values for these observation points is that the model does not account for the open well from the packers to the surface (Figure 3.5). The open well extending to near the pumping screens may act as a conduit for flow of water to the pumping screens, similarly to a high K zone within an otherwise low K aquifer. Higher flow in the well creates greater drawdown at the observation points compared to the drawdown in the adjacent aquifer. The multi dipole RWP model assumes that the K in the well is identical to the K in the aquifer, and therefore will not account for increased flow in the well. This hypothesis was tested by assigning different in well K and aquifer K values within MODFLOW. The difference between a uniform K value for the entire aquifer and using a high K zone in the well was on average 0.0005m whereas the average difference between the observed and modelled hydraulic head values was 0.01m, therefore using high in well K would improve K estimation but does not account for the full difference in values. More

research is needed to understand why using observation points above the well screen (Obs 1, 2, 5 and 6) did not produce accurate K estimates.

The multi dipole experiments, assuming anisotropy, produced K estimates ranging from 204-308 m/d (17 to 116% greater than actual K), when tests using only observation points 1, 2, 5 and 6 are excluded (Table 4.7). Tests using all sample points gave relatively good agreement with aquifer K (17 to 31% greater) with an average K of 216m/d. The change in hydraulic head values of observation 1, 2, 5, and 6 was small in comparison to observation points 3, 4, 7 and 8 and therefore measurements at these points did not greatly affect the analysis. Tests using only observation points 3, 4, 7 and 8 gave a range of 24 to 116% difference compared to the actual aquifer K.

A sensitivity analysis was conducted to determine the effect of changing the observed hydraulic head values on estimated K values. This was conducted on MD4 by altering the observed hydraulic heads by known percentages and inputting these values into the multi dipole model enabling it to optimise K. Table 4.11 shows the observed (original) hydraulic head values together with the altered values used to conduct the analysis.

Table 4.11: Values used in the sensitivity analysis.

	Original Values (m)	+1% (m)	-1% (m)	+5% (m)	-5% (m)	+10% (m)	-10% (m)	+20% (m)	-20% (m)
Obs 1	0.0115	0.0116	0.0114	0.0121	0.0109	0.0127	0.0104	0.0138	0.0092
Obs 2	0.0125	0.0126	0.0124	0.0132	0.0119	0.0138	0.0113	0.0150	0.0100
Obs 3	0.0715	0.0722	0.0708	0.0753	0.0679	0.0787	0.0644	0.0858	0.0572
Obs 4	-0.0610	-0.0616	-0.0604	-0.0642	-0.0580	-0.0671	-0.0549	-0.0732	-0.0488
Obs 5	-0.0185	-0.0187	-0.0183	-0.0195	-0.0176	-0.0204	-0.0167	-0.0222	-0.0148
Obs 6	-0.0170	-0.0172	-0.0168	-0.0179	-0.0162	-0.0187	-0.0153	-0.0204	-0.0136
Obs 7	-0.0765	-0.0773	-0.0757	-0.0805	-0.0727	-0.0842	-0.0689	-0.0918	-0.0612
Obs 8	0.0650	0.0657	0.0644	0.0684	0.0618	0.0715	0.0585	0.0780	0.0520

Analysis was conducted on 3 combinations of observation points, all observation points, observation points 3, 4, 7 and 8, and observation points 1, 2, 5 and 6. All combinations of observation points exhibited a linear response to increasing or decreasing the observed hydraulic head (Figure 4.8, 4.10 and 4.11). This illustrates that the K estimates produced by the multi dipole method are sensitive to the hydraulic head values. A linear response is to be expected because hydraulic head changes linearly with aquifer K. That is, doubling the aquifer K will produce half the drawdown in a well.

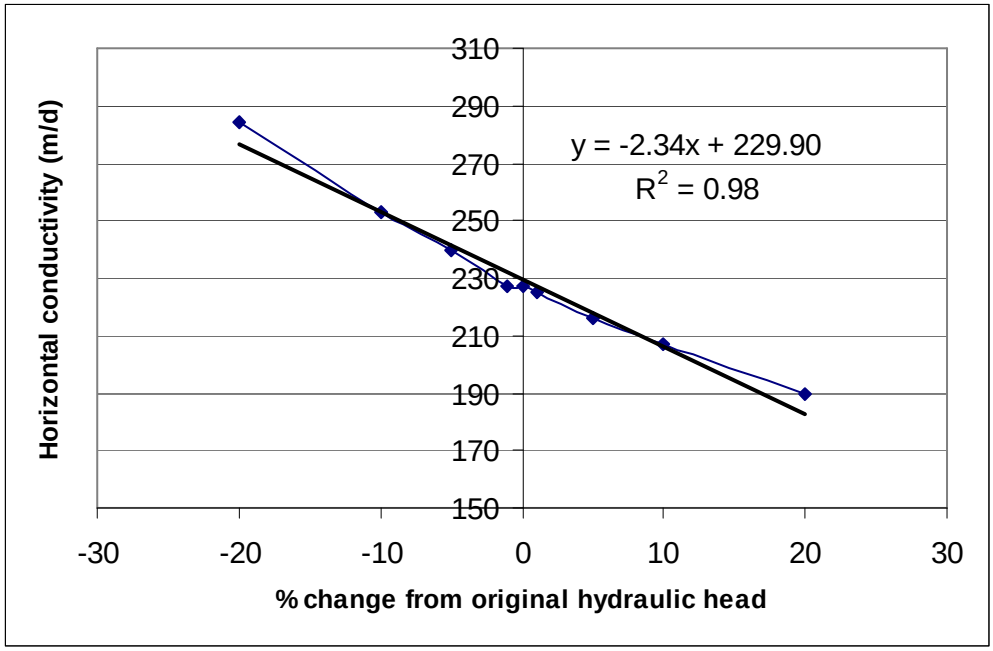

Figure 4.10: Sensitivity results using all observation points

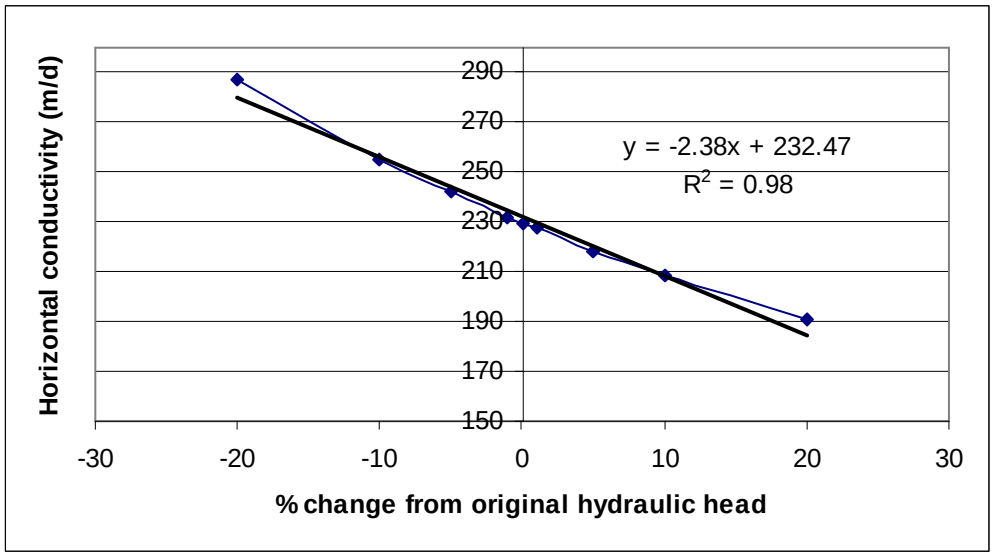

Figure 4.11: Sensitivity results from using only observation points 3, 4, 7 and 8.

Vertical K estimated from the multi dipole method ranged from 4 to 455m/d (Table 4.7). There were no correlations between the estimated vertical K values, except that when estimated horizontal K is large, estimated vertical K is small. Experiments using sample points 1, 2, 5 and 6 produced unrealistic vertical K estimates (vertical greater then horizontal). This is likely to be caused by the higher hydraulic head values in these sample points compared to the modelled values, thus distorting the calculated vertical K estimates. The higher flow rate experiments (MD3-5), when using all observation points, produce vertical and horizontal K estimates that are similar (indicating isotropy). Experiments that did not use observation points 1, 2, 5, and 6 produced estimates of vertical K that were lower than horizontal K. This may indicate that the multi dipole method was not sensitive to variations in vertical K and therefore the method was unable to produce accurate or reliable estimates of vertical K.

When all observation points (excluding tests using only 1, 2, 5, and 6) are used and isotropy is assumed, the multi-dipole RWP model produced estimates of K ranging from 203–306 m/d which were 17 to 76% greater than the actual K (174 m/d) (Table 4.8). This

is very similar to the results when anisotropy is assumed. The average K value for these tests is 231 m/d. If MD1, using only observation point 4, is excluded from this average this range narrows to 17 to 48% greater than the actual K, (average of 228 m/d). As with the analyses assuming anisotropy, observation points 1, 2, 5 and 6 have only a small impact on results of the tests that use all observation points and results are very similar to the values obtained for tests using only observation points 3, 4, 7 and 8.

The results also show that estimates of K do not get better or worse as flow rates increase or decrease. This is consistent with the observed hydraulic heads being proportional to the flow rates (Figure 4.5 and 4.6).

Table 4.12 presents estimated K values from the multi-dipole RWP model when observation values from the 5 multi dipole experiments (MD1-5) are used in the same analysis.

Table 4.12: Multi dipole RWP model results for experiments MD1-5 combined.

	Observation points used	Estimated Horizontal K m/d	% of actual K	Estimated Vertical K m/d	RMSD m	Estimated to actual draw down (r^2)	GA Generations
Anisotropic	1, 2, 3, 4, 5, 6, 7, 8	226	130	188	8.59E-03	0.95	14
	3, 4	299	172	30	6.86E-03	0.98	10
	3, 4, 5, 6	282	162	33	6.78E-03	0.97	13
	7, 8	264	152	42	6.14E-03	0.98	4
	1, 2, 3, 4	71	41	68	3.83E-03	0.98	38
Isotropic	1, 2, 3, 4, 5, 6, 7, 8	221	127	221	8.26E-03	0.95	8
	3, 4	233	134	233	7.19E-03	0.98	23
	3, 4, 5, 6	223	128	223	8.06E-03	0.97	1
	7, 8	215	123	215	7.49E-03	0.98	4
	1, 2, 3, 4	71	41	71	3.72E-03	0.98	4

The results are consistent with the K estimates when single experiments were analysed separately (Tables 4.7 and 4.8). Anisotropic estimates range from 30 to 72 % higher than the actual aquifer K whereas when isotropy is assumed the range is 23 to 34 % higher than

the actual aquifer K (excluding tests using observation points 1, 2, 5, and 6 only). The average K estimate when isotropy is assumed is 223 m/d, which is similar to when single experiments were analysed separately (228 m/d). Apparently, combining multiple tests to optimise for K is not advantageous when compared to single experiments, except in averaging small errors in measurement.

Results from the multi dipole RWP modelling are plotted in Figures 4.12 and 4.13. These figures also highlight the fact that the estimated K values and the tracer test K values (actual) are significantly different. Possible reasons for this discrepancy are discussed in Section 4.4. The figures also show that there is a greater variation in estimated K values when anisotropy is assumed.

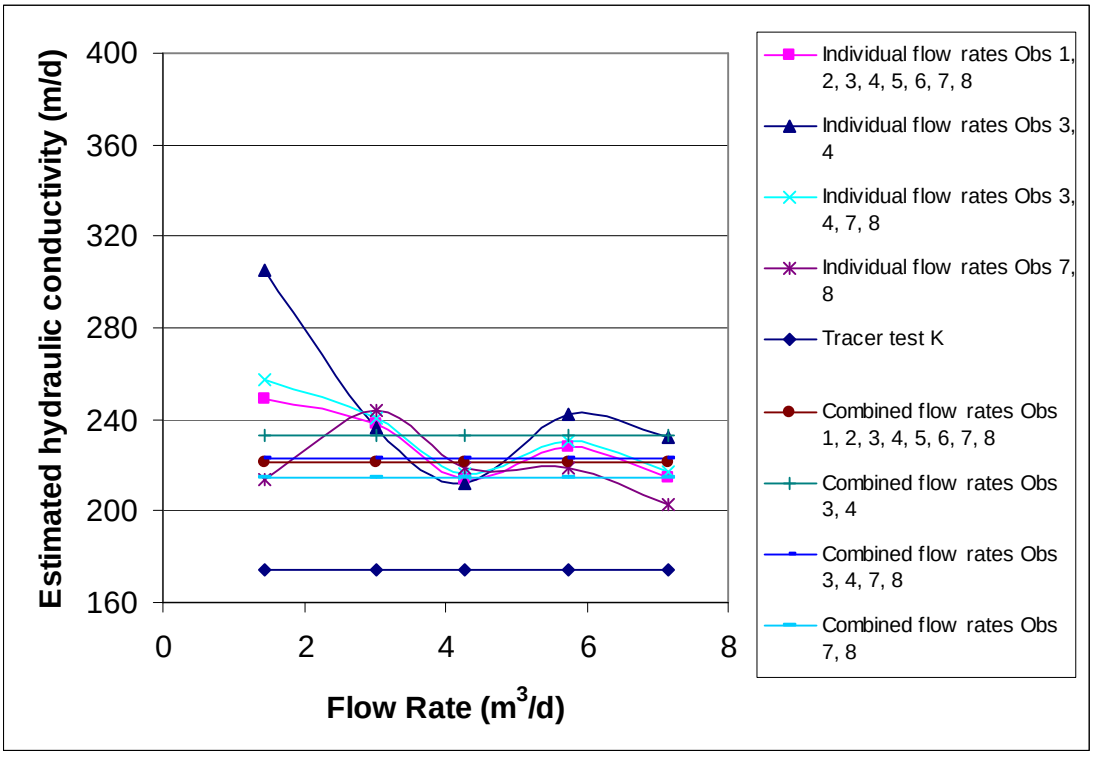

Figure 4.12: Flow rate vs. average hydraulic conductivity estimate comparisons between single and combined multi dipole RWP model results (assuming isotropy).

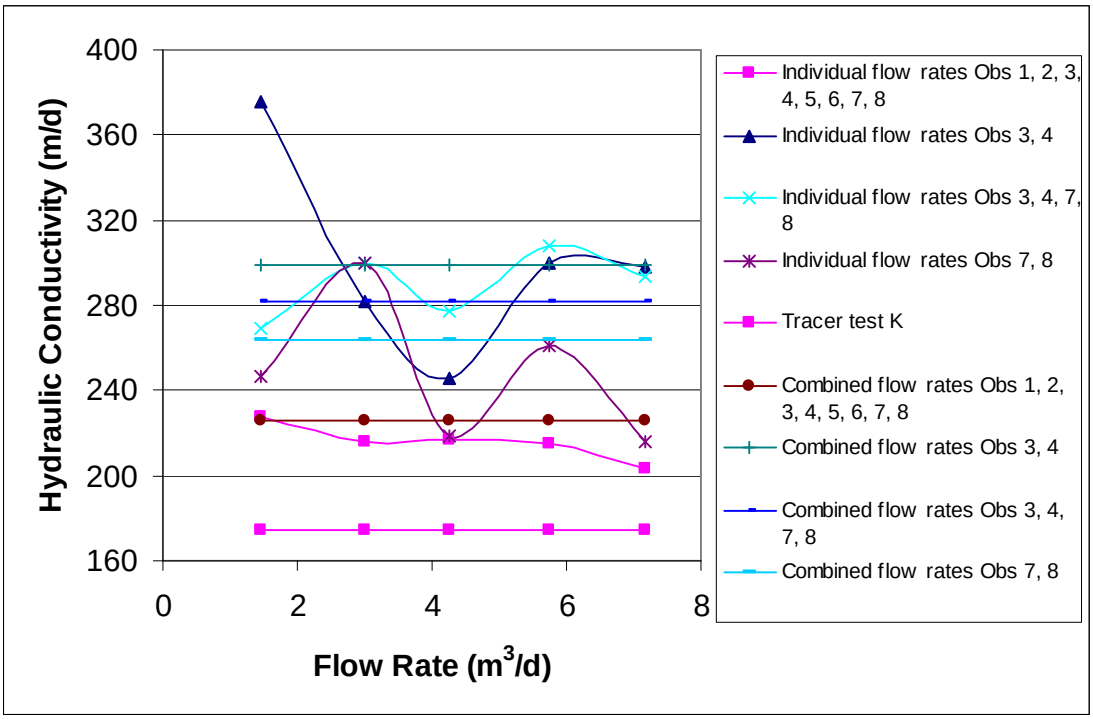

Figure 4.13: Flow rate vs. average hydraulic conductivity estimate comparisons between single and combined multi dipole RWP model results (assuming anisotropy).

Constraining MD6 to be isotropic produced a result that was 18% greater than the actual aquifer K value, whereas if anisotropy is assumed estimated K ranged from 28-56% greater than the actual K (if tests using only sample points 1, 2, 5 and 6 were excluded) (Table 4.9). These are similar to results obtained for experiments MD1-5 (Table 4.7-4.8). When isotropy is assumed, MDA produced a K estimate 4% greater than the actual value and when the aquifer was assumed to be anisotropic it produced estimates 10-11% greater than the actual K values (Table 4.10).

This limited analysis shows that the multi dipole RWP method provides accurate K estimates with incidence angles other than 90 degrees. This finding makes field application of the multi dipole RWP method more practical as determination of groundwater flow direction before a test is undertaken is not of critical importance. Further study however, is needs to be undertaken to verify this.

4.4 Why the Discrepancy between the K Estimates obtained from Multi Dipole RWP Modelling and the Actual K of the Artificial Aquifer?

The K of the artificial aquifer has been calculated by tracer tests as ranging from 168 to 174 m/d in the section of aquifer that the multi dipole tests were conducted (Section 4.1). This shows good agreement with most other methods (Table 4.1) including average K derived from Darcy's Law for the experiments in this study (Table 4.2).

When the multi dipole RWP model was applied to estimate K a range of 203-257 m/d was produced with a 90 degree incidence angle, assuming isotropy (Tables 4.7 and 4.8). This value is significantly different from the values obtained independently from other methods (as illustrated in Figures 4.12 and 4.13). This difference between the observed and modelled K value could be caused by a number of factors, outlined in this section.

One reason why inaccuracies between the observed and modelled heads in the pumping screens, and therefore the K values estimated, may exist is that MODFLOW may not be able to simulate the large draw downs at the pumping wells accurately. Simulation of flow near, or at, a pumping well requires that the change in head due to radial convergence of flow lines are accurately represented (Samani et al., 2004). MODFLOW, which is constructed using a rectilinear grid system generally has not been used to simulate flow near a pumping well and so may not be able to accurately simulate draw downs in a RWP system. Samani et al. (2004) states that head gradients are generally underestimated in conventional discretization schemes (such as MODFLOW) because distances between cell centres, or cells next to the well are too large to capture the steep and rapidly changing head gradients. The model grid employed in this thesis contained relatively small cell

spacing in the vicinity of the well (2.5cm), but this may not have been fine enough to simulate the head gradients accurately.

Another hypothesis is that, because the multi dipole RWP model does not account for the open well, due to the lack of a multi-zone parameterizing option in the multi dipole RWP model, K is overestimated. This effect can be conceptualized in terms of flow through a pipe. As water flows through a pipe it generates a fixed draw down. When this pipe increases in size, maintaining identical flow rate the pressure in the larger diameter pipe is less than in the narrow diameter pipe. In the aquifer the porosity was measured as 0.44 and within the well the porosity is 1 leading to reduced draw down within the well as compared to the aquifer. This will also apply to screens that have mounding. Figure 4.14 illustrates this point. A simple test was conducted in MODFLOW to illustrate this hypothesis.

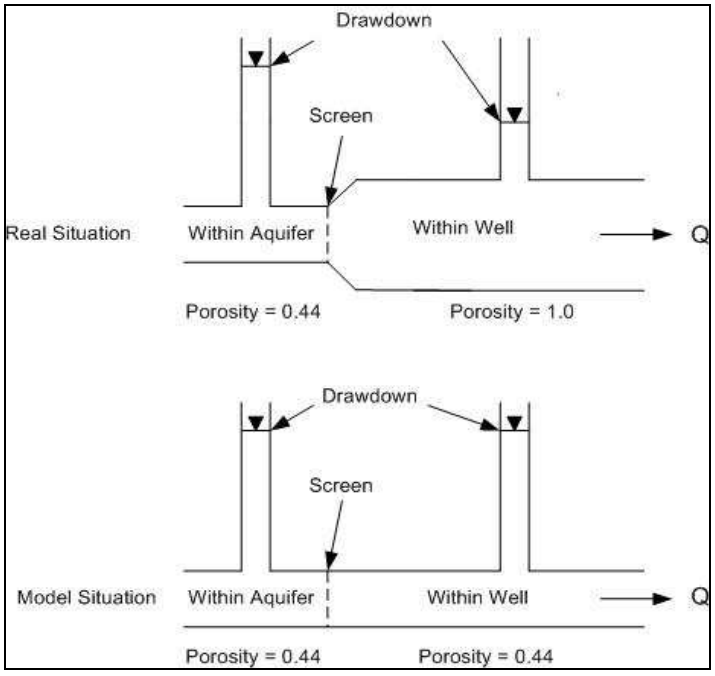

Figure 4.14: Schematic illustrating the effect of having an open well on pumping screen drawdown values as pipe flow.

The MODFLOW grid constructed for the RWP analysis (including the well and packer configuration of the RWP) was used to predict the effect of an open, fully screened well on observed hydraulic heads. Only the effect on observations points 3, 4, 7 and 8 will be analysed because the effect on observation points 1, 2, 5 and 6 was minimal. The analysis was carried out over a range of flow rates (MD1, 3 and 5).

When MODFLOW is run with a global K value of 174m/d it predicts that the hydraulic heads are larger than those observed in the artificial aquifer (Table 4.13). The wells in MODFLOW were then assigned a K value of 10000 m/d and the remaining aquifer assigned 174 m/d in order to simulate the open well (Figure 4.15). A K value of 10000m/d was chosen because this value was large enough to allow hydraulic head within the well to be controlled by the K of the aquifer cells. This assumption was tested by varying the K in the cells in the well until no change in hydraulic head was observed. Results from the scenario are given in Table 4.13. The entire aquifer was then assigned a K value of 221m/d, and the resulting hydraulic heads recorded. A K value of 221m/d was chosen because this was the K obtained when using an average of all tests and all sample points when the aquifer is isotropic (Table 4.12). The results for these simulations are also shown in Table 4.13.

The hydraulic head values for a run when the K of the aquifer is 174 m/d, (except that K in the well is set at 10000m/d) is approximately equal to the hydraulic head values if the entire aquifer is assigned a K of 221 m/d. This analysis shows that if the K within the well is set to a high value in MODFLOW, a more accurate match between the actual aquifer K and the K estimated from the multi dipole RWP model can be achieved.

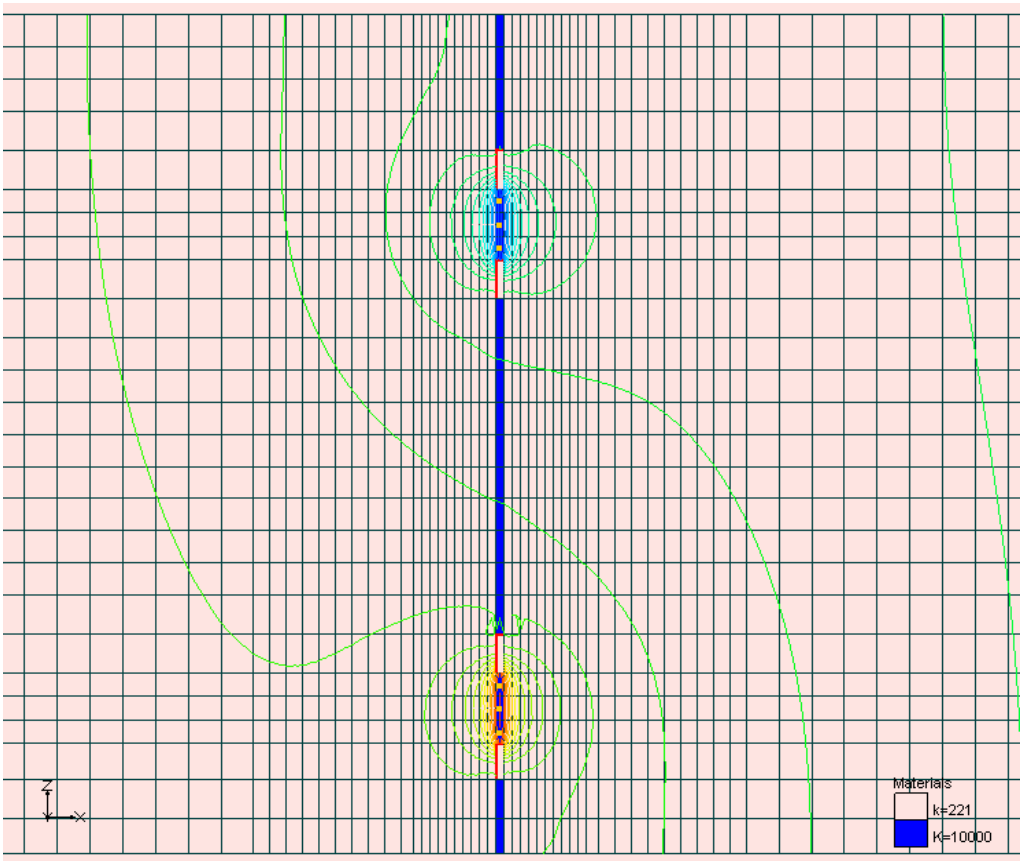

Figure 4.15: MODFLOW configuration of the RWP system used to test the hypothesis that the open well significantly effect estimated K values.

Table 4.13: Results of the analysis of the effect of high in well K.

		Obs 3 (m)	Obs 4 (m)	Obs 7 (m)	Obs 8(m)	Average (m)
MD5 7.16 m^3/d	Observed	0.097	-0.071	-0.096	0.098	0.091
	overall K=174 m/d	0.115	-0.113	-0.113	0.113	0.114
	overall K=174 m/d inwell K=10000 m/d	0.089	-0.087	-0.087	0.087	0.087
	overall K=221 m/d	0.091	-0.089	-0.088	0.089	0.089
MD3 4.26 m^3/d	Observed	0.0535	-0.059	-0.056	0.051	0.055
	overall K=174 m/d	0.069	-0.067	-0.067	0.068	0.068
	overall K=174 m/d inwell K=10000 m/d	0.053	-0.051	-0.052	0.052	0.052
	overall K=221 m/d	0.054	-0.052	-0.053	0.054	0.053
MD1 1.46m^3/d	Observed	0.036	-0.015	-0.005	0.0165	0.018
	overall K=174 m/d	0.023	-0.021	-0.024	0.025	0.023
	overall K=174 m/d inwell K=10000 m/d	0.018	-0.016	-0.018	0.019	0.018
	overall K=221 m/d	0.018	-0.016	-0.019	0.02	0.018

Further modelling and experimentation is required to prove the above hypothesis. This effect may be of greater importance in field situations where the size of the well relative to the area being interrogated by the RWP system is large.

4.5 Fractional Flow Experimental Results

Results from the 5 fractional flow experiments are presented in Figures 4.16-4.20. The results consist of time versus concentration plots for the 4 screens for each tracer species. Screen positions are illustrated in Figure 3.7.

To study the fractional flow between wells, injection wells received a constant input of either bromide or nitrate/chloride. Input time can be seen visually as a sharp decrease in tracer concentration in screens 1 and 3 (Figures 4.16 to 4.20). When input of tracer ceases, injection screen concentrations (S1 and S4) match the corresponding extraction screen concentrations (S2 and S3) for each tracer.

Screens 3 and 4 for the bromide tracer and screens 1 and 2 for the nitrate/chloride tracer theoretically should have equal concentrations. Variations in these concentrations were observed which may be due to analytical error. In this thesis the concentrations of screens 3 and 4, for bromide, and screens 1 and 2 for nitrate/bromide were treated as replicate samples and therefore averaged to obtain steady state values.

The fractional flow RWP model requires steady state tracer concentration at 3 screens (two screens are averaged as discussed previously) for each tracer in order to estimate K. The breakthrough curves reach steady state when the mass of tracer exiting the dipole due to the regional gradient equals the mass of tracer entering the system through the injection pulse. The 2 tracers were injected into the system at a constant concentration through the injection screens. A proportion of this tracer reaches the extraction screen of the same well (S1 to S2 and S4 to S3) and is then mixed with the fresh tracer and injected back into the aquifer. This continues until the amount of mass that is lost through regional flow equals

the input mass. The breakthrough curves show an initial sharp rise in concentration as the tracer is introduced. After this a more gradual rise occurs due to recycling of the tracer and at later time tracer concentrations plateau when steady state is achieved (Figures 4.16 to 4.20).

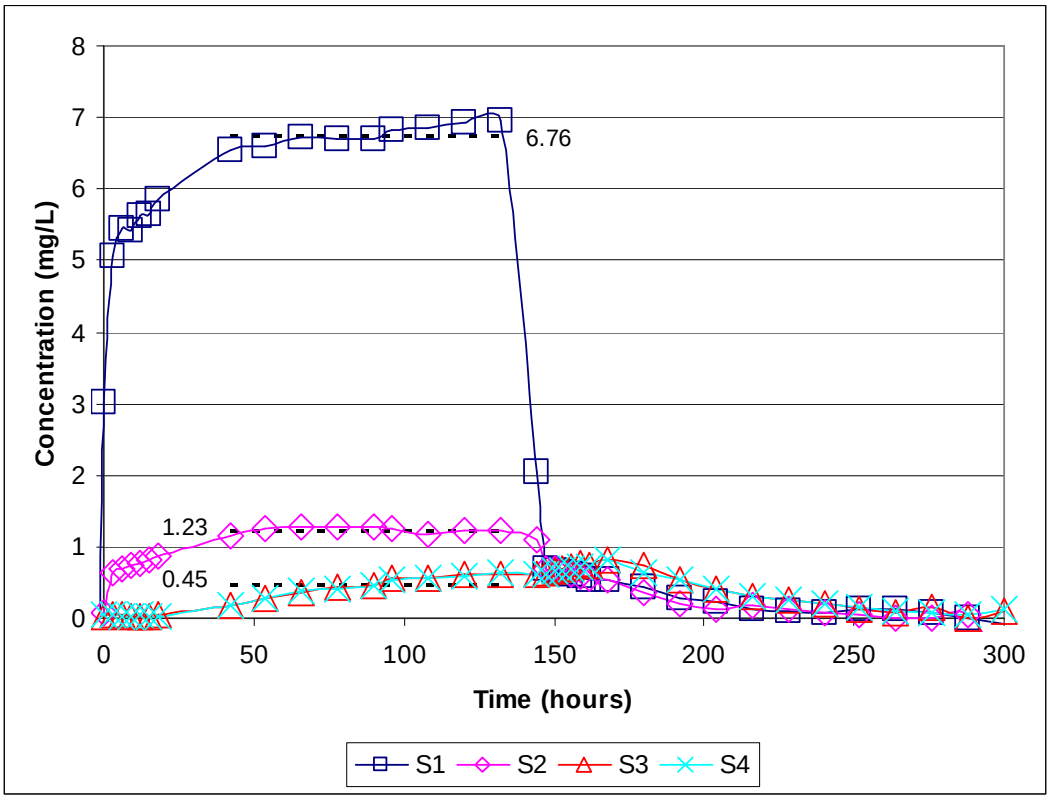

(a)

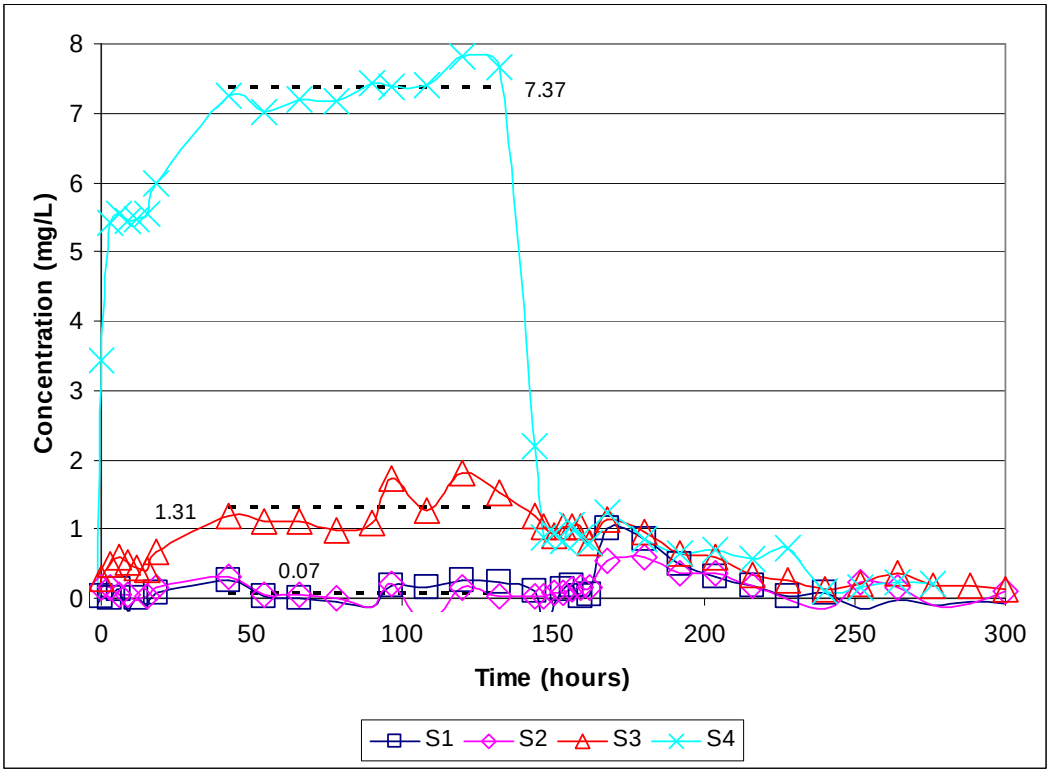

(b)

Figure 4.16: Experiment FF1 bromide (a) and chloride results (b) at the 4 screens in the RWP system. Dotted lines represent the concentrations averaged to obtain the steady state concentration.

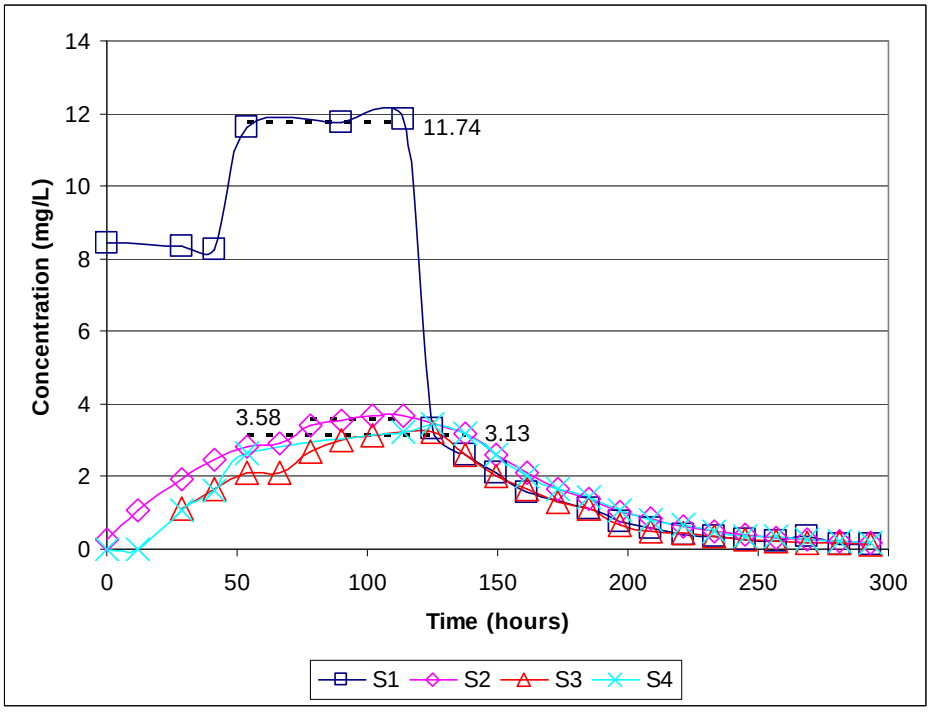

(a)

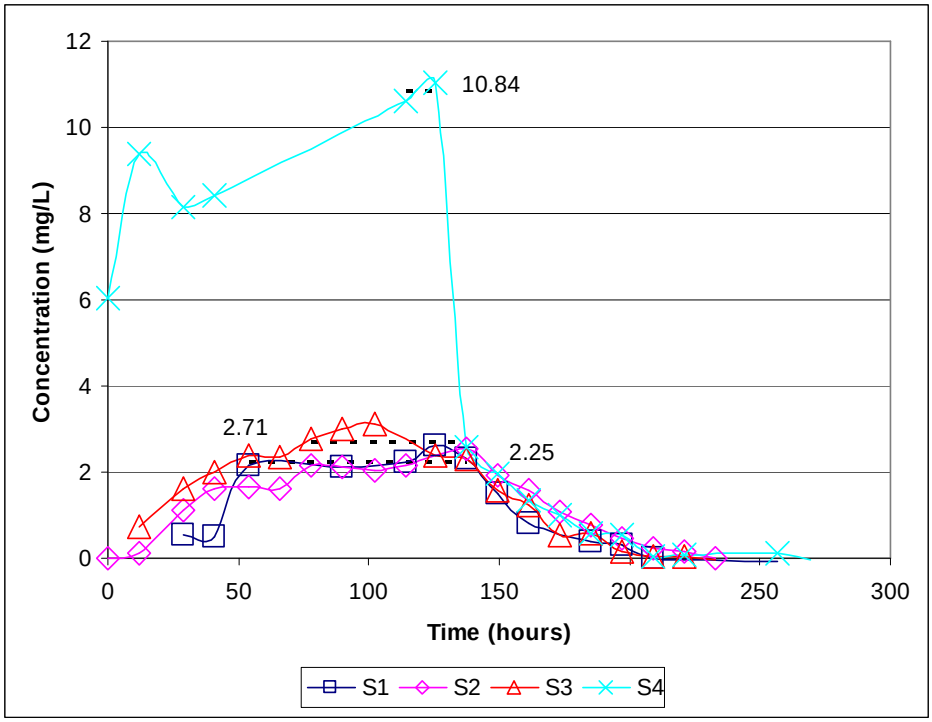

(b)

Figure 4.17: Experiment FF2 bromide (a) and nitrate results (b) at the 4 screens in the RWP system. Dotted lines represent the concentrations averaged to obtain the steady state concentration.

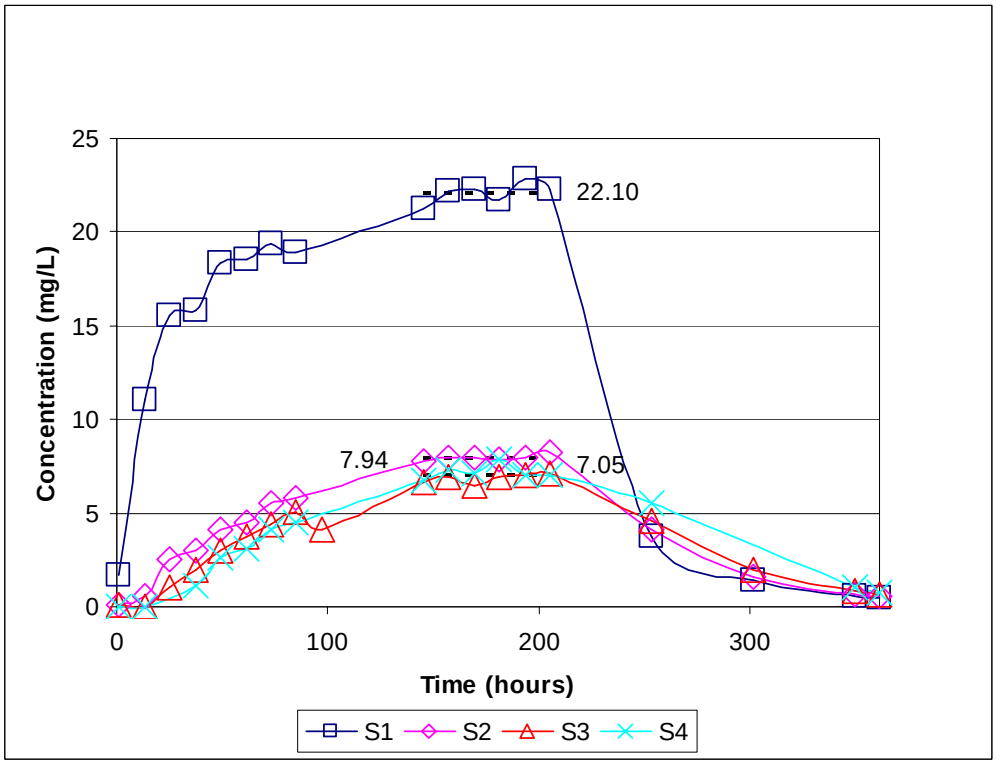

(a)

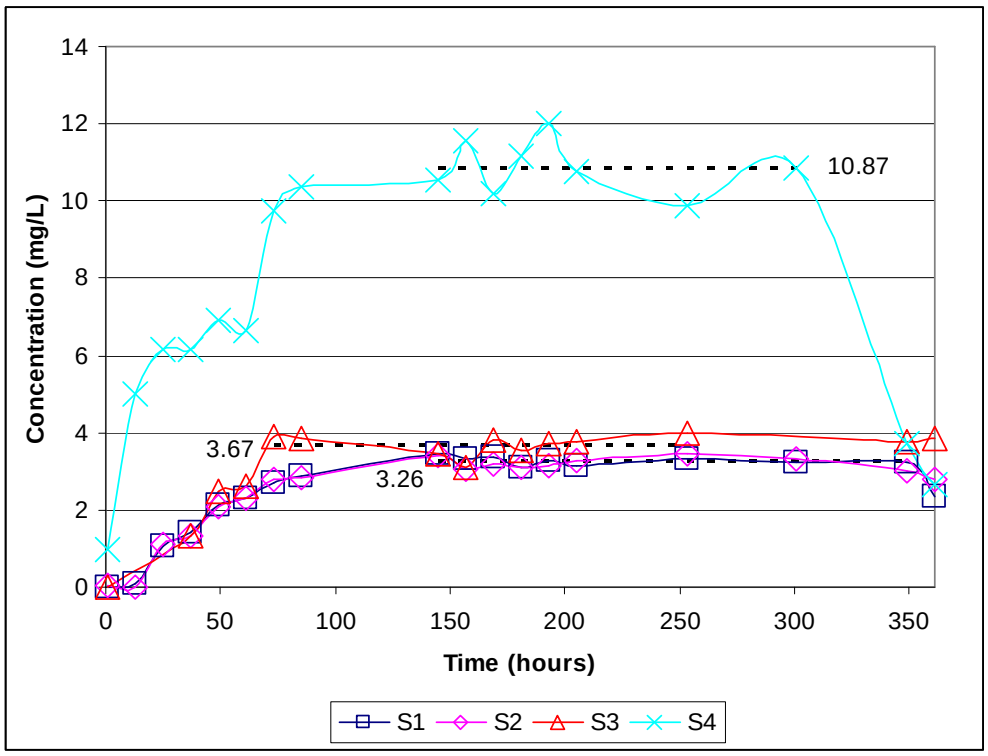

(b)

Figure 4.18: Experiment FF3 bromide (a) and nitrate results (b) at the 4 screens in the RWP system. Dotted lines represent the concentrations averaged to obtain the steady state concentration.

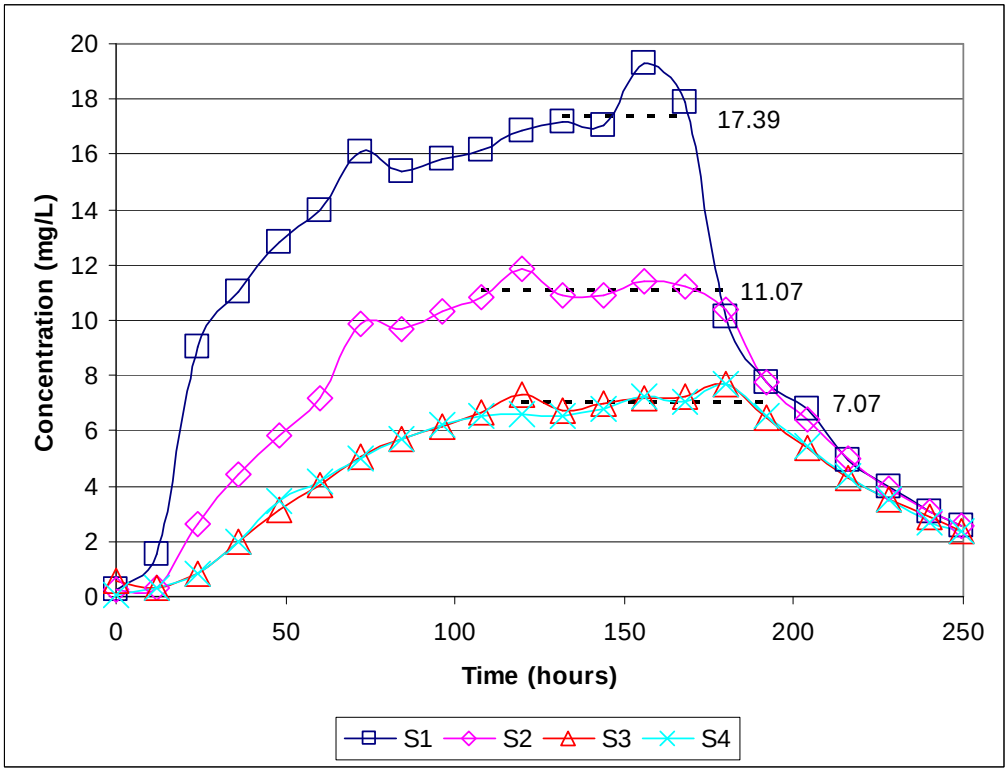

(a)

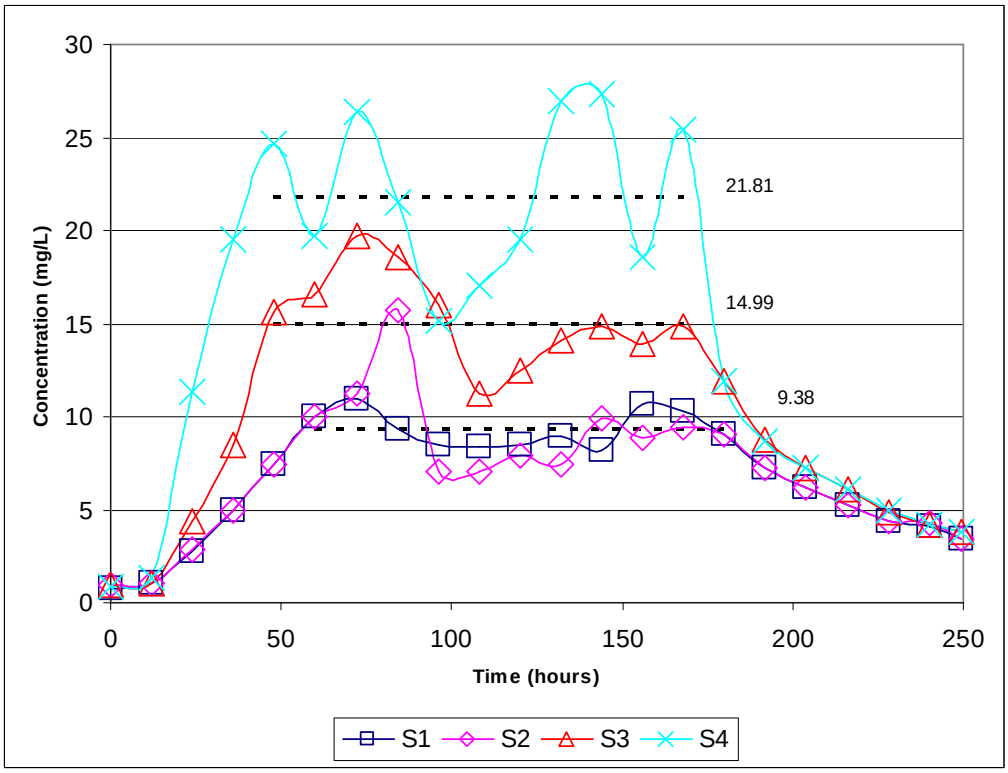

(b)

Figure 4.19: Experiment FF4 bromide (a) and nitrate results (b) at the 4 screens in the RWP system. Dotted lines represent the concentrations averaged to obtain the steady state concentration.

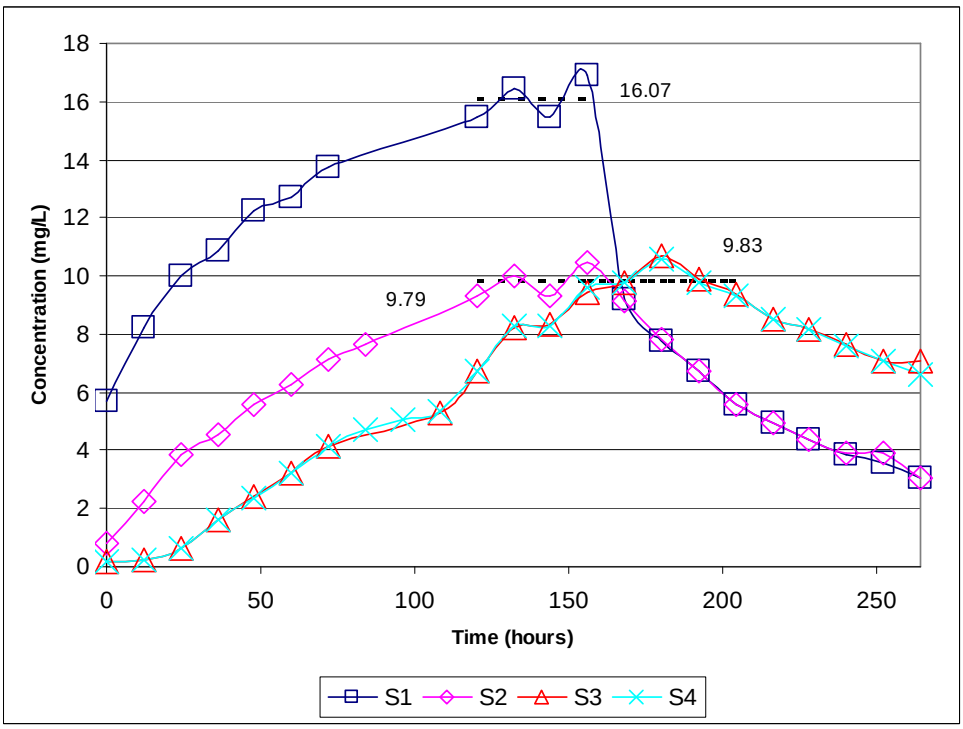

(a)

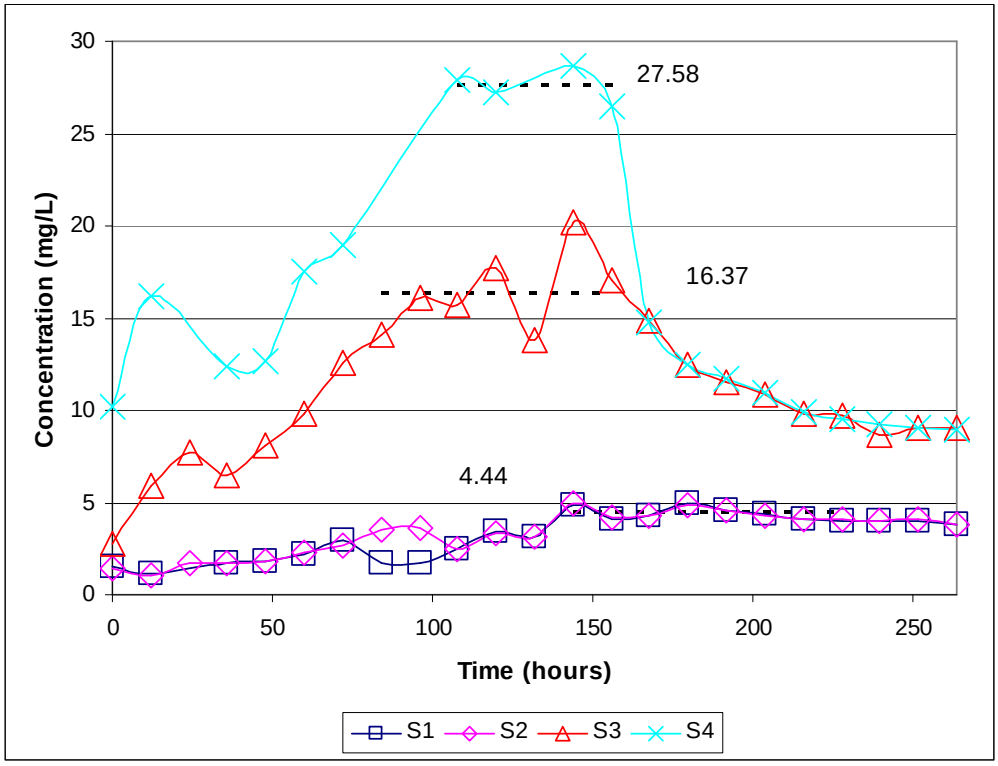

(b)

Figure 4.20: Experiment FF5 bromide (a) and nitrate results (b) at the 4 screens in the RWP system. Dotted lines represent the concentrations averaged to obtain the steady state concentration.

.

FF1 reaches a plateau in concentration after approximately 50 hours (Figure 4.16). Concentration data from 50 hours till 144 hours (time when injection pulse ceased) was averaged to obtain the steady state concentrations used to estimate K. Steady state time for FF2-5 was problematic to determine because of the variability in observed concentration values. Best estimates of steady state concentration values were determined visually. Variability in the plateau concentration values may be caused by not allowing the experiments to run over a sufficient time period. Brief interruptions in the operation of the RWP, due to malfunctioning pumps, also added complications in the interpretation of the breakthrough curves. Malfunctioning automatic samplers produced gaps in the data, leading to poor definition of some of the breakthrough curves.

The fractional flow approach recycles water from the extraction screen and re-injects it via the injection screens after the tracer is added. As recycling continues the concentration increases until tracer lost due to regional flow matches the tracer added at the injection screen. The concentration of tracer being recycled is the concentration in the corresponding extraction screen (S2 and S3). The time taken to reach steady state may be prolonged due to this recycling. Recycling of tracer is dependent on the dipole pumping rate as compared to the regional flow. The greater the pumping rate as compared to the regional flow the longer the time period required to reach steady state. If the RWP creates a perfect dipole with no loss or gain in the system there will be a continuous increase in tracer concentration due to the addition of tracer into the system. This will occur if there is no regional hydraulic gradient. In the experiments performed for this thesis the ratio of dipole pumping rate to regional flow ranged from 0.44 (FF1) to 2.44 (FF5). When conducting the experiments in this study, the experimental duration was not increased to correspond with the increase in dipole pumping rate to regional flow ratio. Prematurely ending the higher flow rate experiments (FF4 and 5) may have resulted in concentration breakthrough curves that did not reach a plateau (steady state). This may produce inaccurate K estimates for these experiments.

The time to steady state can also be calculated theoretically. The time to first breakthrough has been calculated by Cunningham et al. (2004) and this is used by Kim (2005) to estimate the time to reach steady state and therefore optimal duration of a RWP experiment. The method used by Cunningham et al. (2004) assumes a homogeneous aquifer and that there is no hydraulic connection between the upper and lower screens. In this thesis there is hydraulic connection between the upper and lower screens but a rough estimate should still

be gained from this method. Cunningham et al. (2004) calculated the time to first breakthrough from Equation 4.6.

$$t_{\min} \approx \frac{4}{3}\pi \frac{a^2 HNe}{Q} \quad \textbf{(4.6)}$$

where t_{min} is the minimum tracer breakthrough time, a is the distance between the injection and extraction screens, H is the thickness of the aquifer, Ne is the effective porosity and Q is the wells pumping rate.

Kim (2005) analysed both measured and predicted breakthrough curves produced by Cunningham et al. (2004) and estimated that it took approximately 20 times longer than the first breakthrough time to reach steady state. Applying this to the RWP experiments carried out in the artificial aquifer produces a range of steady state values from 7.3 days for FF1 to 1.3 days for FF4. These estimates do not take into account the increase in the proportion of tracer being recycled and therefore produce a low estimate of the time to steady state.

Several methods have the potential to decrease the time required for the RWP system to reach steady state. The RWP system could be operated without recirculating the water, instead disposing of the water from the extraction screens and injecting fresh water into the injection screens. Large amounts of clean water would be required inject into the aquifer, and large amounts of water from the extraction screen would need to be disposed of negating some of the benefits of the RWP system and rendering this method unfeasible. Another possibility is to use a filter within the RWP system, enabling the recirculation of clean water. Sutton et al. (2000), when performing the dipole flow test used rhodamine WT as a tracer and filtered this out with charcoal filters before re-injection into the aquifer. An

alternative method would be to use a volatile substance that could be easily removed from the extraction flow before re-injection. A volatile tracer (SF_6) was used by Johnson and Simon (2007) to measure recirculation in a dipole flow test. The SF_6 was stripped out at each recirculation simplifying the analysis of the tracer concentrations and reducing the time taken to reach steady state. A constant input concentration can be maintained with this method. This method would reach steady state in a reduced time frame and therefore would be less time consuming and costly to implement.

When the RWP fractional flow method was used to estimate mass flux, Kim (2005) investigated the use of different segments of the breakthrough curve as the steady state value. Kim (2005) analysed the average concentration when the tracer curve reached a plateau, the shoulder of the concentration curve, at peak tracer concentration and using a point concentration during steady state by the fractional flow approach. Kim (2005) found that K values were not sensitive to the method used to estimate steady state tracer concentration at the well screens especially when isotropy was assumed (230-243m/d).

This insensitivity may be a result of the methods Kim (2005) employed to estimate the steady state values. Kim (2005) measured concentrations at different time periods consistently across the 4 screens. This would result in the proportions of tracer (fractional flow) being similar regardless of the time period being measured unless a measurement was made at a very early time. Figure 4.21 illustrates this point with a theoretical example. At time A tracer is being recycled and concentrations are increasing. At time B steady state has been reached and therefore concentrations are stable. The proportions of tracer at time A and time B are almost identical (depending on when each individual screen reaches equilibrium) and therefore concentration values at both these times will produce near

identical K estimates. This indicates that steady state concentration is not critically important, rather that the proportions of tracer in each concentration curve need to be stable.

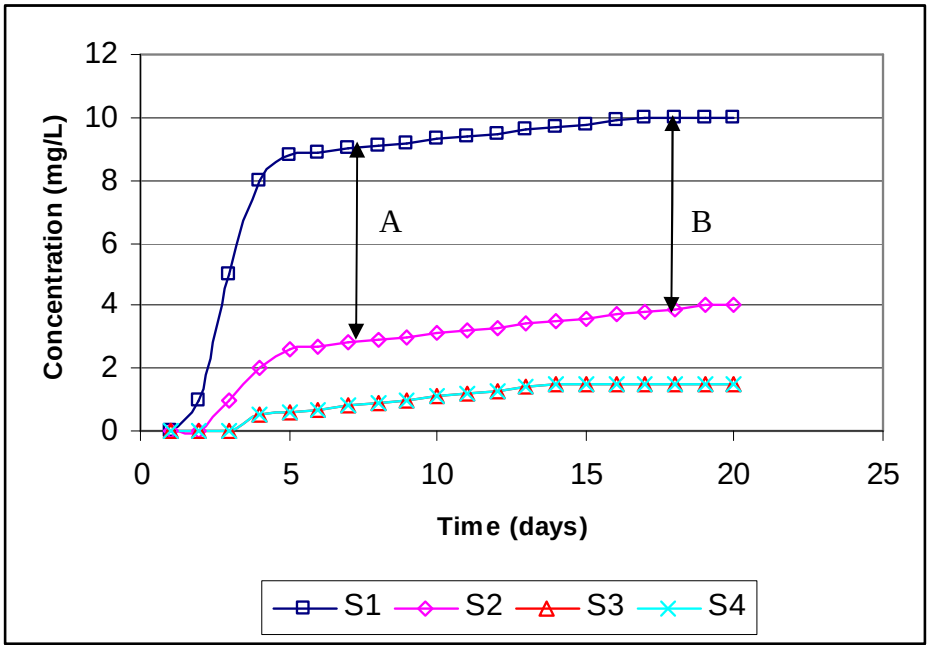

Figure 4.21 Tracer proportion approximately equal regardless of whether steady state has been reached.

A real example is given in Figure 4.20. S1 (input) concentrations minus concentrations from the remaining 3 screens from FF4 bromide were graphed. Subtracting S2, S3 and S4 from screen S1 concentrations result in constant concentration values when the tracer proportions are the same. Comparing Figure 4.22 to Figure 4.19a shows that even though steady state was not reached until approximately 120 hours the proportions are stable at approximately 70 hours and therefore reliable ‘steady state’ values can be obtained from this shorter time period.

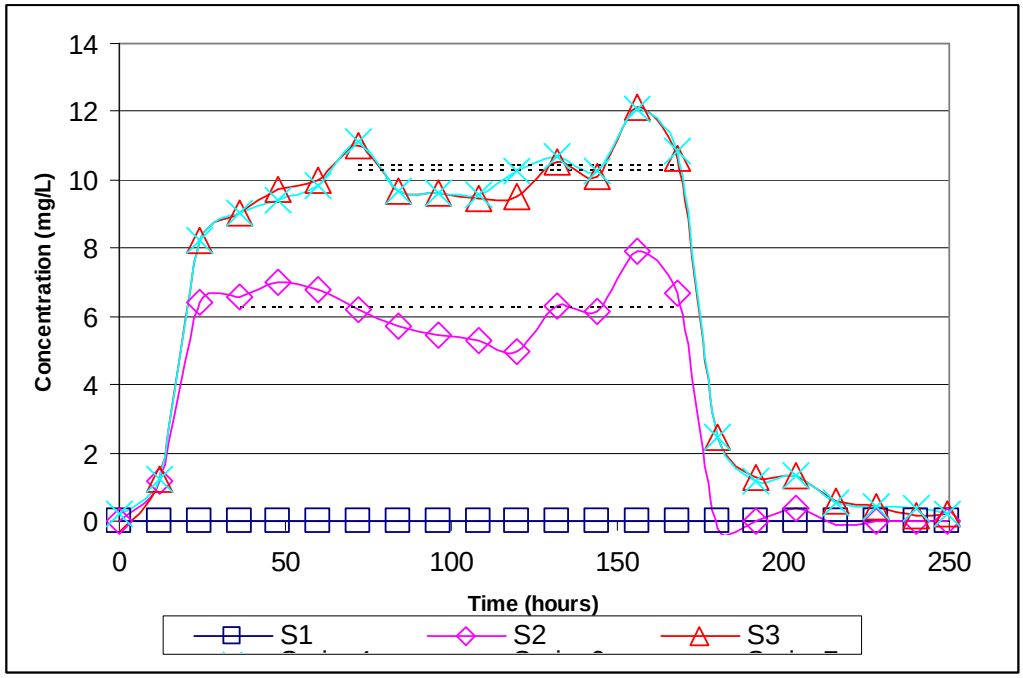

Figure 4.22: Difference between S1 concentrations and concentrations of other screen to determine when proportions between screens are stable.

This study has determined the steady state value when the proportions between the concentration curves of the screens stabilise. The segment of the curve used to determine this number and the average of the values over this time are shown in Figure 4.16-4.20.

The average tracer concentration values derived from Figures 4.16–4.20 are summarised in Table 4.14 together with the proportions of the injection screen concentration (S1, S4) reaching the remaining 3 screens. The physical set-up and the pumping rates of the two well pairs were symmetrical and therefore, theoretically, the proportions of tracer should be equal for the two tracers. The fractional flow results for the bromide compared to the nitrate/chloride dipole are similar but not equal. This may be caused by errors in calculating the average value at steady state as discussed above or may be the result of heterogeneity in the artificial aquifer. The flow rates for the two dipoles were not matched precisely which may also result in the observed uneven fractional flow. This difference in

the flow rates of each dipole in a single test were accounted for by the fractional flow model used to calculate K.

FF5 was performed on a 45 degree angle which produced nearly equal concentrations of bromide in both dipoles. A proportionately smaller amount of nitrate reached screens 1 and 2 due to the effects of the regional hydraulic gradient.

Table 4.14: Tracer concentration used to calculate hydraulic conductivity and the fraction of the injection concentration reaching each screen.

		Bromide				Nitrate or Chloride			
		S1	S2	S3	S4	S1	S2	S3	S4
FF 1	Steady state concentration (mg/L)	6.76	1.23	0.45	0.45	0.11	0.03	1.31	7.37
	Fraction of injection concentration	1.00	0.18	0.07	0.07	0.01	0.00	0.18	1.00
FF 2	Steady state concentration (mg/L)	11.74	3.58	3.12	3.14	2.29	2.20	2.71	10.84
	Fraction of injection concentration	1.00	0.30	0.27	0.27	0.21	0.20	0.25	1.00
FF 3	Steady state concentration (mg/L)	22.10	7.94	7.26	6.84	3.27	3.24	3.69	10.87
	Fraction of injection concentration	1.00	0.36	0.33	0.31	0.30	0.30	0.34	1.00
FF 4	Steady state concentration (mg/L)	17.39	11.07	7.09	7.05	9.34	9.42	14.99	21.82
	Fraction of injection concentration	1.00	0.64	0.41	0.41	0.43	0.43	0.69	1.00
FF 5	Steady state concentration (mg/L)	16.07	9.79	9.81	9.84	4.42	4.47	16.37	27.58
	Fraction of injection concentration	1.00	0.61	0.61	0.61	0.16	0.16	0.59	1.00

Results summarised in Table 4.14 are applied with the fractional flow RWP model in the following section.

4.6 Fractional Flow RWP Model Results

Results obtained for the fractional flow RWP modelling are shown in Table 4.15. Results were modelled assuming either an isotropic or anisotropic aquifer. Estimated horizontal and vertical K values are shown together with the percentage of actual K this represents (Section 4.1). The goodness of fit between the predicted and observed well interflows is shown using a regression co-efficient (r^2). The root mean square deviation (RMSD) is also calculated for the difference between predicted and observed well interflows. The number of GA generations the model required to estimate the K values is also given.

Table 4.15: Fractional flow experimental results.

		Estimated Horizontal K m/d	% of actual K	Estimated Vertical K m/d	Estiamted to actual fractional flow (r^2)	RSMD (fractional flow)	GA generations
FF 1	Isotropic	136	93	136	0.98	0.04	3
	Anisotropic	135	92	134	0.98	0.09	38
FF 2	Isotropic	172	117	172	0.97	0.06	8
	Anisotropic	164	111	105	0.98	0.04	37
FF 3	Isotropic	140	95	140	0.97	0.06	4
	Anisotropic	132	90	87	0.99	0.04	42
FF 4	Isotropic	149	86	149	0.97	0.07	5
	Anisotropic	114	68	111	0.97	0.07	65
FF 5	Isotropic	249	148	249	0.99	0.02	3
	Anisotropic	223	133	192	1.00	0.01	37

As described in Section 3.4 experiments FF 1-3, FF4 and FF5 were undertaken in different sections of the aquifer. The corresponding actual K values for the sections of the artificial aquifer in which these experiments were carried out were 147 m/d for FF1-3, 174 m/d for FF4 and 168 m/d for FF5 (Section 4.1).

Estimated K values ranged from 114 to 249 m/d or 68-148 % of the calculated values (Table 4.15). The 4 experiments conducted with a 90 degree well configuration (FF1 to FF4) produced K estimates from 68-117 % of the actual K value. A range of 86 – 117 % of actual values was determined when the model was constrained to being isotropic. The estimated K values matched the actual values satisfactorily. The accuracy achieved also compares favourably to the accuracy achieved by Kim (2005) and Goltz et al. (2008).

FF2 and FF4 exhibited greater variation between actual and estimated K compared to FF1 and FF3. An explanation for this deviation may be found in the quality of data that were obtained from the RWP tests for these 2 experiments. The injection screen breakthrough curves (S1 for bromide and S4 for nitrate) for FF2 (Figure 4.17) were inconsistent and

contained limited data points, resulting in uncertainty in the steady state concentration values. This uncertainty may result in inaccurate estimates of K. Comparing FF2 to FF3 which was conducted at a similar flow rate (average of 2.31m^3/d vs. 2.46m^3/d), we see that the two experiments produced significantly different fractional flow results (Table 4.14). Again, this indicates that estimates of steady state obtained from the tracer breakthrough curve may not be accurate. Additionally, the 2 dipoles of FF2 did not produce similar interflow values (Table 4.14) as should occur theoretically if both dipoles were similar. This also indicates that steady state estimates were incorrect.

FF4 produced breakthrough curves for the nitrate dipole that were erratic (Figure 4.19b). Nitrate interflow was also higher than the bromide which was the opposite of the other 3 experiments. Low r^2 and relatively high RSMD values indicate the model did not fit the data accurately. Due to the erratic nitrate breakthrough curves the steady state bromide concentrations were used in a simulation for both dipoles. Theoretically the fractional flow in each dipole should be equal. This improved the match between the actual and estimated K values when anisotropy was set in the model but did not improve estimated K when isotropy was assumed (Table 4.16).

Table 4.16: FF4 results when bromide concentration values used for both dipoles.

		Estimated Horizontal K m/d	% of actual K	Estimated Vertical K m/d	Estiamted to actual fractional flow (r^2)	RSMD (fractional flow)	GA generations
FF 4	Isotropic	149	86	149	0.97	0.05	6
	Anisotropic	158	91	145	0.97	0.07	8

The fractional flow RWP model produces vertical conductivities ranging from 87 to 134 m/d for experiments FF1-4 (Table 4.15). These values are relativity close to the estimated horizontal K values, especially for experiments FF1 and FF4.

FF5 (performed on a 45 degree incidence angle to the regional gradient) fractional flow RWP model results produced a poor match with the actual horizontal K When Isotropic conditions were assumed the model produced K estimates 48% greater than the actual value (249m/d compared to168m/d). When anisotropy is assumed, a horizontal K estimate of 223 m/d and vertical K of 192 m/d is determined. This horizontal K value is 33 % greater than the actual K value determined for this section of aquifer. If isotropy is assumed, K was estimated to be 249 m/d which is 48% greater than the actual K value of the aquifer.

The fractional flow RWP model matched the observed interflows of FF5 closely as demonstrated by the r^2 value approaching 1 and the low RSMD values. This indicates that the discrepancies may be due to: (1) the steady state values determined for the experiment are not correct, or (2) that the physical conditions of the experiment were not adequately incorporated into the model. As discussed previously, experiments with high flow rates may not have obtained steady state concentration values in the experimental time frame which may have resulted in the inaccurate K estimates. FF4, performed at a similar flow rate to FF5 reached steady state concentration values sooner than FF5. This may be a result of the greater distance between dipoles in the FF5 experiment, perhaps contributing to uncertain steady state values in the FF5 experiment. Additional experiments are required to determine if increasing the duration of the experiments will result in better estimates of K for experiments conducted at a 45 degree incidence angle.

5. Conclusions

5.1. Summary

The purpose of this study was to assess the effect of changing recirculating well pair (RWP) system parameters on the estimation of hydraulic conductivity (K) from RWP models.

To assess the effect of changing RWP system parameters a series of RWP experiments were conducted in an artificial aquifer. Two RWP methods and their corresponding models were assessed, the multi dipole method and the fractional flow method. The multi dipole method uses steady state hydraulic head data at various locations in the RWP system to estimate K. The fractional flow approach is based on conducting a tracer test and measuring the steady state concentration values at the four screens in the RWP system.

Five multi dipole experiments were conducted to assess the effect of varying dipole flow rates. Two RWP experiments were undertaken to assess the effect of changing the incidence angle of the pumping wells as compared to the regional flow. The effects of altering the dipole pumping rate and altering the incidence angle of the pumping wells on estimation of K was studied from five RWP fractional flow experiments. Results of the experiments were modelled to obtain estimates of K.

Estimated K results were compared to K values obtained from a modified natural gradient tracer test to assess the accuracy of the methods. The results were assessed assuming both isotropic and anisotropic conditions. The performance of both methods was compared.

5.2. Conclusions

This study re-analysed a natural gradient tracer test to determine the actual K values of the artificial aquifer. The aquifer was found to have a certain degree of heterogeneity. As the RWP methods average the K of the aquifer within the methods area of influence, it was appropriate that K values derived from well to well tracer tests also be averaged. Average K values from the well tracer tests where then use as "baseline" values to compare against predicted K values from the RWP methods.

Multiple values of actual K were determined corresponding to the sections of artificial aquifer in which the RWP experiments were conducted. For the sections of aquifer in which the RWP experiments were conducted, K values ranging from 147 m/d to 174 m/d were determined. These K values were consistent with K calculated utilizing other methods.

Dipole pumping flow rate did not influence the estimation of K from the multi dipole method. This knowledge leads to a greater confidence in the method in field applications where the ratio between the regional flow and the dipole pumping rate is not known before installation of the wells. When anisotropic conditions were assumed in these experiments, greater variation in the estimated K occurred compared to when isotropy was assumed (resulting from either the artificial aquifer being isotropic or the greater number of parameters being estimated in the anisotropic situation giving greater uncertainty in parameter estimation).

A comparison of a multi dipole experiment conducted on a 45 degree incidence angle (MDA) with a corresponding experiment conducted on a 90 degree incidence angle (MD6)

resulted in MDA producing a more accurate K estimate than MD6 (118% compared to 108% of the actual value). Again, assuming the aquifer is isotropic generated more accurate K estimates as compared to if anisotropy was assumed. Although these results are promising, the results may be fortuitous and therefore more experimentation is required to fully determine the effects of altering the incidence angle on K estimation.

For all multi dipole experiments using well observation points above the packer, estimates of K were significantly lower than the actual K of the aquifer. The estimates appear not to be a result of measurement error or the result of not modelling the high in-well K in the multi dipole model.

Hydraulic conductivity values determined by the multi dipole RWP model were consistently higher than the actual K values determined for the aquifer. It was proposed that this discrepancy was caused by the open well not being simulated by the multi dipole RWP model. To test this hypothesis hydraulic head values were determined with MODFLOW from simulations that included the open well. The hydraulic head values determined from these simulations were very close to the observed hydraulic head values. Therefore, if the multi dipole RWP model was modified to incorporate this open well, K estimations with a greater accuracy may be achieved.

Hydraulic conductivity estimates from the fractional flow model were not affected by the dipole pumping rate. Similarly to the multi dipole approach, this finding leads to greater confidence in the field application of the method, where the ratio between the regional flow and the dipole pumping rate is not known before installation of the wells. Assuming the aquifer was isotropic or anisotropic produced similar K estimates.

Comparison of the fractional flow experiment conducted on a 45 degree incidence angle (FF5) to the corresponding experiment conducted on a 90 degree angle (FF4) indicates that FF5 does not estimate K accurately (133-148% of the actual aquifer K). The cause of this discrepancy is not known, although it may be a result of the experiment not reaching steady state concentration values. Also, as only one replicate of this experiment was conducted, experimental variation may have caused this error

The fractional flow RWP method produced estimates of K that were more accurate as compared to the multi dipole method for experiments conducted at 90 degrees (Table 5.1). The accuracy was reversed when experiments conducted at 45 degrees were examined.

Table 5.1: Comparison of the multi dipole and fractional flow methods as percentages of actual K.

		Multidipole		Fractional Flow	
		Average (%)	Range (%)	Average (%)	Range (%)
90 degree experiments	Isotropic	119	105-157	98	86-117
	Anisotropic	151	117-216	90	68-111
45 degree experiments	Isotropic	108	107-108	148	-
	Anisotropic	114	114-115	133	-

5.3. Recommendations

- The fractional flow method produced more accurate estimates of K compared to the multi dipole method for experiments conducted at 90 degrees to the regional flow, and therefore the fractional flow method is recommended in this situation. Having said this, the multi dipole method should not be discounted as a K measurement method as it can be performed in a short time period and does not require costly sample analysis as compared to the fractional flow approach.

- In the experiments conducted on an angle of 45 degrees the multiple dipole method produced results that were more accurate than the fractional flow method. This result could be fortuitous and therefore it is recommended that further research is conducted to validate the both RWP methods that are conducted on an angle.

- Further investigation is required into the effect of the open well on the estimation of K by the multi dipole method. The multi dipole RWP model needs to be amended so that multi K zones can be incorporated. Re-modelling the current data with the amended model may result in more accurate estimation of K from the technique. Field applications of the multi dipole method with larger diameter wells with gravel packs will lead to a greater influence of the open well and hence lead to an increase in errors associated with the method. An experiment could be performed with peizometers observing draw down in the aquifer next to the pumping well to determine if drawdown in the pumping well is different to drawdown in the aquifer.

- Further experimentation, over a range of angles, needs to be undertaken to further ascertain the effect of varying the incidence angle of the RWP system to the

regional gradient. The multi dipole method produced accurate estimates of K whereas the fractional flow approach produced inaccurate estimates.

- When applying the RWP system a step drawdown test should be conducted to access the well loss in the system. If well loss is occurring it should be taken into account in the calculation of the K for the multi dipole method. Step drawdown tests should be undertaken with the RWP system as well loss is specific to specific well configurations.

- An investigation into the time period required to reach steady state concentration values when applying the fractional flow approach for varying flow rates and well configurations is also required. This could perhaps best be undertaken using MOFLOW simulations.

References

Allen-King, R. M., R. M. Halket and R. Gaylord (1998). "Characterizing the heterogeneity and correlation of perchloroethene sorption and hydraulic conductivity using a facies-based approach." Water Resources Research 34(3): 385-396.

Avci, C. B. (1992). "Parameter estimation for step-drawdown tests." Ground Water 30(3): 338-342.

Bal, A. A. (1996). "Valley fills and coastal cliffs buried beneath an alluvial plain: Evidence from variation of permeabilities in gravel aquifers, Canterbury plains, New Zealand." Journal of Hydrology (NZ) 35(1): 1-27.

Bear, J. (1979). Hydraulics of groundwater. New York, McGraw Hill.

Beyer, W. (1964). "On the determination of hydraulic conductivity of gravels and sands from grain-size distributions." Wasser-wirtschaft-Wassertechnik 14: 165–169.

Bouwer, H. (1978). Groundwater Hydrology, McGraw-Hill, Inc.

Bouwer, H. and R. C. Rice (1976). "A slug test for determining hydraulic conductivity of unconfined aquifers with completely or partially penetrating wells." Water Resources Research 12: 423-428.

Bright, J., F. Wang and M. Close (2002). "Influence of the amount of available K data on uncertainty about contaminant transport prediction." Ground Water 40(5): 529-534.

Cameron, K. C., D. F. Harrison, N. P. Smith and C. D. A. McLay (1990). "A method to prevent edge-flow in undisturbed soil cores and lysimeters." Australian Journal of Soil Research 28: 879-886.

Carman, P. C. (1937). "Fluid flow through granular beads." Transactions of the Institute of Chemical Engineering 15: 150-156.

Carman, P. C. (1938). "Determination of the specific surface of powders." Trans. J. Soc. Chem. Indus. 57: 225-234.

Carroll, D. L. (1996). "Chemical laser modelling with genetic algorithms." American Institute of Aeronautics and Astronautics Journal 34(2): 338-346.

Christ, J. A., M. N. Goltz and J. Huang (1999). "Development and application of an analytical model to aid design and implementation of *in situ* remediation technologies." Journal of Contaminant Hydrology 37(3-4): 295-317.

Cieniawski, S. E., J. W. Eheart and S. Ranjithan (1995). "Using genetic algorithms to solve a multi-objective groundwater monitoring problem." Water Resources Research 31(2): 399-409.

Cirpka, O. A. and P. K. Kitanidis (2001). "Travel-time based model of bioremediation using circulation wells." Ground Water 39(3): 422-433.

Close, M., J. Bright, F. Wang, L. Pang and M. Manning (2008). "Key features of artificial aquifers for use in modelling contaminant transport." Ground Water 46(6): 814-828.

Close, M. E., G. J. Stanton and L. Pang (2002). "Use of rhodamine WT with xad-7 resin for determining groundwater flow paths." Hydrogeology Journal 10: 368-376.

Cooper, H. H., J. D. Bredehoeft and I. S. Papadopulos (1967). "Response of a finite diameter well to an instantaneous charge of water." Water Resources Research 3: 263-269.

Cunningham, J. A., T. P. Hoelen, G. A. Hopkins, C. A. Lebrón and M. Reinhard (2004). "Hydraulics of recirculating well pairs for ground water remediation." Ground Water 42(6/7): 880-889.

Dann, R. L., M. E. Close, L. Pang, M. J. Flintoft and R. P. Hector (2008). "Complementary use of tracer and pumping tests to characterize a heterogeneous channelized aquifer system in New Zealand." Hydrogeology Journal 16: 1177-1191.

Dietrich, P., J. J. Butler Jr and K. Faiß3 (2008). "A rapid method for hydraulic profiling in unconsolidated formations." Ground Water 46(2): 323-328.

Fetter, C. W. (2001). Applied hydrogeology. New Jersey, Prentice-Hall, Inc.

Freeze, R. A. (1994). "Henry Darcy and the fountains of Dijon." Ground Water 32(1): 23-30.

Freeze, R. A. and J. A. Cherry (1979). Groundwater. Englewood Cliffs, NJ, Prentice-Hall, Inc.

Gandhi, R. K., G. D. Hopkins, M. N. Goltz, S. M. Gorelick and P. L. McCarty (2002). "Full-scale demonstration of *in situ* cometabolic biodegradation of trichloroethylene in groundwater 1. Dynamics of a recirculating well system." Water Resources Research 38(4).

Gaspar, E. and M. Oncescu (1972). Radioactive tracers in hydrology. New York, Elsevier Science.

Goltz, M. N., M. E. Close, H. Yoon, J. Huang, M. J. Flintoft, S. Kim and K. Enfield (2009). "Validation of two innovative methods to measure contaminant mass flux in groundwater." Journal of Contaminant Hydrology 106: 51-61.

Goltz, M. N., J. Huang, M. E. Close, M. J. Flintoft and L. Pang (2008). "Use of tandem circulation wells to measure hydraulic conductivity without groundwater extraction." Journal of Contaminant Hydrology 100(3-4).

Grove, D. B. and W. A. Beetem (1971). "Porosity and dispersion constant calculations for a fractured carbonate aquifer using the two well tracer method." Water Resources Research 7(1): 128-134.

Harbaugh, A. W. (2005). Modflow-2005, the U.S. Geological survey modular ground-water model -- the ground-water flow process. U.S. Geological Survey Techniques and Methods 6-A16, variously paged.

Hazen, A. (1892). Some physical properties of sands and gravels, with special reference to their use in filtration. Annual Report, Massachusetts State Board of Health: 539-556.

Holland, J. H. (1975). Adaptation in natural and artificial systems. Ann Arbor, MI, University of Michigan Press.

Huang, J. and M. N. Goltz (2005). "A three-dimensional analytical model to simulate groundwater flow during operation of recirculating wells." Journal of Hydrology 314(1-4): 67-77.

Hunt, B (2005). "Visual Basic Programs for Spreadsheet Analysis." Ground Water 43(1): 138-141.

Hvorslev, M. J. (1951). Time lag and soil permeability in ground water observations. U. S. A. C. o. E. W. E. Station. Bulletin 36: 50.

Illman, W. A., A. J. Craig and X. Lui (2008). "Practical issues in imaging hydraulic conductivity through hydraulic tomography." Ground Water 46(1): 120-132.

Johnson, R. L. and M. A. Simon (2007). "Evaluation of groundwater flow patterns around a dual-screened groundwater circulation well." Contaminant Hydrology 93: 188-202.

Kabala, Z. J. (1993). "The dipole flow test: A new single borehole test of aquifer characterization." Water Resources Research 29(1): 99-108.

Kim, S. (2005). "Validation of an innovation groundwater contamination flux measurement method." Department of System and Engineering Management,. Dayton, Air Force Institute of Technology. Master of Science in Environmental Engineering and Science: 84.

Leap, D. I. and P. G. Kaplan (1988). "A single-well tracing method for estimating regional advective velocity in a confined aquifer: Theory and preliminary laboratory verification." Water Resources Research 24(7): 993-998.

Levy, B. S., L. J. Pannell and J. P. Dadoly (1993). "A pressure-packer system for conducting rising head tests in water table wells." Journal of Hydrology 148(1-4): 189-202.

Mace, R. E. (1997). "Determination of transmissivity from specific-capacity tests in a karst aquifer." Ground Water 35(5): 738-742.

McCarty, P. L., M. N. Goltz, G. D. Hopkins, M. E. Dolan, J. P. Allan, B. T. Kawakami and T. J. Carrothers (1998). "Full-scale evaluation of *in situ* cometabolic degradation of trichloroethylene in groundwater through toluene injection." Environmental Science Technology 32(1): 88-100.

Molz, F. J., R. H. Morin, A. E. Hess, J. G. Melville and T. O. Güven (1989). "The impeller meter for measuring aquifer permeability variations: Evaluations and comparisons with other tests." Water Resources Research 25 (7): 1677–1686.

Neimann, W. L. and C. W. Rovey (2000). "Comparison of hydraulic conductivity values obtained from aquifer pumping tests and conservative tracer tests." Ground Water Monitoring and Remediation 20(3): 122-128.

Odong, J. (2008). "Evaluation of empirical formulae for determination of hydraulic conductivity based on grain- size analysis." Journal of American Science 4(1).

Palmer, C. D. (1993). "Borehole dilution tests in the vicinity of an extraction well." Journal of Hydrology 146: 245-266.

Peursem, D. V., V. Zlotnik and G. Ledder (1999). "Groundwater flow near vertical recirculatory wells: Effect of skin on flowgeometry and travel times with implications for aquifer remediation." Journal of Hydrology 222(1-4): 109.

Pitterle, M. T., R. G. Andersen, J. T. Novak and M. A. Widdowson (2005). "Push-pull tests to quantify *in situ* degradation rates at a phytoremediation site." Environmental Science Technology 39: 9317- 9323.

Pollock, D. W. (1989). Documentation of computer programs to compute and display pathlines using results from the U.S. geological survey modular three- dimensional finite-difference ground-water flow model, US Geological Survey. Open-file Report 94-464. 1-249.

Razack, M. and D. Huntley (1991). "Assessing transmissivity from specific capacity data in a large and heterogeneous alluvial aquifer." Ground Water 29(6): 856-861.

Rorabaugh, M. J. (1953). "Graphical and theoretical analysis of step-drawdown test of artesian wells." Proceedings of the American Society of Civil Engineers 79(362): 1-23.

Rovey, C. W. and D. S. Cherkauer, (1995). "Scale dependency of hydraulic conductivity measurements." Ground Water 33(5): 769-780.

Rovey, C. W. and W. L. Niemann (2001). "Wellskins and slug tests: Where's the bias?" Journal of Hydrology 243(1-2): 120-132.

Samani, N., M. Kompani-Zare and D. A. Barry (2004). "MODFLOW equipped with a new method for the accurate simulation of axisymmetric flow." Advances in Water Research 27: 31-45.

Slichter, C. S. (1899). Theoretical investigations of the motion of ground waters. U.S. Geological Survey 19th Annual Report, Part 2.

Sorensen, K. I., F. Efferso, E. Auken and L. Pellerin (2002). "A method to estimate hydraulic conductivity while drilling." Journal of Hydrology 260: 15 - 29.

Sutton, D. J., Z. J. Kabala, D. E. Schaad and N. C. Ruud (2000). "The dipole-flow test with a tracer: A new single-borehole tracer test for aquifer characterization." Journal of Contaminant Hydrology 44(1): 71-101.

Theis, C. V. (1935). "The lowering of the piezometric surface and the rate and discharge of a well using ground-water storage." Transactions, American Geophysical Union 16: 519-524.

Theis, C. V., R. H. Brown, and R. R. Meyer (1963). Estimating the transmissivity of a water table aquifer from the specific capacity of wells. U.S. Geological Survey Water Supply Paper 1536-I: 331-341.

Thorbjarnarson, K.W., D. Huntley and J. J. McCarty (1998). "Absolute hydraulic conductivity estimates from aquifer pumping and tracer tests in a stratified aquifer." Ground Water 36 (1) 87-97.

Toride, T., F. J. Leij and M. T. van Genuchten (1995). The CXTFIT code for estimating transport parameters from laboratory or field tracer experiments. Riverside, California: U.S. Department of Agricultural Research.: 121.

Van der Kamp, G. (1976). "Determining aquifer transmissivity by means of well response tests: The underdamped case." Water Resources Research 12(1): 71-77.

Vandenbohede, A. and L. Lebbe (2003). "Combined interpretation of pumping and tracer tests: Theoretical consideration and illustration with a field test." Journal of Hydrology 277: 134 - 149.

Vandenbohede, A. and L. Lebbe (2006). "Double forced gradient tracer test: Performance and interpretation of a field test using a new solute transport model." Journal of Hydrology 317: 155-170.

Wenzel, L. K. (1942). Methods for determining permeability of water bearing materials with special reference to discharging well methods, U.S. Geological Survey Water-Supply paper 887.

White, P.A. and M. R. Rosen (2001). "Introduction" *in* Groundwaters of New Zealand, M.R. Rosen and P. A. White (eds). New Zealand Hydrological Society Inc., Wellington. 1-3.

Xiang, J. and Z. J. Kabala (1997). "Performance of the steady-state dipole flow test in layered aquifers." Hydrological Processes 11(12): 1595-1605.

Yang, Y. G. and T. M. Gates (1997). "Wellbore skin effect in slug-test data analysis for low permeability geological materials." Ground Water 35(6): 931-937.

Yoon, H. (2006). "Validation of methods to measure mass flux of a groundwater contaminant." Department of Systems and Engineering Management. Dayton, Air Force Institute of Technology. Master of Science in Environmental Engineering and Science: 1-50.

Zlotnik, V. and G. Ledder (1996). "Theory of dipole flow in uniform anisotropic aquifers." Water Resources Research 32(4): 1119-1128.

Zlotnik, V. A., D. E. Eisenhauer, D. J. Schlautman, B. R. Zurbuchen and D. Van Peursem (2007). "Entrapped air effects on dipole flow test in sand tank experiments: Hydraulic conductivity and head distribution." Journal of Hydrology 339(3-4): 193-205.

Zlotnik, V. A. and B. R. Zurbuchen (2003). "Estimation of hydraulic conductivity from borehole flowmeter tests considering head losses." Journal of Hydrology 281: 115 - 128.

Zlotnik, V. A. and B. R. Zurbuchen (1998). "Dipole probe: Design and field applications of a single-borehole device for measurements of vertical variations of hydraulic conductivity." Ground Water 36(6): 884-893.